DYNAMIC MODELING AND DESIGN EVALUATION OF INTERACTIONS OF FISH AND A HEAD-REMOVAL MACHINE

By

Franco Steven Bussani

B. A. Sc. University of British Columbia

A THESIS SUBMITTED IN PARTIAL FULFILLMENT OF

THE REQUIREMENTS FOR THE DEGREE OF

MASTERS OF APPLIED SCIENCE

in

THE FACULTY OF GRADUATE STUDIES

MECHANICAL ENGINEERING

We accept this thesis as conforming

to the required standard

THE UNIVERSITY OF BRITISH COLUMBIA

December 1993

In presenting this thesis in partial fulfilment of the requirements for an advanced degree at the University of British Columbia, I agree that the Library shall make it freely available for reference and study. I further agree that permission for extensive copying of this thesis for scholarly purposes may be granted by the head of my department or by his or her representatives. It is understood that copying or publication of this thesis for financial gain shall not be allowed without my written permission.

Mechanical Engineering
The University of British Columbia
2075 Wesbrook Place
Vancouver, Canada
V6T 1W5

Date: Dec. 29, 1993

Abstract

Commercial salmon processing is a five-hundred million dollar industry in British Columbia. This research is part of the work undertaken at the Industrial Automation Laboratory of the University of British Columbia to address the need to increase the raw product recovery rate during the processing of salmon, in view of dwindling stocks and increasing production costs. The scope of this research is limited to the analysis of positioning the salmon for head removal on a conventional machine (Iron Butcher). A better understanding of the dynamic interactions in this stage of processing will lead to establishing design improvements that will increase the raw product recovery rate of the Iron Butcher.

Finite element models are developed to simulate the static and dynamic interaction of a salmon with the Iron Butcher. The finite element models are verified by comparing experimental results to simulation results obtained from the models. Verification ensures the simulation results are accurate and also provides an estimate of the error in the finite element models.

The finite element model is first used to analyze the fish–machine interaction during the conveying process. Simulations provide information on how to better configure the machine so that reliable conveying of fish in different situations is achieved. The finite element model is also used to analyze the operation of the Iron Butcher in its present configuration to determine the causes of positioning error, termed overfeed and underfeed. Once the mechanisms which cause these errors are identified, the model of the processing machine is modified so that the effectiveness of these modifications can be determined prior to the building of a prototype machine.

These simulation results lead to the establishment of possible design improvements for conveying, indexing and holding the salmon. Recommendations are made for the design and configuration of machine components which will result in an improved performance of the the Iron Butcher.

Table of Contents

Abstract ii

List of Tables viii

List of Figures x

Acknowledgement xvi

1 Introduction 1

1.1 History of Fish Processing 1

1.2 The Iron Butcher 3

1.3 Motivation of the Research 5

1.4 Research Objectives 9

1.5 Organization of the Thesis 12

2 Literature Review 14

2.1 Manipulation of Sliding Objects 14

2.2 Impact, Contact and Grasp 16

2.3 Material Properties of Fish Tissue 18

3 Model of the Fish 22

3.1 The Finite Element Method 22

3.1.1 Solution Procedure in the Finite Element Method 23

3.1.2 Application of the Finite Element Method to Biological Systems . 26

3.2 Material Properties of Salmon Tissue 26
3.2.1 Material Properties of Muscle 27
3.2.2 Material Properties of Organs 28
3.2.3 Material Properties of Bone 29
3.3 Model Assumptions 29
3.3.1 Assumptions Pertaining to Material Properties of Biological Tissues 29
3.3.2 Assumptions Pertaining to the Fish Geometry 31
3.4 Details of the Model 31
3.4.1 Development of the Fish Geometry 32
3.4.2 The Collar–bone and Gill Cover 36
3.4.3 Assigning Values for Material Properties 37
3.5 Verification of the Finite Element Model of a Fish 38
3.5.1 Model Validation 38
3.5.2 Mesh Refinement Study 44

4 Model of the Processing Machine **48**
4.1 Model Assumptions 48
4.2 Model of the Iron Butcher 49
4.2.1 The Table Surface 49
4.2.2 The Conveying System 50
4.2.3 The Holding Mechanism 51
4.2.4 The Indexing System 52
4.2.5 The Fish–Machine Interface 53
4.3 Verification of the Conveying Model 54
4.3.1 Order of Magnitude Calculation 55
4.3.2 Simulation Results 57

4.3.3 Discussion of Results 58
4.4 Verification of the Indexing and Holding Model 59
4.4.1 Operation of the Iron Butcher 59
4.4.2 Simulation Results 60
4.4.3 Discussion of Results 61
4.5 Limitations of the Model 62

5 Finite Element Simulation of Conveying **66**
5.1 Conventional Conveying 66
5.2 Modified Iron Butcher Conveying 67
5.2.1 Pulsed Conveyor Motion of the Current Iron Butcher 72
5.2.2 Conveying Using Staggered Lugs 75
5.2.3 Conveying Using Holding Pans 82
5.3 Summary of Results and Design Recommendations 84

6 Investigation of Indexing Errors **93**
6.1 Investigation of Underfeed Error 93
6.2 Investigation of Overfeed Error 97
6.2.1 The Role of Friction in Overfeed Error 98
6.2.2 The Role of Structural Deformities 104
6.3 Summary of Results and Design Recommendations 104

7 Implementation of Design Improvements **108**
7.1 Laboratory Prototype 108
7.2 Industrial Prototype 111

8 Conclusions and Recommendations **113**
8.1 An Overview of the Research 113

8.2 Recommendations for Design Improvement 114
8.3 Recommendations for Further Work 115

Bibliography **117**

List of Tables

2.1 The modulus of deformability and the upper limit on the linear region of the true stress–strain curves for various species of fish, as determined by Johnson et al. 20

2.2 Recorded values of Young's modulus and the associated coefficient of variation for various species of fish, as determined by Borderias et al. 20

3.1 Material properties for soft and firm fish used in the finite element simulations. 39

3.2 Experimental results for the bending of Fish No.1 and Fish No.3. 40

3.3 Simulation results for the bending of Fish No.1 and Fish No.3. 42

3.4 The percentage error between experimental and simulation results for the bending of Fish No.1 and Fish No.3. 44

3.5 Convergence curve data for the model of Fish No.3. CPU times are for simulations on a Sun SPARC station IPX using release 5.0 of ANSYS. . . 46

4.1 Overshoot and steady–state resting position for the simulations of conveying firm and soft fish. 58

4.2 A comparison of the actual size of the machine components and the corresponding component size in the finite element models. 62

6.1 Variation in the minimum gill cover–fish gap size for successful indexing using the current design of the Iron Butcher. 95

6.2 Variation in the minimum gill cover–fish gap size for successful indexing when the nose push–down device is added to the Iron Butcher. 97

List of Figures

1.1 The Iron Butcher: (a) positioning (conveying and indexing) the fish for the head cut (b) feeding fish onto the conveyer. Conveyer motion is from right to left. 4

1.2 An illustration of anatomical features of salmon which are of interest when processing salmon on the Iron Butcher. 5

1.3 Positioning a salmon on the feeding table. 6

1.4 Lugs, used for conveying the salmon, are shown on either side of an indexer. 7

1.5 An indexer is locked into the collar–bone region of a fish and is indexing the fish for the head cut while a weight rests on the tail–end of the fish. . 8

1.6 The indexer retracts from the fish just prior to the removal of the fish head by the cutter. 9

1.7 A schematic representation of the Iron Butcher, showing the crucial components. 10

1.8 A comparison of the amount of meat attached to the fish head (waste) resulting from a good cut (on the right) with that from a cut where overfeeding error occurred (on the left). 11

2.1 The orthogonal axes for fish muscle, as defined by Petrell et al. 19

3.1 The metameric structure of fish muscle. The pattern of lines on the cross (1) and longitudinal (2) sections represents the arrangement of sheets of connective tissue (myosepta) in the muscle. 27

3.2 Simplification of the fish geometry. 32

3.3 The equipment setup for acquiring the image of a salmon. 33
3.4 Calculation of the major principal axis and θ, the angle of orientation of the principal axis. 34
3.5 Measurement of the perpendicular distance from points on the contour of the fish to the major principal axis. 35
3.6 The cross–section of the finite element model of the fish (right) is based on the drawing (left). 37
3.7 The captured image of the bending experiment of Fish No.1 (on the left) and Fish No.3 (on the right). 41
3.8 Dimensionalized experimental results for the bending experiments. 41
3.9 Simulation results for the bending of fish using the material property values from Petrell et al.: (a) Material property values from the low end of the range (b) Material property values from the high end of the range. 42
3.10 Simulation results for the bending of fish using material property values which are an order of magnitude smaller than those cited by Petrell et al.: (a) Material property values from the low end of the range (b) Material property values from the high end of the range. 42
3.11 Simulation results for the bending of (a) Fish No.1 (b) Fish No.3. 43
3.12 Models used in the mesh refinement study. 45
3.13 Convergence curves for the finite element model of the fish. 47

4.1 Two views showing the finite element model of the Iron Butcher. 50
4.2 Orientation of the lugs for (a) straight conveying (b) staggered conveying. 51
4.3 Displacement profiles (motion sources) that specify the motion of the lugs for (a) continuous conveying (b) pulsed conveying. 52

4.4 The force–deflection relationships for a CONTACT49 element specified with (a) rigid friction (b) elastic friction. 55
4.5 Position of the fish mass center for the simulation of the conveying of (a) firm fish (b) soft fish. 58
4.6 Schematic representation of the Iron Butcher showing the location and motion of the lugs, indexer and holder during the indexing and holding process. (1) Initial position (2) Position when the indexer and holder drop onto the fish (3) Final position when indexing is completed. 60
4.7 Simulation results for the validation of indexing and holding processes of small fish. 64
4.8 Simulation results for the validation of indexing and holding processes of large fish. 65

5.1 Constant speed conveying of small, soft fish using the existing configuration of the Iron Butcher. The transient "rocking" motion is sufficiently settled at Time = 0.61 s. 68
5.2 Constant speed conveying of small, firm fish using the existing configuration of the Iron Butcher. The transient "rocking" motion is sufficiently settled at Time = 1.01 s. 69
5.3 Constant speed conveying of large, soft fish using the existing configuration of the Iron Butcher. The transient "rocking" motion is sufficiently settled at Time = 0.81 s. 70
5.4 Constant speed conveying of large, firm fish using the existing configuration of the Iron Butcher. The transient "rocking" motion is sufficiently settled at Time = 1.61 s. 71

5.5 Pulsed conveying of a small, soft fish using the existing configuration of the Iron Butcher shows that an error in the lateral position of the fish is introduced after only two cycles of the conveyor motion. 74
5.6 Simulation results for the pulsed conveying of a large, soft salmon with a single parallel holder show that a successful hold is not achieved. 76
5.7 Simulation results for the pulsed conveying of a large, soft salmon with two parallel holders show that a successful hold is possible. 77
5.8 Simulation results for the pulsed conveying of a large, soft salmon when two parallel holders are used: (a) the holding forces, (b) the undeformed state of the fish prior to starting the holding process and (c) the deformed state of the fish during the holding process. 78
5.9 Simulation results for the pulsed conveying of a large, soft salmon when one slanted holder is used, show that a successful hold is possible. 79
5.10 Simulation results for the pulsed conveying of a large, soft salmon when two slanted holders are used, show that a successful hold is possible. . . . 80
5.11 Simulation results for the pulsed conveying of a large, soft salmon when one slanted holder is used: (a) the holding force, (b) the undeformed state of the fish prior to starting the holding process and the deformed state of the fish (c) viewed from the dorsal (back) side of the fish (d) viewed from the ventral (belly) side of the fish. 81
5.12 Simulation results for the pulsed conveying of a large, soft salmon when two slanted holders are used to hold the fish: (a) the holding force, (b) the undeformed state of the fish prior to starting the holding process and the deformed state of the fish (c) viewed from the dorsal (back) side of the fish (d) viewed from the ventral (belly) side of the fish. 82

5.13 (a) The approximate model for the staggered–lug conveying process and (b) the resulting free–body diagram for the pusher. 83
5.14 Constant speed conveying of a large, firm fish, using staggered lugs. . . . 84
5.15 Pulsed conveying of a large, soft fish using staggered chain lugs, with the holders oriented perpendicular to the line created by the lugs. 85
5.16 Pulsed conveying of a large, soft fish using staggered chain lugs with the edges of the holders parallel to the corresponding sides of the table. . . . 87
5.17 A sketch of the holding pan used in the simulations. 88
5.18 Pulsed conveying of a large, soft fish using a pan and parallel holders. . . 89
5.19 Pulsed conveying of a large, soft fish using a pan and slanted holders. . . 90
5.20 Holding forces for the pulsed conveying of a large, soft fish using a holding pan with (a) parallel holders (b) slanted holders. 91
5.21 Pulsed conveying of a large, soft fish using a rotated pan and slanted holders. 92

6.1 The fish–gill cover gap. 94
6.2 Components of the push–down mechanism: (a) the finite element model and (b) simulation result for indexing. 96
6.3 Overfeed motion (in the x–direction) of the fish when the fish conforms to the table surface under gravity loading ($\mu_{fish-table} = 0.1$). 99
6.4 Overfeed motion (x–direction) of the fish as a function of the coefficient of friction between the fish and indexer ($\mu_{fish-table} = 0.1$). Simulation results for indexing large fish with (a) firm muscle (b) soft muscle. 100
6.5 Overfeed motion (x–direction) of the fish as a function of the coefficient of friction between the fish and indexer ($\mu_{fish-table} = 0.05$). Simulation results for indexing large fish with (a) firm muscle (b) soft muscle. 101

6.6 Overfeed motion (x–direction) of a large, soft fish when the holder is not used ($\mu_{fish-table} = 0.1$). 102

6.7 Overfeed motion (x–direction) of a large, soft fish as a function of the coefficient of friction between the fish and indexer, when the position of the holder is corrected ($\mu_{fish-table} = 0.1$). 103

6.8 A movable carousel system to permit the manual adjustment of the holder position. 107

7.1 The laboratory prototype head–butchering machine. 109

7.2 The industrial prototype head–butchering machine. 111

Acknowledgement

I would like to thank Dr. C. W. de Silva for his constant supervision and guidance throughout this research. Funding for this research was provided by the Natural Sciences and Engineering Research Council's Industrial Automation Chair held by Dr. C. W. de Silva, and through a G. R. E. A. T. scholarship awarded by The B. C. Science Council. I thank Mr. A. Beatty for his help with the vision component of the research. I would like to thank my family for their constant support and encouragement. Last but not least, I thank my wife Angelina for her support, understanding and patience.

Chapter 1

Introduction

1.1 History of Fish Processing

The principles of canning had been established by 1809 and have not changed significantly to this day, although canning methods and canning machinery have changed considerably. The world's first salmon cannery was established on the Sacramento River in 1864 by the Hume Brothers, William, G.W., and R.D., and by Percy Woodson [1]. At that time all the operations on the canning line were performed manually. By the early 1900's, several labor–saving machines were developed. The Jensen can filler automatically filled cans to the required weight. A topper was employed to automatically seal the lids on the cans. In 1903, the first Iron Butcher (also known as the Iron Chink), was introduced in a cannery in Bellingham, Washington, [1]. This machine greatly increased the production rates for preparing round (whole, undressed) salmon for canning and enabled the industry to expand rapidly. Over the years the Iron Butcher has been refined in an attempt to increase the throughput rates and to improve the raw product recovery, but the basic mechanical design remains virtually unchanged.

As advances in food science and mechanical engineering were made, new machinery were developed for the fish processing industry. Filleting machines employ two parallel knives which are separated by a distance slightly greater than the diameter of the fish backbone. Feeding a fish lengthwise into the machine results in two cuts being made along the length of the fish and on either side of the backbone. The backbone and the

attached strip of fish meat is discarded from the two resulting fillets. Skinning machines are comprised of a steel drum which uses a refrigerant to freeze the outer surface of the drum, and a conveyer to transport fish past the drum. The drum rotates so that the surface speed of the drum is identical to the speed of the conveyer. As a fish moves past the drum the skin touches and freezes to the drum, and is peeled from the fish. Head cutting machines and large vacuum pumps for unloading fish from boats have also been developed. Technology employed in the fish processing industry is for the most part mechanical in nature. These first–generation machines are typically hydraulically driven and employ little or no sensing to perform their desired task. Sensors used have been almost exclusively limited to primitive mechanical sensors. For example, the weigh station, which automatically weighs cans after they are filled, uses a lever–arm balance to determine if the cans are under–weight, over–weight, or filled to the correct weight. Correctly filled cans are sent to the topper for the lids to be fit and are vacuum sealed, while those cans which are under–weight are diverted to filler stations for correction.

The use of electronics and image processing techniques in fish processing has received attention only recently. Some recent developments can be pointed out. Automated weighing stations grade fish on the basis of weight, sending fish in a specific weight range to a specific location. The HD1S Herring Sex Discriminator [1] uses an infra–red light source and sensor to separate herring according to the sex of the fish. In order to standardize the procedures and to ensure that high government standards are met when cooking the cans of salmon, the retorts have been retrofitted from manual operation to computer control with manual supervision.

The Fisheries Technology Group Ltd, Canada, has developed a Fish Monitoring System (FMS 1000) [2]. The FMS 1000 captures a computer image of backlit fish and uses a

[1] HD1S Herring Sex Discriminator is manufactured by Neptune Dynamics Ltd. 180–6751 Graybar, Richmond, British Columbia, Canada

[2] FMS 1000 is a registered trademark of Fisheries Technology Group Ltd, P.Ø. Box 9190, St. Johns,

fish species recognition formula to determine the particular species of fish. Results from the image analysis and an automated weighing station are used to determine the weight of the fish and generate drive signals for operating the gates for sorting the fish by species and weight.

A machine that was first tested in the fish processing industry but that has potential applications throughout all food processing industries is Sentinel Vision Inc.'s Seam Sensor [3]. The Seam Sensor uses image processing to inspect, in real–time, the seal on each can after it is sealed. Improperly sealed cans are removed from the processing line, reducing the likelihood of botulism in the canned product.

1.2 The Iron Butcher

The Iron Butcher, which was developed to replace the skilled manual labour of butchers, employs fixed average settings. As long as the size of the fish being processed is the same as what the Iron Butcher is set–up to process, assuming that the machine operates properly, the raw product recovery rate of the Iron Butcher approaches that of manual operation, while the processing efficiency of the machine exceeds that of manual labor. However, since the Iron Butcher has no means of adjusting to the size of each fish run through it, the processing efficiency quickly falls below that of manual labor as the raw product recovery rate falls.

Salmon placed on the Iron Butcher is headed (the head is removed), split, eviscerated, and further cleaned before moving on for subsequent processing. Figure 1.1 is a picture of the Iron Butcher from the feeding to cutting operations. The operation of the Iron Butcher is as follows: A worker places a salmon on the feeding table so that the salmon is oriented with its head pointed towards the cutter and its belly facing away from the

Newfoundland, Canada A1A 2X9

[3]Sentinel Vision Inc. 4–7449 Hume, Ladner, British Columbia, Canada

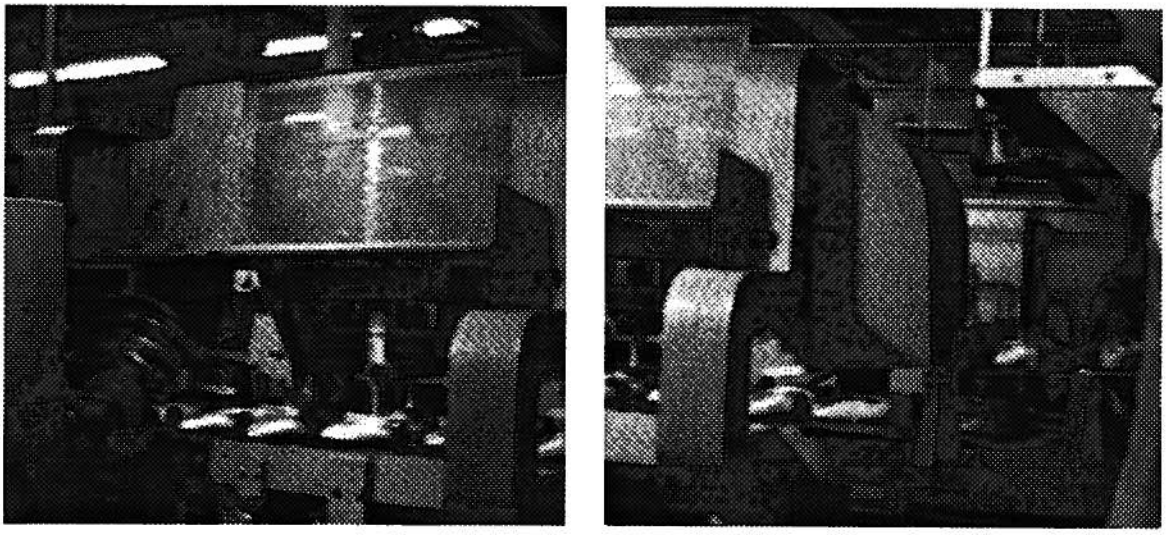

(a) (b)

Figure 1.1: The Iron Butcher: (a) positioning (conveying and indexing) the fish for the head cut (b) feeding fish onto the conveyer. Conveyer motion is from right to left.

direction of the conveyer motion. The worker must also align the salmon so that the end of the gill cover, which also corresponds to the collar–bone location, lies between two markers (see Figures 1.2 and 1.3). The feeding table has a horizontal door that pivots about one end, allowing the salmon to slide onto the conveyer bed. Pivoting motion of the feeding door is synchronized with the conveying mechanism.

Conveying of the fish is accomplished by three chains which move in recessed slots in the machine bed. Lugs, extending 5.5 cm beyond the level of the machine bed, are attached to the chains with an inter–lug spacing of 23 cm. These lugs push the fish in the direction of the conveyer motion (see Figure 1.4). Lateral indexing (incremental positioning) of the salmon starts when a metal foot (indexer) drops onto the fish; a weight also drops onto the tail end of the fish simultaneously, to hold down the fish. The indexer and weight move along the machine bed at the same speed as the chains, but in addition the indexer simultaneously moves laterally towards the cutter, as a result sliding across the lengthwise direction of the fish toward its head. When the indexer foot reaches the

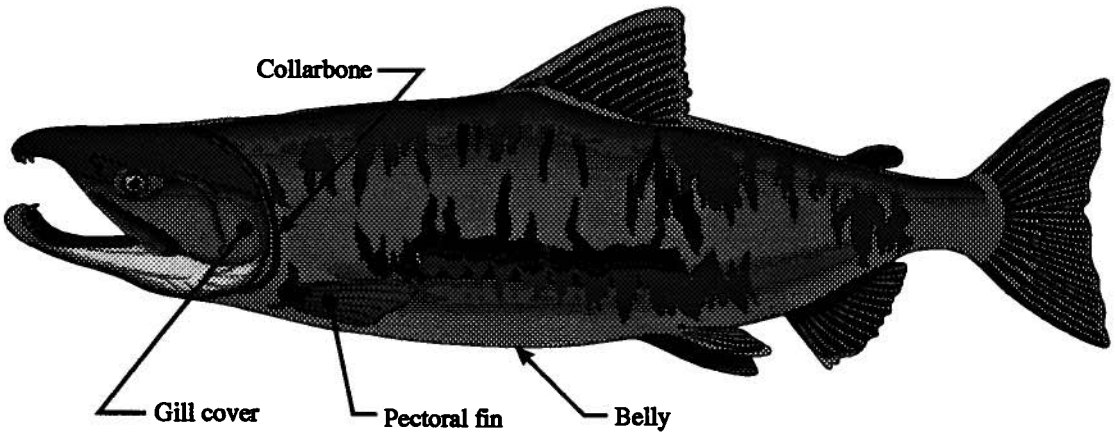

Figure 1.2: An illustration of anatomical features of salmon which are of interest when processing salmon on the Iron Butcher.

collar–bone, near the gill cover, it is expected to lock in with this region of the fish and the entire fish is pulled laterally by the indexer toward the cutting line (see Figure 1.5). The indexer positions the fish so that the collar–bone of the fish is just beyond the cutting line. The indexer then retracts from the fish just prior to the removal of the head by the cutter (see Figure 1.6). The cutting blade is specially shaped to remove both the fish head and pectoral fin while minimizing the amount of meat (i.e., waste) which is left attached to the head. A schematic diagram of the Iron Butcher, showing its main components, is shown in Figure 1.7.

1.3 Motivation of the Research

When the Iron Butcher is adjusted correctly for the size and the species of fish being processed, the head is severed from the body no more than 6 mm posterior of the collar–bone and pectoral fin; this is considered a good cut. Two major errors can occur when indexing the salmon for a head–removal operation, and both involve improper positioning of the fish with respect to the cutter.

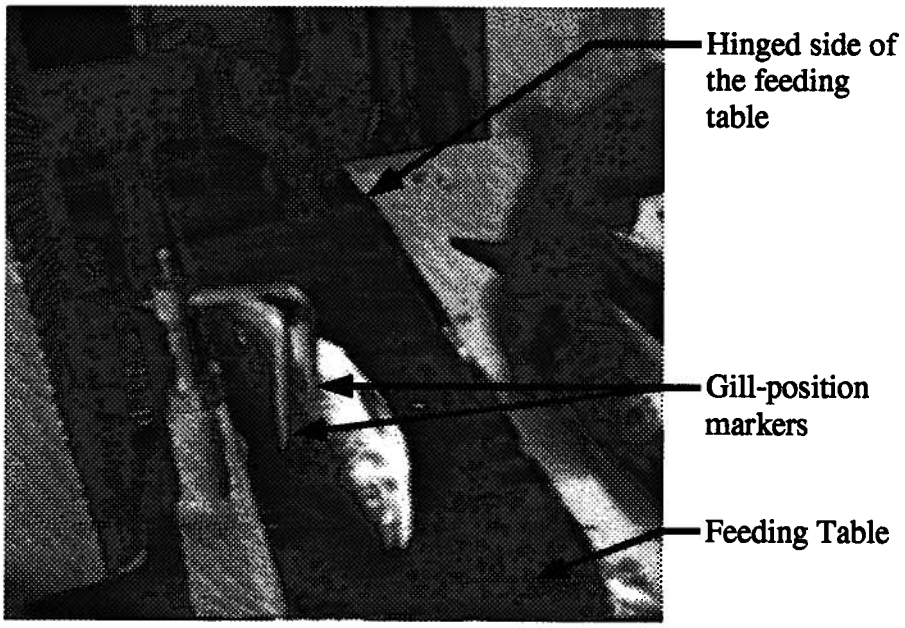

Figure 1.3: Positioning a salmon on the feeding table.

The first type of error, underfeed, occurs when the fish is not moved enough, so rather than the cutter removing the head and collar–bone from the body, the cutter cuts through the head itself, leaving part of the head and all of the collar–bone attached to the body. This happens when the indexer foot does not engage with the collar–bone, but either depresses the soft gill cover towards the nose, or completely slips over the gill cover. Underfeed requires the fish to be re–processed, either by the Iron Butcher or manually. In either case, the throughput of the machine is reduced and added expense is required to remove the head and collar–bone correctly. The second type of error, overfeed, occurs when the fish is moved too much, so that the cutter removes the head from the body more than 6 mm posterior of the collar–bone (see Figure 1.8). This situation occurs when the indexer foot becomes engaged with a different structural region prior to reaching the collar–bone, possibly due to softness or physical defect of the fish body. In many cases the wastage can be so significant that the positioning error is as high as 75 mm posterior of the collar–bone.

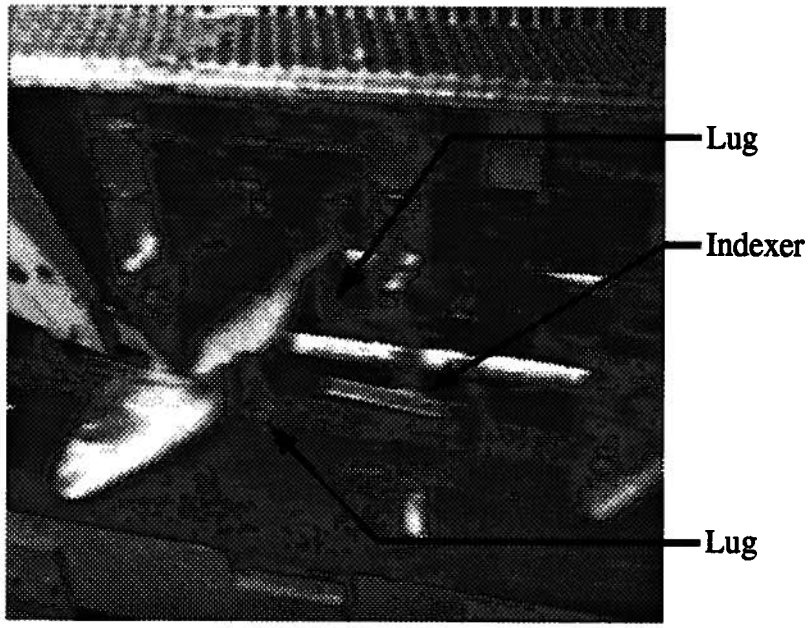

Figure 1.4: Lugs, used for conveying the salmon, are shown on either side of an indexer.

The ability of the fish processing industry in British Columbia to maintain its global competitiveness will depend upon several factors. Increasing the productivity and reduction of the wastage it currently incurs while processing the raw product are two such crucial factors. In the past, when the price of the raw material was low and the fish stocks were apparently high, the processors could afford to accept the wastage that these labour–saving machines inherently produced. But with limitation of the catch, mostly due to dwindling stocks, and the sharp increase in price of the raw product over the last few years, processors are finding it more difficult to remain competitive while accepting the wastage incurred when these machines are used for processing. The head cut on the Iron Butcher accounts for the largest percentage of raw product loss during the processing of salmon for canning. Every one percent increase in the raw product recovery rate will save the fish processing industry in British Columbia approximately five–million dollars annually [4]. It follows that wastage reduction has direct economic benefits, if not being a

[4] 1990 figures

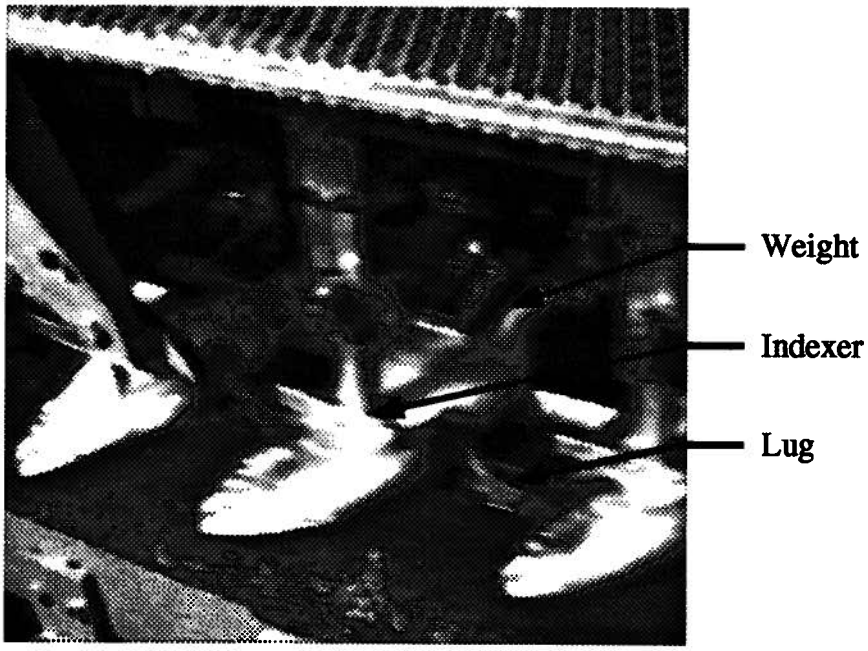

Figure 1.5: An indexer is locked into the collar–bone region of a fish and is indexing the fish for the head cut while a weight rests on the tail–end of the fish.

requirement for survival of the industry.

A pioneering effort in developing advanced technology for fish processing automation has been undertaken with the establishment of the Industrial Automation Laboratory in the Department of Mechanical Engineering at the University of British Columbia [2]. Specific projects include knowledge–based hierarchical control of a fish processing cell to address the concerns of raw product recovery, throughput rate and the quality of cutting while subject to various specifications. Model–based vision is being used to infer complex features of an object from simple geometric attributes of the object. This methodology has been successfully applied to the generation of cutting contours for Pacific salmon. Coordinated manipulation and control is being applied to the holding and manipulation of a fish while it is being cut. The grasping and handling of a non–homogeneous object has been addressed by the development of an innovative gripper.

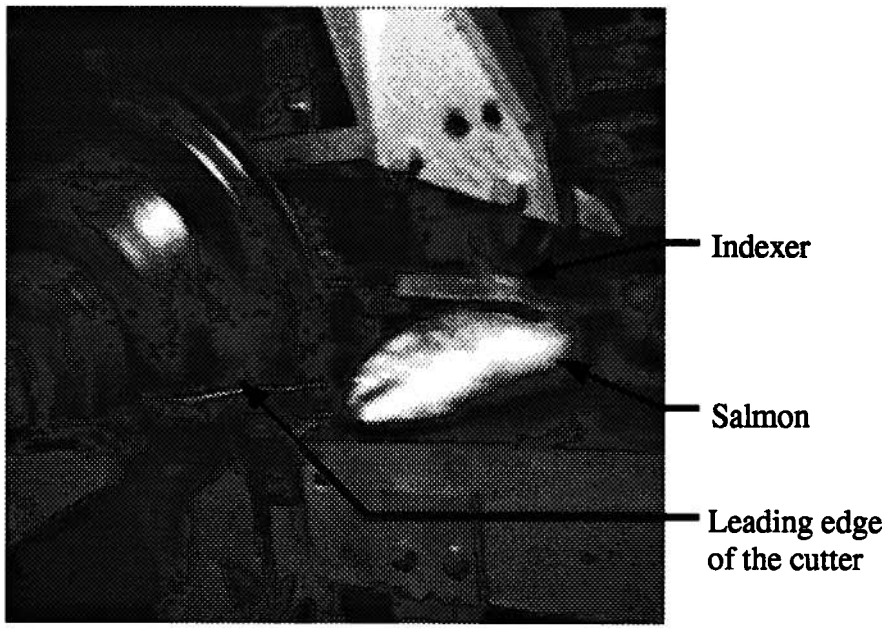

Figure 1.6: The indexer retracts from the fish just prior to the removal of the fish head by the cutter.

1.4 Research Objectives

Positioning a salmon for the head cut on an Iron Butcher is neither an accurate nor highly repeatable operation. The ultimate goal of the research described in this dissertation is to recommend design improvements which may be used in a redesign of the Iron Butcher that will result in better accuracy and repeatability. These improvements will lead to an increase in the raw product recovery rate. In order to accomplish this, the following objectives are defined:

1. **Develop a model of the fish–machine interactions for the processing of fish on the Iron Butcher.** The model is an analytical computer–simulation tool used to investigate the problems encountered during the conveying and indexing processes on the Iron Butcher. Simulation has the benefit of easy variation of

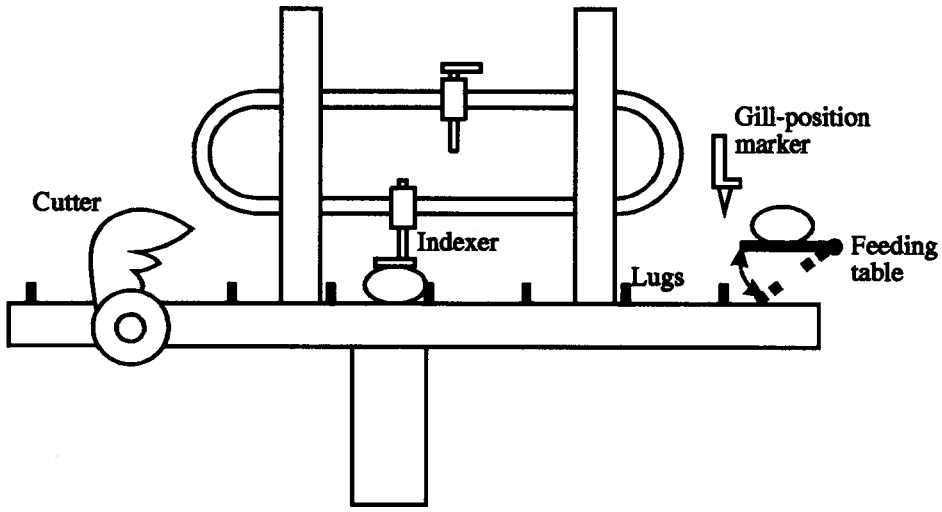

Figure 1.7: A schematic representation of the Iron Butcher, showing the crucial components.

system parameters and evaluation of the dynamic response, thereby providing insight into the underlying problems with the Iron Butcher without the cost of time and resources required to construct or modify prototypes and conduct controlled experiments.

2. **Identify the magnitudes and locations of the forces to be applied to a salmon for proper holding and conveying.** While the salmon is being conveyed, it is desirable to constrain the fish to maintain a fixed orientation with respect to both the cutter and the indexer while achieving a stable motion prior to cutting. Also, different stages of relative motion may be needed. For example, initially the indexer foot will slip over the top surface of a fish, but the fish itself will not slip laterally on the conveyer. Next the fish is expected to slip laterally as pushed by the indexer, but there should not be any slip between the indexer and the fish. The magnitude of holding forces should be minimized to reduce bruising

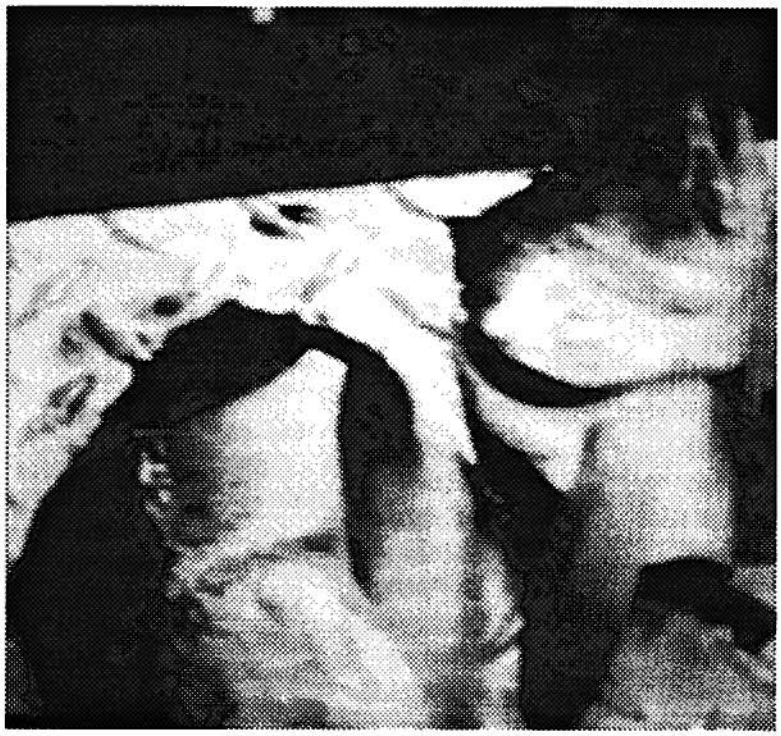

Figure 1.8: A comparison of the amount of meat attached to the fish head (waste) resulting from a good cut (on the right) with that from a cut where overfeeding error occurred (on the left).

of the fish body, while maintaining them at sufficient levels to achieve the required motion stages. Two types of conveying are investigated, conveying at a constant speed and pulsed or intermittent conveying.

3. **Identify and quantify the parameters which will lead to the elimination of both underfeed and overfeed errors.** Many parameters and variables are active during indexing, but the role each plays in determining if the salmon is improperly indexed (primarily underfeed or overfeed) has to be investigated. After identifying possible "problem" parameters and variables, the significance of each variable in determining the success/failure of the indexing process can be systematically determined. Finally, an acceptable operating range for each problem parameter is

required in order to determine design guidelines for the new machine.

4. **Establish design guidelines and make recommendations for the crucial components of a typical butchering machine.** The results of objectives 1–3 will lead directly to the establishment of design guidelines for the conveying, indexing and holding mechanisms. These recommendations may take many forms (e.g., parametric, geometric, active or conceptual).

1.5 Organization of the Thesis

This chapter has provided an introduction of the development of fish processing in British Columbia. The operation of the Iron Butcher has been explained. Finally, the motivation for and the formal objectives of this research were presented. Chapter 2 contains a review of literature relevant to this work.

Chapter 3 begins with an introduction to the finite element method, followed by a discussion of the material properties of salmon tissue. Assumptions which are required for the formulation of the finite element model of the salmon, along with details of the model development, are then presented. The chapter ends with the verification of the fish model.

Chapter 4 deals with the model of the processing machine. The details of the model are presented after the assumptions required for modeling the processing machine are discussed. Next, the verification of the model of the processing machine is presented, and the chapter concludes with a discussion of the limitations of the model.

Chapter 5 provides an analysis of the conveying process on the Iron Butcher. Simulations examine the operation of the machine in both its existing mode and in possible modified modes. Some modifications to the design of the machine are made and are simulated to determine if the operation of the machine, in its new configuration and in

the new mode, is satisfactory. The analysis of the indexing process of the Iron Butcher is presented in Chapter 6. Simulation results identify mechanisms or dynamic interactions which may be responsible for underfeed and overfeed errors. Modifications to the design of the Iron Butcher are simulated to show that the design can be improved. Both Chapter 5 and Chapter 6 conclude with discussions of the design recommendations for improved performance of the Iron Butcher.

Chapter 7 discusses the implementation of design suggestions on two prototype head–cutting machines. Finally, Chapter 8 summarizes the thesis, outlines the main contributions, and makes recommendations for future work.

Chapter 2

Literature Review

The task of conveying and lateral indexing a salmon for the head cut on the Iron Butcher may be considered primarily as a problem of how to manipulate a flexible object that is able to slide, by pushing it on a flat surface. Because of the similarities that exist in the manipulation of sliding objects and the analysis and design of part–feeders, with the conveying and positioning of fish on the Iron Butcher, literature dealing with these topics is reviewed in section 2.1. In the analysis of the dynamic interactions between a fish and the Iron Butcher, the high processing speed and the interaction between objects that undergo relative motion on the Iron Butcher necessitate the inclusion of impact and contact dynamics of deformable bodies. A review of the impact, contact and grasp in robotic applications is presented in section 2.2, as these applications were the only relevant sources found in the literature review conducted. Biomechanic and food–texture studies which experimentally studied the material properties of fish tissue are reviewed in section 2.3, in view of the importance of such experimental data in this investigation.

2.1 Manipulation of Sliding Objects

An important issue in positioning a fish for the head cut is how to deal with the uncertainties in the initial location of the fish and shape of the fish. Mason [3] introduces a method that is different from structuring the environment or using sensors to attack this problem. In that work, it is proposed that the task mechanics be used to eliminate the uncertainty without the need for sensing. A funnel has been defined as any operation

that eliminates uncertainty mechanically, and converges towards the positioning objective. The funnel will achieve the goal of positioning an object despite variation in the initial location and shape of the object. Task mechanics are invaluable when manipulating flexible materials, as pointed out in that work. Rather than directly controlling all motion degrees of freedoms of the flexible material, one must only exploit the natural tendencies of that material.

Mason [4], having recognized the importance of pushing as an essential component in many robotic manipulator tasks, presents a theoretical basis for analyzing and planning pushing operations. Coulomb friction is assumed and the frictional forces are considered to dominate over inertial forces. The motion of the object is determined, which depends on whether or not the object rotates, and on the direction of rotation.

Brost [5] presents a method for the automatic planning of robot grasp motions for a parallel–jaw gripper that is insensitive to bounded uncertainties in the location of the object. His method uses the physics of friction to generate all grasp plans that utilize either a squeeze–grasp, offset–grasp, or push–grasp motion. These three motions are essentially examples of Mason's mechanical funnel [3] as applied to a parallel–jaw gripper. Brost only examines planar motion and uses Mason's work in [4] to determine the direction of rotation of the object.

Peshkin and Sanderson [6] have developed a method to plan the manipulation of an object that is free to slide without knowing the exact distribution of frictional forces between the object and the surface it is sliding over. They have simplified the problem by assuming the following:

- Zero friction at the pusher–object contact.
- The support force distribution is confined to a disk.
- The object is a 2–D rigid body which is pushed across a level surface.

- A point contact exists between the pusher and the object.
- Coulomb friction exists between the object–surface interface.
- All motions are slow (quasi–static).

Peshkin and Sanderson have extended their work [7, 8] to compute configuration maps that provide a basis for planning the operation sequences which occur in parts–feeder designs or in more general sensorless manipulation strategies for robots.

Gilmore [9] provides a rule–based algorithm to predict the dynamic motion of parts–feeders or pushing operations of manipulators. The algorithm automatically determines, predicts or detects the kinematic–constraint changes and reformulates the dynamic equations of motion, automatically simulating the dynamic behavior of systems with unpredictable or unforeseen kinematic–constraint changes. The rules have been developed using kinematics, system dynamics and geometric modeling, but ignoring frictional effects and body deformations.

The methods outlined thus far have in common Mason's idea of a funnel. Except for Gilmore [9], all assume slow motions. If the motion of the pusher and object is not slow, and if instantaneous relative motions occur, then impact dynamics must also be considered. Furthermore, the methods presented do not address the pushing of deformable bodies.

2.2 Impact, Contact and Grasp

Impact dynamics must be considered for robotic and pusher operations when impulsive–type forces exist and inertial effects are not negligible compared to frictional effects. Wang and Mason [10] have explored the planar impact of two objects and developed a graphical method for predicting the mode of contact, the total impulse and the resultant

motions of the objects. The analysis includes the effects of elasticity and friction and is based on the seminal work by Routh [11].

Once the pusher and object are in contact, the relative motion between them is also of interest. Cai and Roth [12] have derived equations for the study of roll–slide motions between rigid curves with point contact under planar motion, by considering only the instantaneous time based kinematics. It has been assumed that a tactile sensor [13] is available to measure the relative motion at the point of contact and that the elastic deformation of the sensor is negligible. Equations have been derived for the case of two point contacts as well, and this work has been further expanded to examine the 3–D case of planar motion with point contact [14]. The derived equations for both the 2–D and 3–D case were applied to sensor–based robotic path planning.

In a different approach which does not require sensing of the motion of the contact point, Montana [15] uses differential geometry to derive a set of contact equations which describes the motion of a point contact over the surfaces of two touching objects in response to a relative motion of these objects. Two assumptions, that the objects are rigid bodies and that there is only point contact between the objects, are made. Montana uses his contact equations to investigate the rolling of a sphere between two arbitrarily shaped fingers and for fine grip adjustment. He then extends this work to non–rigid bodies and derives compliant contact equations to model the kinematics of contact with compliance [16]. Results of his experiments show that compliance can cause large deviations from the rigid–body model, which supports the requirement of a compliant, or deformable, fish model in studying the dynamic interaction during the conveying, indexing and holding operations of the Iron Butcher.

Saliba and de Silva [17] have studied the dynamics of planar objects on a flat surface, during grasping with a robotic hand. A hand has been designed and built for the experimental investigations. The innovative hand uses fewer actuators than it has degrees of

freedom, and furthermore, a novel switch based on Coulomb friction has been employed in order to eliminate the need for electronic sensors in limit sensing and overload protection. The effects of Coulomb friction and various geometric and kinematic parameters on the dynamics of the grasped object have been analyzed and studied through both laboratory experimentation and computer simulation. The use of a gripper of this type in handling fish for an Iron Butcher–type machine has been investigated [18].

Although certain aspects of the above work are applicable to the problem at hand, certain limitations exist. The various studies outlined above investigate specific tasks, while the problem at hand requires an integrated study that encompasses pushing, impact, contact and grasp of a flexible body with nonlinear and anisotropic material properties.

2.3 Material Properties of Fish Tissue

Measurement of mechanical properties of biological tissues is used in the study of biomechanics and in texture studies of food. Biomechanics seeks to understand the mechanics of living systems, and data is available primarily for the human body. Texture study of food attempts to provide a relationship between palatability (a subjective measure) and mechanical properties of the food (an objective measure). Data collected for texture studies of fish deal with mechanical properties of both raw and processed fish.

Petrell et al. [19] performed a preliminary study to determine the elastic properties of the transversely anisotropic structure of salmon muscle subjected to compression tests. The test samples consisted of blocks of muscle tissue, and consisted of both myotomes (muscle fibre) and myosepta (connective tissue between muscle fibres). They found a large variation in the values of the moduli of elasticity E_{11} and E_{22} along the orthogonal axes 1 and 2 (see Figure 2.1), but established the approximate range of values as:

- $300\ kPa \leq E_{11} \leq 625\ kPa$

- $700\ kPa \leq E_{22} \leq 1100\ kPa$
- $300\ kPa \leq G_{12} \leq 550\ kPa$ [1]

The moduli E_{11} and E_{22} were calculated using engineering stress and strain so that they are only valid for small strains. Many factors have been proposed as contributing to the wide variability in these elastic constants. "These include high intramuscular fat levels, insufficient exercise, pre–slaughter stress, pre–slaughter starvation, improper post–mortem handling and time since slaughter" [19].

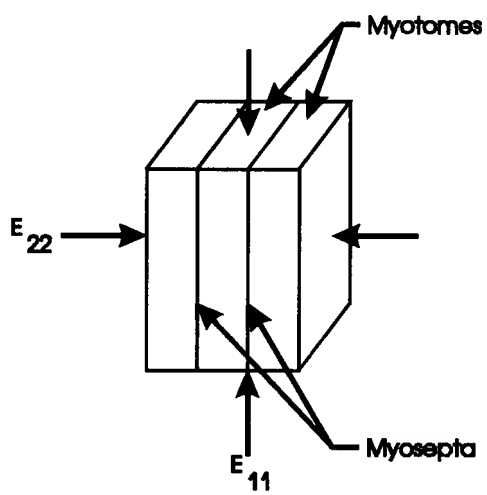

Figure 2.1: The orthogonal axes for fish muscle, as defined by Petrell et al.

Johnson et al. [20] developed a procedure to measure the response of both fresh and cooked fish muscle subjected to compression by an Instron Universal Testing Machine. The modulus of deformability, M, defined as $M = \sigma_T/\epsilon_T$, where σ_T and ϵ_T are the true stress and true strain respectively, was used to characterize the overall resistance of the material to deformation, instead of Young's modulus E, because, strictly speaking, Young's modulus is only applicable to linear elastic strains. Experimental results

[1] From a discussion with R.J. Petrell, August 6, 1992.

indicated the linear region of the true stress versus true strain curves ranges from 20% to 40% and depends strongly on the species of fish. The deformability modulus varied between species of fish as well as between samples within a species of fish and the values are summarized in Table 2.1.

Table 2.1: The modulus of deformability and the upper limit on the linear region of the true stress–strain curves for various species of fish, as determined by Johnson et al.

Fish Species	M (kPa)		Upper limit of linear region (% strain)
	Test #1	Test #2	
Hake	17 – 31	23 – 38	20 – 25
Pollock	20 – 54	15 – 39	20 – 25
Flounder (Pseudopleuronecetes americanus)	15 – 88		25 – 35
Bluefish (Potatomus soltatrix)	16		25
Cod (Godus morhua)	73		25 – 30

Table 2.2: Recorded values of Young's modulus and the associated coefficient of variation for various species of fish, as determined by Borderias et al.

Fish Species	Test #1		Test #2	
	$E_{average}$ (kPa)	coefficient of variation	$E_{average}$ (kPa)	coefficient of variation
Trout	86	18	137	19
Sardine	53	26	98	8
Conger	120	36	129	16
Horse Mackerel	76	28	88	21
Blue Whiting	111	32	80	48

Borderias et al. [21] attempted to establish a link between sensory analysis of fish texture with instrumental testing of the mechanical properties of fish flesh. The experimental investigation of texture was performed using an Instron model 1140 Texturometer

and each test consists of five replicates. A summary of the Young's moduli and the corresponding coefficients of variation from compression tests on various species of fish are shown in Table 2.2.

Petrell et al. [19] did not report any values of Poisson's ratio ν for salmon muscle, but this parameter is estimated to be in the range of $0.3 \leq \nu \leq 0.5$, and is dependent on the water content of the muscle tissue, as disclosed in private conversations [2]. When the fish is alive the water content of the tissue is at its maximum ($\nu \approx 0.5$). As the time since slaughter increases, the water content of the tissue decreases ($\nu \longrightarrow 0.3$). Chow and Odell [22] performed a finite element analysis to investigate the deformations and stresses in the buttocks of a sitting person. They measured the muscle material properties in vivo and found $\nu_{human\ muscle} = 0.49$.

Due to anatomical and structural mutations occurring post–mortem, the mechanical properties of soft tissue change, normally within a few hours of death. Yamada [23] analyzed data obtained from stress–strain tests performed on a variety of human skeletal muscles. He found that, "in general, the post–mortem decrease in the ultimate strength of muscle tissue occurs quite rapidly during the first 24 hrs, slows down somewhat between 24 and 36 hrs, and becomes substantially constant at 48 hrs." Although Yamada's observation is for human muscle, it illustrates the rapid post–mortem deterioration in the strength of muscle tissue which is common to all animal species.

[2]From a discussion with R.J. Petrell, August 6, 1992.

Chapter 3

Model of the Fish

It is required to analyze the dynamic interactions of a fish with the Iron Butcher during the holding, conveying and indexing processes. The purpose of the analysis is to predict the dynamic behaviour of a fish when acted upon by various components of the Iron Butcher during processing. Parametric studies based on this may be employed to predict whether specified conditions and structural modifications will result in a better hold on the fish while conveying and indexing, and what conditions are necessary to better convey and index the fish. The main objective is accurate positioning and the reduction of wastage at the head cut. The development of a model of the fish is the first step toward these goals. The present chapter begins with a brief introduction of the Finite Element Method in section 3.1. A discussion of the material properties of salmon tissue in section 3.2 provides the framework for establishing the model assumptions in section 3.3. Details of the fish model are elaborated upon in section 3.4, and the chapter concludes with the verification of the fish model in section 3.5.

3.1 The Finite Element Method

Huebner and Thornton [24] write:

> Continuum problems are concerned with fields of temperature, stress, mass concentration, displacement, and electromagnetic and acoustic potentials, to name just a few examples. These problems arise from phenomena in nature that are *approximately* characterized by partial differential equations and their

> boundary conditions. ...However, the number of problems with exact solutions is severely limited, and most of these have already been solved. They are the classical problems.

In such cases where the problem is so complex that an exact closed–form solution cannot be found, numerical methods of analysis are a viable alternative. Of these, two of the most popular are the finite difference method and the variational methods (e.g., the Ritz method). Because they do not support non–rectangular or non–uniform meshes, these methods encompass difficulties in defining boundary conditions along curved boundaries and difficulties in accurately modeling geometrically complex domains. With the finite element method (FEM), the assumed trial functions are defined over the element, not the entire solution domain, and must only satisfy certain continuity conditions, not boundary conditions. As a result, the FEM can be applied to geometrically complex domains.

In the processes under investigation, the loading on a fish varies with time. The fish is a complex structure comprised of hard tissue (bone) and soft tissue (muscle, internal organs, connective tissue and skin). As a result, the numerical method of analysis chosen must be capable of both static and dynamic analyses, and must account for the nonlinear, deformable and anisotropic material of the fish. Because the FEM is able to handle such requirements, this particular method is used in the present research to model a fish.

3.1.1 Solution Procedure in the Finite Element Method

The solution of a problem by the finite element method follows an orderly process. The following steps summarize in general terms how the solution process of the finite element method proceeds.

1. **Discretize the solution domain.** The solution domain is divided into sub–regions called elements. A variety of element shapes is available to be selected

from, and if care is taken, more than one element shape may be used in the same solution domain.

2. **Select interpolation functions.** For each element, assign nodes and then choose the type of interpolation function (shape function) to represent the variation of the field variable over that element.

3. **Determine the element properties.** Select the parameter values for the element properties and determine the matrix equations expressing the properties of the individual elements.

4. **Obtain the system equations by assembling the element properties.** Combine the matrix equations describing the behavior of the elements to form the matrix equations defining the behaviour of the entire solution region or domain. The system equations are modified to account for the boundary conditions of the problem. A vector for the loading applied to the system has to be defined at this stage.

5. **Solve the system equations.** The system equations (a set of second–order simultaneous differential equations in the general dynamic case) are solved to obtain the unknown nodal values of the field variable. Solutions can be obtained whether the system equations are linear or nonlinear. For a dynamic analysis, the equation to be solved is

$$[M]\{\ddot{X}\} + [C]\{\dot{X}\} + [K]\{X\} = \{F\} \tag{3.1}$$

where $[M]$, $[C]$ and $[K]$ are the global mass, damping and stiffness matrices respectively, $\{\ddot{X}\}$, $\{\dot{X}\}$ and $\{X\}$ are the global acceleration, velocity and displacement vectors respectively, and $\{F\}$ is a vector of applied forces.

6. **Perform additional computations if required.** The solution of the system equations can be used to calculate other important parameters. For example, if the

solution of the equations for a structural analysis gives the displacement at each node in the solution domain, these results can be used to approximate the stress field in the solution domain.

The above procedure is followed to arrive at a solution using the finite element method. However, once a solution is obtained, it must be validated. Validation usually involves comparing the finite element solution results to one or more of the following:

- Experimental results.
- An exact solution, if it exists. (Sometimes an exact solution may exist for a special case of the problem being investigated. The finite element model is developed for a general situation, which then is reduced to this special case for which an exact solution exits, so that a comparison can be made. If the results are in agreement within an allowable tolerance, then, assuming that the special case is sufficiently representative, the finite element model of the general case is considered valid, by association).
- Other simulation results that are available and known to be valid.
- An order of magnitude calculation.

In addition to validating the finite element solution, an estimate of the error in this solution, arising from the assumptions made to simplify the model (e.g. geometric approximations) and from round–off error, is required [25]. A convergence study, also known as a mesh refinement study, has to be performed as well, to generate a convergence curve. To generate the convergence curve, the finite element simulation is solved several times, each time using a finer element mesh for successive simulation runs. One of the field variables being solved for is selected and is graphed against the simulation run–time. The

resulting curve should show a decrease in simulation error with increasing solution times. Simulation error is estimated by the change in the value of the selected field variable from two successive simulation runs. This approach will provide information for selecting the mesh size for a particular problem.

3.1.2 Application of the Finite Element Method to Biological Systems

Since its introduction, use of the finite element method has progressed from analyzing simple structural problems through thermo–fluid processes to complex biological systems. Biological models typically consider either the bone structure (hard tissue), the soft tissue, or some combination of the two. Modeling soft tissue presents the most difficulty since the normal behaviour of soft tissues is time dependent. In addition, the experimental data regarding the mechanical properties of soft tissues are either scarce or unavailable. Even when data for the soft tissues are available, the conditions under which they are collected often generate more questions than answers. As a result, assumptions regarding the mechanical properties of soft tissues are extremely difficult to stipulate.

3.2 Material Properties of Salmon Tissue

A salmon is a complex biological system comprised of hard tissue (bone) and soft tissue (muscle, connective tissue, organs, skin and fat). Because the mechanical behaviour of soft tissues is time dependent while the mechanical behaviour of hard tissue is time independent, in general, the material properties of hard tissue are more accurately known and are more widely available. Nonetheless, the material properties of both soft and hard tissue must be defined for the salmon to be modeled using the finite element method.

3.2.1 Material Properties of Muscle

In a fish such as salmon, the flesh muscle is divided into layers of contractile fibres called myotomes which are held together by a thin connective tissue called myosepta. The myotomes and myosepta are structured in a complex geometry, as shown in Figure 3.1. In addition to the complexity of the organization of the myotomes and the myosepta, the

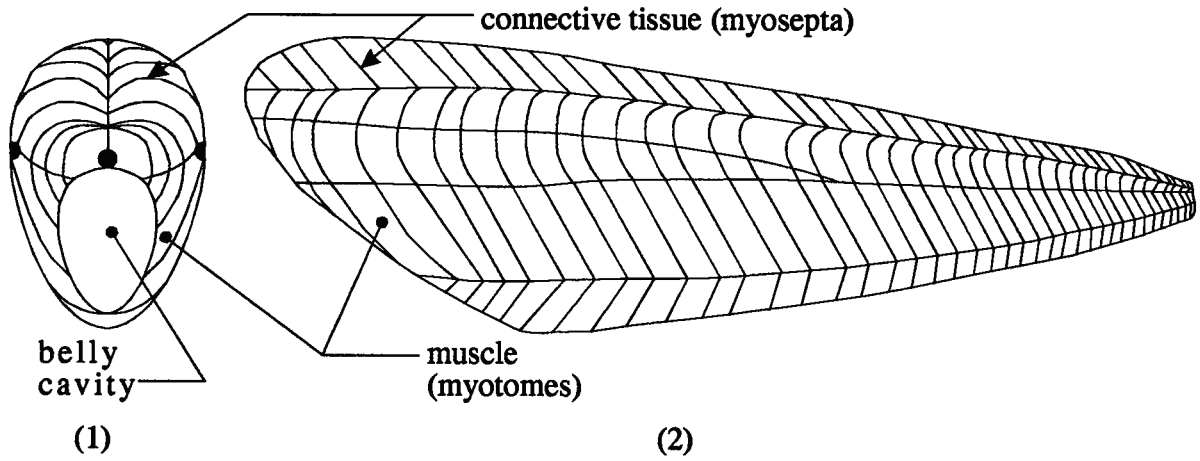

Figure 3.1: The metameric structure of fish muscle. The pattern of lines on the cross (1) and longitudinal (2) sections represents the arrangement of sheets of connective tissue (myosepta) in the muscle.
[26]

myotomes themselves may be curved, and have a non–uniform cross–section that often results in coning (the tapering of the cross–section to a point). The complexity of the pattern of myotomes and myosepta, combined with the shape of the muscle fibre results in the fish muscle behaving like an anisotropic, composite material. However, certain regions of the fish muscle (the mid–anterior in either the epaxialis or hypaxialis) are straight and are of uniform cross–section. In these areas, the fish muscle can be considered to be transversely isotropic and can be characterized by the independent elastic moduli, E_{11} and E_{22} in the two orthogonal directions (i.e., along the muscle fibres and perpendicular to the muscle fibres), the Poisson's ratio ν, and an in–plane shear modulus G_{12}.

As outlined in section 2.3, Petrell et al. [19] measured the elastic moduli E_{11} and E_{22} of salmon tissue prepared from these special regions of the fish. However, their results are one order of magnitude larger than results obtained by Johnson et al. [20] and Borderias et al. [21], who measured the modulus of deformability ($M = \sigma_T/\epsilon_T$) and Young's modulus ($E = \sigma/\epsilon$), respectively, of samples prepared from fillets of various species of fish. It is unlikely that this order of magnitude difference is the result of the method used to calculate E or M, since both Petrell et al. and Borderias et al. calculated E using engineering stress and strain, while Johnson et al. used true stress and strain to calculate M. Further comparison of E for other animals shows that for beef, 6.3 kPa $< E^{beef}_{muscle} <$ 126 kPa [27], for sheep, $E^{ovine}_{muscle} \approx$ 157 kPa [28] , and for humans, $E^{human}_{muscle} \approx$ 15 kPa.

As will be shown in section 3.5.1 of this work, reducing the values of E_{11}, E_{22} and G_{12} which Petrell et al. report, by one order of magnitude, results in simulation results obtained using the finite element model of the fish which are characteristic of a fish with firm muscles, as would be expected from fish in rigor mortis. The values of the material properties for characterizing soft fish are determined by comparing simulation results to experimental results.

3.2.2 Material Properties of Organs

By observation, the belly region (comprised of muscle tissue and the organs in the belly cavity) of a salmon is softer than the dorsal region (comprised of solid muscle and some bone) of the salmon. Post–mortem changes also cause a build–up of gas in the belly cavity. No data are available to define the material properties of the contents of the belly cavity, but it can be characterized as a spongy solid with a Young's modulus lower than the Young's modulus for fish muscle. The Poisson's ratio for the contents of the belly cavity is considered to be about 0.49.

3.2.3 Material Properties of Bone

Bone is a nonhomogeneous, anisotropic and composite material primarily composed of collagen and hydroxyapatite. Bone is hard and has a stress–strain relationship similar to many engineering materials [29]. A comparison of the Young's moduli for bone and muscle shows that in humans, the stiffness of bone tissue is approximately 670,000 times larger than that of muscle tissue ($E^{muscle} \approx 15kPa$, $E^{bone} \approx 10,000,000kPa$ [23]). This comparison reveals that under identical loading, deformation of bone is negligible when compared to the deformation of muscle (soft tissue). Although approximate values for the Young's modulus for fish bone is not available, experience shows that, as in the case of human tissue, fish bone is much harder than fish muscle.

3.3 Model Assumptions

A fish is a complex biological system, and simplifying assumptions have to be made before it can be modeled mathematically. This simplification is achieved by making assumptions regarding the material properties of the tissues and the geometry of the fish. These assumptions then serve as a basis upon which a finite element model can be developed.

3.3.1 Assumptions Pertaining to Material Properties of Biological Tissues

The following assumptions are used to simplify the representation of the material properties of biological tissues in the finite element model of a salmon.

1. The fish muscle is transversely isotropic. The associated elastic constants are: Young's moduli E_{11}^{muscle}, E_{22}^{muscle} corresponding to orthogonal axes 1 and 2 (see Figure 2.1), Poisson's ratio ν_{12}^{muscle}, and the in–plane shear modulus G_{12}^{muscle}.

2. The elastic constants $E_{11}^{muscle}, E_{22}^{muscle}$ and G_{12}^{muscle}, and the Poisson's ratio ν^{muscle} for fish muscle are assigned the following range of values:

   - $15.3 \text{ kPa} \leq E_{11}^{muscle} \leq 62.5 \text{ kPa}$
   - $31.4 \text{ kPa} \leq E_{22}^{muscle} \leq 110 \text{ kPa}$
   - $15.7 \text{ kPa} \leq G_{12}^{muscle} \leq 57.9 \text{ kPa}$
   - $\nu^{muscle} \approx 0.5$

3. The fish muscle has a structural damping factor of $0.10 \leq \beta^{muscle} \leq 0.12$, which is used to calculate the viscous damping matrix [C] in the dynamic equations.

4. The effects of the fish skin are insignificant compared to the effects of the fish muscle.

5. The internal organs in the belly cavity behave like a spongy solid and are characterized by a Young's modulus of $E^{belly} = (0.1) \times E_{11}^{muscle}$, a Poisson's ratio of $\nu^{belly} = 0.49$, a shear modulus of $G^{belly} = (0.1) \times G_{12}^{muscle}$, and a structural damping factor of $\beta^{belly} = \beta^{muscle}$.

6. The fish bone is linear elastic and isotropic. The Young's modulus for the fish bone is one order of magnitude greater than the Young's modulus for fish muscle, i.e., $E^{bone} = 10 \times E_{22}^{muscle}$. Similarly, $G^{bone} = 10 \times G_{12}^{muscle}$. The Poisson's ratio for fish bone is estimated as $\nu^{bone} = 0.3$ [30].

7. The mass density of all tissue is approximately the same, and is in the range $1141\ kg/m^3 \leq \rho \leq 1373\ kg/m^3$.

3.3.2 Assumptions Pertaining to the Fish Geometry

The following assumptions are used to generate the geometry of the finite element model of the salmon.

1. The geometry of the model is based on a 1.48 kilogram, farmed, Chinook salmon that was selected at random. It is assumed that the geometry of this fish is representative of the geometry of all fish (salmon) processed on the Iron Butcher.

2. The fish is divided into three distinct regions, the head, the back, and the belly (see Figure 3.2).

   - The head of the fish is solid bone. The boundary between the head and the body of the fish is defined by the collar–bone.
   - The back region is solid muscle.
   - The belly region is a muscle layer surrounding the spongy belly cavity.

3. The collar–bone is straight but need not be perpendicular to the long axis of the fish, which runs from the nose to the tail.

4. The nose of the fish is cut–off to facilitate meshing of the finite element model.

5. All fins are removed.

3.4 Details of the Model

In this section, the procedure for developing the geometry for the finite element model of the fish from an actual salmon is discussed, and furthermore, the limitations which are imposed by the procedure followed are outlined. The manner in which the material property values for the salmon tissue are assigned to the fish model is also presented.

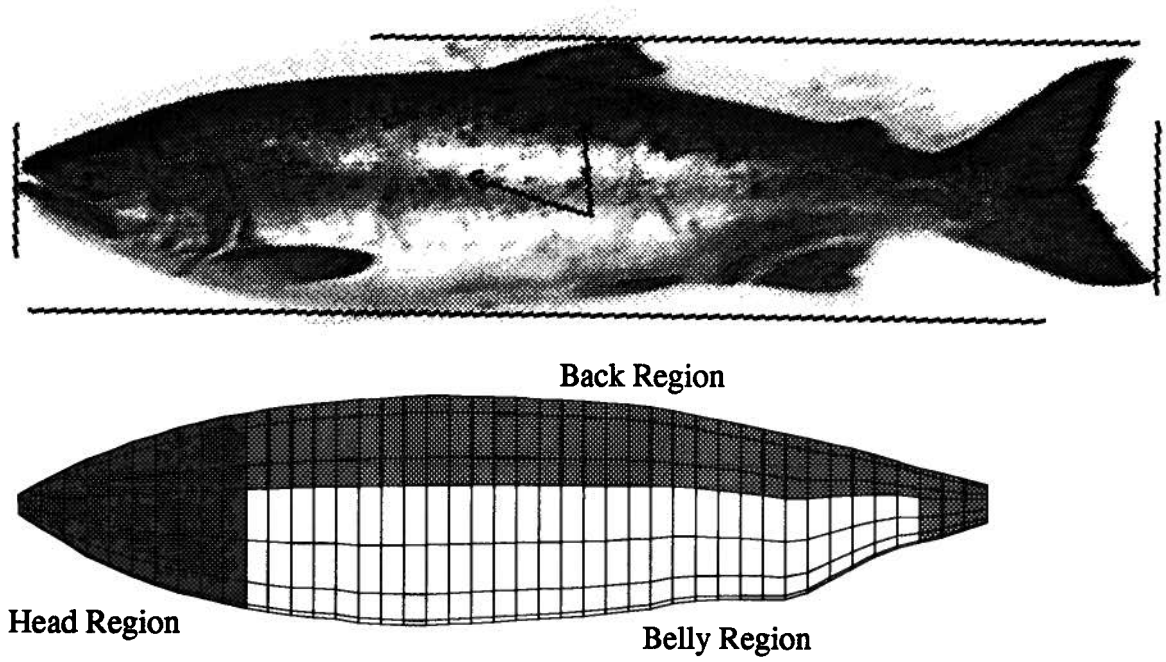

Figure 3.2: Simplification of the fish geometry.

3.4.1 Development of the Fish Geometry

The profile and thickness of the finite element model of fish is based on the geometry of a 1.48 kg, farmed, Chinook salmon made available by B. C. Packers Ltd. Standard image processing techniques are used to extract the required data. The geometry of the cross–section is based on the cross–section shown in Figure 3.1, and not from the cross–section of the actual fish, because the required steak of the fish would lose much of its structural rigidity, so that the observed cross–section would not be accurate.

The entire model is set up in a non–dimensional form that is related to the fish length. By changing only one model variable, the fish length, finite element models for fish of any arbitrary size can be easily created. However, it is noted that although a fish of any size may be easily modeled, the proportional size of various features of the fish is assumed to remain the same from model to model, (i.e., models are "geometrically similar") since all

features are related to the fish length. This method of defining all coordinates of a node in terms of the fish length implies that the problems associated with conveying, indexing and holding are either independent of, or are weakly associated with, the slight variation in fish geometry that occurs from fish to fish. This assumption may be easily relaxed by increasing the number of representative geometric parameters, but is not done so here for the sake of brevity.

The fish model is established such that the profile is defined in the x–y plane (as shown in Figure 3.2), with the length of the fish measured as the x–coordinate, the fish width (the belly to back distance) measured as the y–coordinate and the fish thickness measured as the z–coordinate.

Determining the Fish Profile

The profile of the fish is determined by placing the salmon on a white, horizontal surface. The camera is positioned vertically above the fish and structural lighting is used to reduce the shadows cast by the fish onto the background (see Figure 3.3). The lens aperture

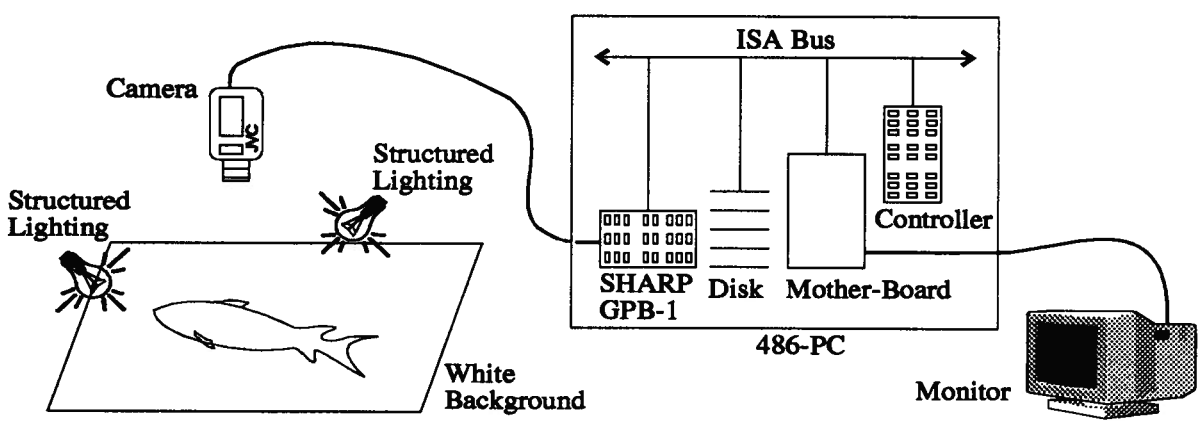

Figure 3.3: The equipment setup for acquiring the image of a salmon.

is set so that the contrast between the background and the fish is enhanced. An image

is captured and sent to a SHARP GPB-1 image processing board residing in an IBM-compatible personal computer based on the 486 processor. Standard image processing techniques are used to analyze the image. First, the image is thresholded to distinguish the fish from the background. Next, the silhouette of the fish is established by identifying the boundary. The major principal axis of this silhouette is calculated along with θ, the angle the major principal axis makes with the horizontal (see Figure 3.4). The fish

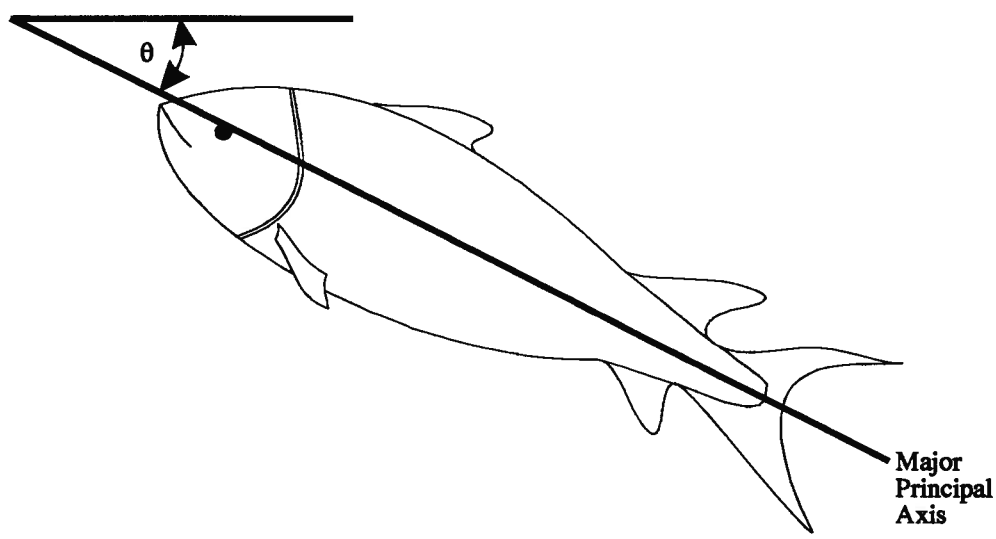

Figure 3.4: Calculation of the major principal axis and θ, the angle of orientation of the principal axis.

silhouette is rotated about its center of area so that the principal axis is horizontal and is divided into n ($n = 100$) equal sections. Finally, the perpendicular distance from the principal axis to the edge (boundary) of the silhouette is determined at each of the n sections along the principal axis (see Figure 3.5). These distances are saved in a file as a fraction of the overall fish length.

The number of points selected on the back profile of the fish equals the number of points selected on the belly profile in order to simplify the eventual meshing of the

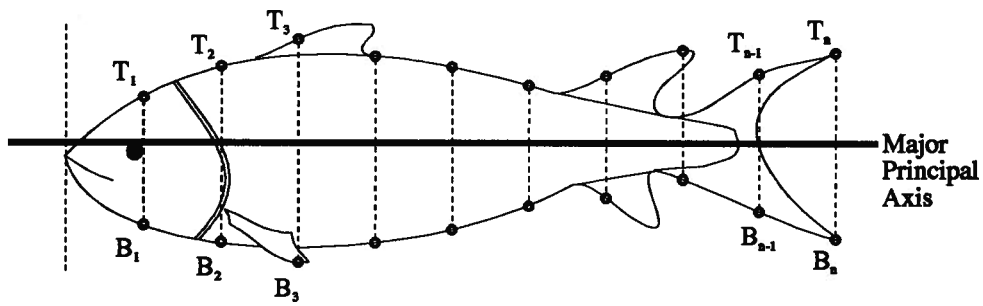

Figure 3.5: Measurement of the perpendicular distance from points on the contour of the fish to the major principal axis.

finite element model. The straight line joining the corresponding points on the back and belly represents a cross–section of the fish (e.g., the line joining points T_1 and B_1, in Figure 3.5, forms a cross–section). The number of cross–sections, and hence the number of points defining the profile, is determined by the results of the mesh refinement study, as described in section 3.5.2.

Determining the Fish Thickness

Using a similar set–up to what is used for determining the profile of the fish, an image of the thickness of the fish is obtained. An image of the fish thickness is acquired and image processing measures the distance, perpendicular to the major principal axis, of points on the edge of the image, and saves this data as a fraction of the overall fish length. This non–dimensional data is a measure of the maximum fish thickness, as a fraction of the fish length, at discrete locations along the fish length. A linear regression is performed on this data to find a fourth order polynomial expression to describe the maximum fish thickness along the fish length. This equation is used directly in the finite element code for the fish model.

Geometry of the Fish Cross–section

The fish cross–section is based on the cross–section shown in Figure 3.1. Nodes are selected so as to:

- adequately define the contour of the outer surface and the belly cavity
- allow the cross–section to be easily meshed with the minimum number of elements
- allow the coordinate axes of the elements to approximate the orientation of the muscle fibres
- ensure the elements which are formed will satisfy the geometric constraints imposed on them by the mathematics used to formulate the element type (e.g., for 3–D brick elements, the recommended range for the angle between adjacent edges is $90° \pm 45°$).

The cross–section of the finite element model uses 30 nodes and 23 elements to define its geometry while observing the above constraints (see Figure 3.6). The coordinates of the nodes on the cross–section are defined as a fraction of the maximum width and maximum thickness at the cross–section. These fractions are kept constant along the length of the fish.

3.4.2 The Collar–bone and Gill Cover

The combination of the physical characteristics of the collar–bone and gill cover enable the indexer to lock into this region of the fish and position the fish for the head cut. These structures are simplified and combined into one structure in the finite element model of the fish. Three–dimensional spar elements (ANSYS LINK8 elements) have one end defined at the junction of the fish head and body, along the side of the fish. The other end of the LINK8 element extends above the side of the fish body. An indexer

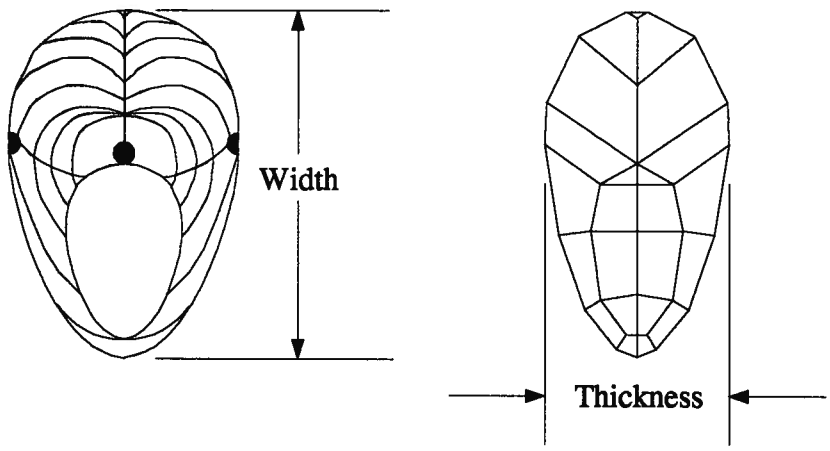

Figure 3.6: The cross–section of the finite element model of the fish (right) is based on the drawing (left).

sliding on the top surface of the fish body will contact the protruding end of the LINK8 elements (i.e., lock into this region of the fish), enabling the indexer to push the fish until it is positioned for the head cut. The distance which the LINK8 elements extend above the side of the fish can be altered to simulate the degree of opening of the gill cover (e.g., a gill cover that is depressed into the head or that is raised above the collar–bone).

3.4.3 Assigning Values for Material Properties

The results given by Petrell et al. [19] provide an estimate of the Young's moduli of a group of muscle fibres in two orthogonal directions (E_{11} and E_{22}). Although a range of values is given for both E_{11} and E_{22}, that work does not provide any data on the pairing of the Young's moduli for each sample. Therefore, in the present work, the maximum value of E_{11} is paired with the maximum value of E_{22}, and the minimum value of E_{11} is paired with the minimum value of E_{22}. A linear distribution of parameter values is assumed within the range of these two extremes.

Having created a criterion to generate pairings of E_{11} and E_{22} of fish muscle in this

manner, and by assuming the value given by Chow and Odell [22] for Poisson's ratio ($\nu = 0.49$), it is possible to estimate a value for the shear modulus of the muscle fibre. Specifically, the shear modulus for fish muscle is defined according to

$$G_{12} = \frac{E_{11} + E_{22}}{2(1+\nu)} \tag{3.2}$$

This results in values for G_{12} which fall within the range reported by Petrell.

The freshness of the fish, which may be categorized by the firmness of the fish muscle, is one parameter which must be varied to determine the role it plays in the effectiveness of a fish processing machine in accurately positioning various salmon for processing. In order to reduce the required number of simulations to a practical level, however, only those material property values corresponding to what can be loosely classified as "soft" and "firm" fish are used in the simulations. A fish categorized as firm is indicative of a fish which is extremely fresh, has been properly stored and handled, and may be in rigor, while a fish categorized as soft has either been improperly handled, improperly stored, or has been previously frozen and thawed. Table 3.1 lists the material properties to be used in modeling soft and firm salmon.

3.5 Verification of the Finite Element Model of a Fish

Verification of the finite element model of a fish is a two–step process. First, the simulation results are validated by comparing them to data which are known to be accurate. Second, the error in the finite element model of the fish is estimated and a suitable mesh density is determined from the results of a mesh refinement study.

3.5.1 Model Validation

Since there are no known results which relate the response of a salmon to external forcing functions applied to it, it is necessary to conduct an experiment to determine such results.

Table 3.1: Material properties for soft and firm fish used in the finite element simulations.

Parameter	Soft Fish	Firm Fish
E_{11}^{muscle} (kPa)	15.3	62.5
E_{22}^{muscle} (kPa)	31.4	110
G_{12}^{muscle} (kPa)	15.7	57.9
ν^{muscle}	0.49	0.49
β^{muscle}	0.10	0.12
E^{belly} (kPa)	1.53	6.25
G^{belly} (kPa)	1.57	5.79
ν^{belly}	0.49	0.49
β^{belly}	0.10	0.12
E^{bone} (kPa)	314	1100
G^{bone} (kPa)	157	579
ν^{bone}	0.30	0.30

In the experiment, a salmon is simply supported on two horizontal rails and is allowed to bend due to gravity. The rails are constructed from a square channel section of aluminum that is rigidly mounted on a wall such that the rails are horizontal. Results of the experiment are recorded using the computer vision system and procedure discussed in section 3.4.1.

Although experimental and simulation data exist for many points along the length of the fish, accurately matching the data points of the experiment with corresponding data points in the simulation is difficult because of the slight geometric differences which exist between the actual fish and the idealized finite element model of the salmon, and because of the large deformations which occur when the fish bends over the rails. However, two points on the fish are easily identifiable and correspond to the same location on the fish in both the experiment and the simulation, and are used in the comparative studies. The first point is at the intersection of the side of the fish which rests on the supports and the tip of the fish nose, and is referred to as the nose. The second point is at the location on

the side of the fish which rests on the supports where the caudal (tail) fin joins the body, and is referred to as the tail. These points are marked in Figure 3.8. Measurements of the nose and tail are made relative to the rail nearest the nose and nearest the tail respectively, and are given in polar coordinates.

Experimental Results

Experiments are conducted for two fish, designated Fish No.1 and Fish No.3. Both fish were stored in a freezer prior to the experiment, but were completely thawed before being placed on the supports. Slowly freezing biological tissue (i.e., taking it under room temperature conditions and placing it into a freezer) will allow ice crystals to form inside the cells, and as the ice crystals grow they may rupture the cell wall. When the tissue is subsequently thawed it is softer and weaker than before it was frozen, since the cells with ruptured walls do not contribute to either the structural rigidity or strength of the tissue. Because the fish used in the experiments have gone through a process of slow freezing, they can be considered as representative of very soft fish.

For each experiment, an image is captured and processed to obtain non–dimensional measurements (see Figure 3.7). The data is dimensionalized using the distance which separates the supports, and is plotted in Figure 3.8. Table 3.2 lists the location of the nose and the tail relative to the supports.

Table 3.2: Experimental results for the bending of Fish No.1 and Fish No.3.

FISH No.1				FISH No.3			
Nose		Tail		Nose		Tail	
r (m)	θ (deg)	r (m)	θ (deg)	r (m)	θ (deg)	r (m)	θ (deg)
0.1288	206.4	0.1462	318.0	0.1525	222.4	0.1429	328.2

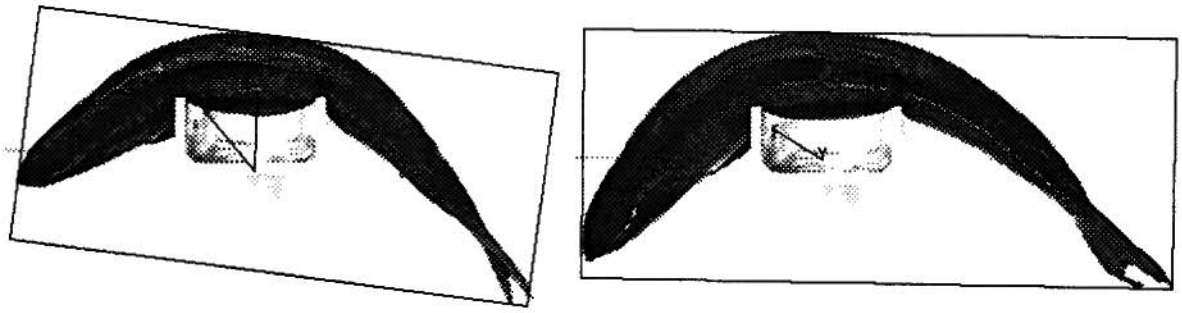

Figure 3.7: The captured image of the bending experiment of Fish No.1 (on the left) and Fish No.3 (on the right).

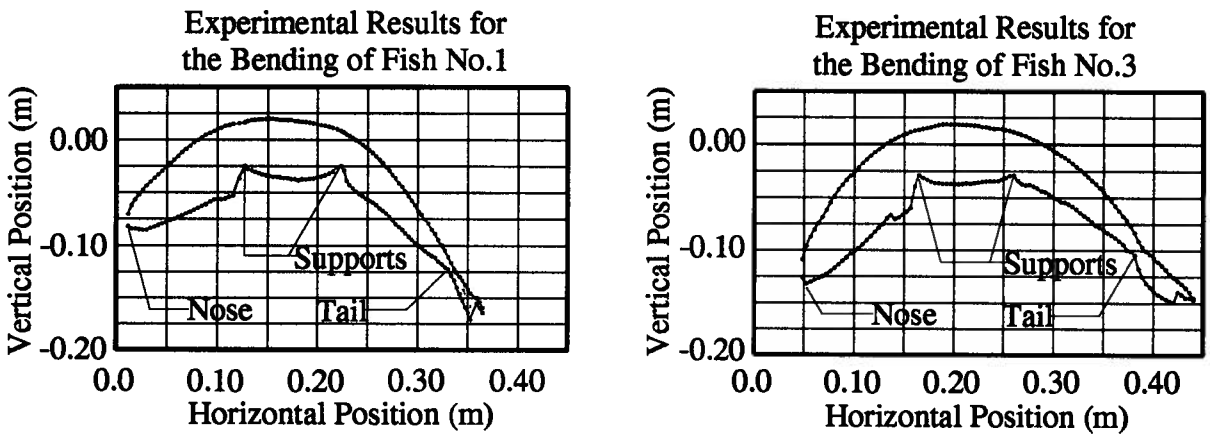

Figure 3.8: Dimensionalized experimental results for the bending experiments.

Simulation Results

Simulations were run to verify that the material properties chosen to represent soft and firm fish lead to general agreement between experiments and simulations which incorporate the finite element model of the fish developed in this chapter. The simulations in this section are static analyses, which investigate the bending of a fish which is simply supported in the same manner as in the experiments.

Figure 3.9 shows the simulation results for the case when the fish material properties

cited by Petrell et al. are used. The results for the case where the values of the fish material properties cited by Petrell et al. are reduced by one order of magnitude, are shown in Figure 3.10. Finally, Figure 3.11 shows the simulation results when the fish material properties are modified to obtain general agreement with the experimental results for the bending of soft fish (Fish No.1 and Fish No.3). The location of the nose and tail relative to the supports for the simulations of the bending of soft fish is given in Table 3.3.

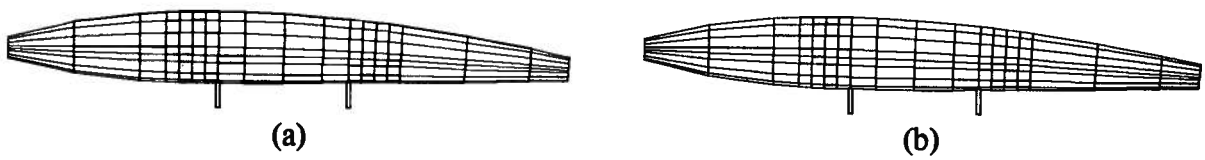

Figure 3.9: Simulation results for the bending of fish using the material property values from Petrell et al.: (a) Material property values from the low end of the range (b) Material property values from the high end of the range.

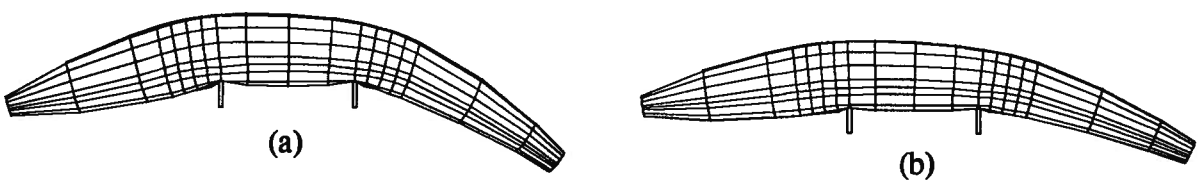

Figure 3.10: Simulation results for the bending of fish using material property values which are an order of magnitude smaller than those cited by Petrell et al.: (a) Material property values from the low end of the range (b) Material property values from the high end of the range.

Table 3.3: Simulation results for the bending of Fish No.1 and Fish No.3.

FISH No.1				FISH No.3			
Nose		Tail		Nose		Tail	
r (m)	θ (deg)	r (m)	θ (deg)	r (m)	θ (deg)	r (m)	θ (deg)
0.1265	189.8	0.1355	313.9	0.1586	215.0	0.1365	314.6

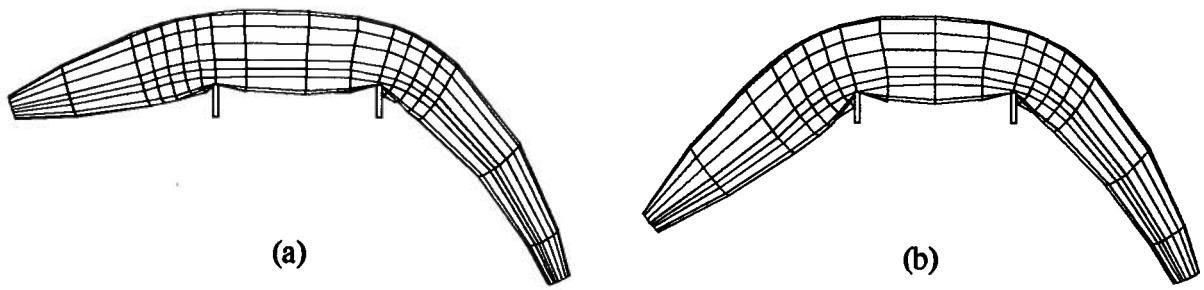

Figure 3.11: Simulation results for the bending of (a) Fish No.1 (b) Fish No.3.

Discussion of Results

When the material properties cited by Petrell et al. are used in the model of the simply supported fish, virtually no bending occurs. However, when these values are reduced by an order of magnitude, the simulation results are representative of a firm fish, such as fish in rigor. These values provide an upper limit on the values of the material properties which can be input to the finite element model of the fish.

The percentage error between the experimental and simulation results for the bending of Fish No.1 and Fish No.3, listed in Table 3.4, is calculated according to the equations

$$error_r = \frac{r_i^{experiment} - r_i^{simulation}}{r_i^{simulation}} \times 100\% \tag{3.3}$$

$$error_\theta = \frac{\theta_i^{experiment} - \theta_i^{simulation}}{\theta_i^{simulation}} \times 100\% \tag{3.4}$$

where r and θ are the polar coordinates and i denotes a measurement for the nose or the tail. The larger error between the experimental and simulation results for Fish No.1 is attributed to the process by which the material properties for soft fish are determined; the material properties are varied until the percentage error between the experimental and simulation results for Fish No.3 are below 5%. As an additional check of the validity of the model of the fish, the same material properties are used in the simulation of Fish

Table 3.4: The percentage error between experimental and simulation results for the bending of Fish No.1 and Fish No.3.

Fish No.1				Fish No.3			
Nose		Tail		Nose		Tail	
$error_r$ (%)	$error_\theta$ (%)	$error_r$ (%)	$error_\theta$ (%)	$error_r$ (%)	$error_\theta$ (%)	$error_r$ (%)	$error_\theta$ (%)
-1.80	-8.04	-7.30	-1.29	3.98	-3.33	-4.53	-4.14

No.1. A general agreement between the experimental and simulation results for Fish No.1 indicates that these material properties are adequate for modeling soft fish using the model developed here.

3.5.2 Mesh Refinement Study

The mesh refinement study provides an estimate of the error in the analysis results. This error is inversely related to the number of degrees of freedom in the model; as the number of degrees of freedom increases, more CPU time is required to run the simulation, so a reduction in the analysis error comes only at the expense of added CPU time. Based on the information provided by the mesh refinement study, a suitable mesh density is selected for further simulation runs.

A simulation of a simply supported fish is carried out using a coarse mesh for the fish. Three additional simulations, each having a successively finer mesh than the previous simulation (see Figure 3.12) are carried out to generate the convergence curve data shown in Table 3.5. The convergence curves of the data are plotted in Figure 3.13, which reveal the characteristic knee. The steeper part of the curve, before the knee, indicates that a small increase in the number of degrees of freedom results in a sizable change in the solution. The shallower section of the curve, after the knee, indicates that a large increase in the number of degrees of freedom results in a small change in the solution;

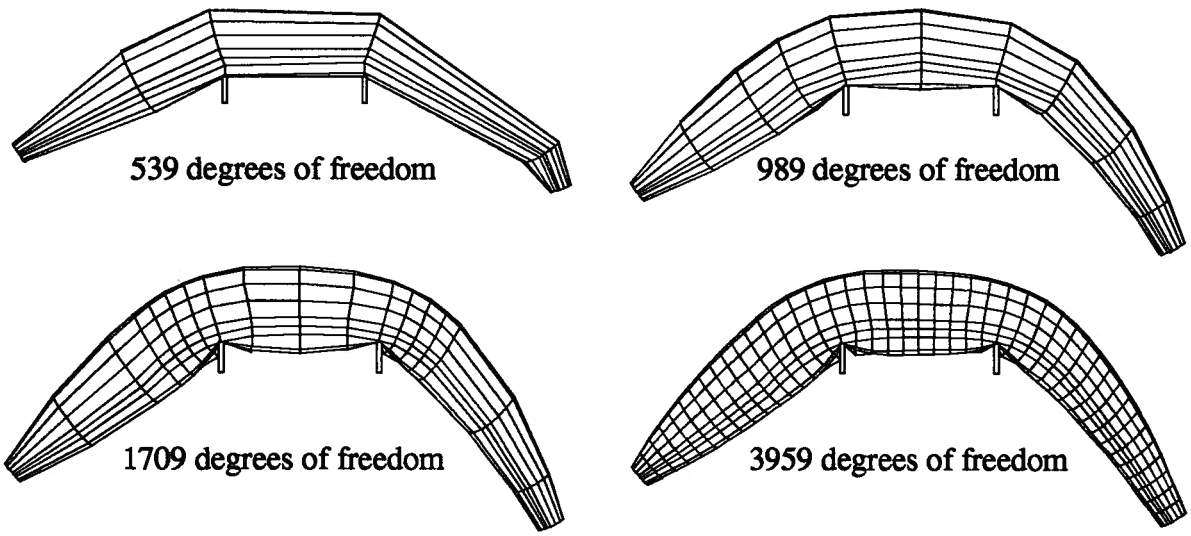

Figure 3.12: Models used in the mesh refinement study.

therefore it buys little added accuracy. If it is accepted that the model with the greatest number of degrees of freedom (3959) yields an approximation that is closer to the exact solution, and if it is accepted that this approximation is a converged solution, then it is evident that the percentage difference between the 3959 degree of freedom approximation and the 1709 degree of freedom approximation is really a measure of the error in the 1709 degree of freedom approximation. The 3959 degree of freedom approximation can be considered converged since the changes in ΔX and ΔZ from the 1709 degree of freedom approximation are less than 5 mm. Thus the error in the 1709 degree of freedom approximation of the fish is approximately 8.0 %. Although the 3959 degree of freedom model has less error associated with it than the 1709 degree of freedom model, the added CPU time prohibits its use in the study of the fish–machine interactions in the subsequent work. For the work which is reported in the following chapters, the model from the 1709 degree of freedom approximation is modified so that the cross–sections are distributed more evenly over the length of the fish.

Table 3.5: Convergence curve data for the model of Fish No.3. CPU times are for simulations on a Sun SPARC station IPX using release 5.0 of ANSYS.

	D. O. F.	CPU Time (s)	ΔX (m)	Change in ΔX (%)	ΔZ (m)	Change in ΔZ (%)
Nose	539	582.510	0.017571		-0.083743	
	989	1925.620	0.027771	57.7	-0.099534	18.9
	1709	2966.860	0.035029	26.4	-0.11165	12.2
	3959	78460.488	0.038004	8.49	-0.11679	4.60
Tail	539	582.510	-0.025580		-0.078353	
	989	1925.620	-0.048834	90.9	-0.10379	32.5
	1709	2966.860	-0.055368	13.4	-0.11162	7.5
	3959	78460.488	-0.058717	6.05	-0.11497	3.00

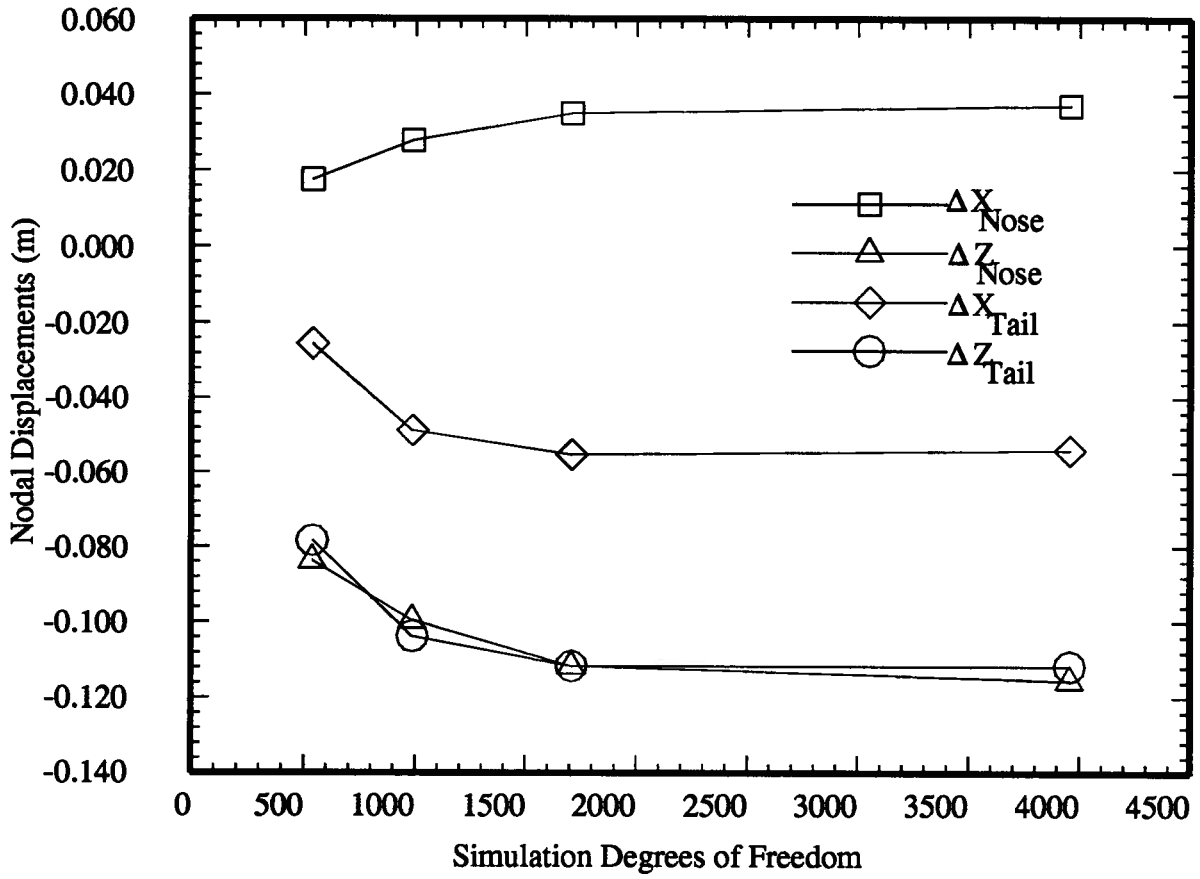

Figure 3.13: Convergence curves for the finite element model of the fish.

Chapter 4

Model of the Processing Machine

In the preceding chapter, a finite element model for a salmon has been established. Next, it is necessary to identify the various components of the Iron Butcher and the interactions between the fish and the machine. Operation of the Iron Butcher is recorded on video and studied in play–back, and particularly in slow–motion, to gain an understanding of the entire processing sequence. Geometric measurements of the Iron Butcher provide additional spatial information. Section 4.1 lists the assumptions which are required to model the machine. The model details are presented for each of the machine components in section 4.2. This section includes a discussion of modeling the contact behaviour between the fish and machine. The verification of the model of both the processing machine and the fish–machine interactions is presented in sections 4.3 – 4.4. The model limitations are discussed in section 4.5.

4.1 Model Assumptions

The following assumptions are made to simplify the process of modeling the Iron Butcher using finite element analysis.

1. All machine components on the Iron Butcher are rigid compared to the fish.

2. The process of moving the fish from the feeding table on to the conveyor is not specifically modeled. Instead, the simulations are initiated with the fish properly oriented (i.e., the back of the fish facing the direction of the conveyor motion and

the fish head on the side of the conveyor edge nearest the cutter) and lying flat on the table of the Iron Butcher. The fish is initially at rest.

3. The table surface is flat, horizontal and continuous (for example, the table does not have recessed slots for housing the chains which convey the fish).

4.2 Model of the Iron Butcher

A complete description of the components and operations of the Iron Butcher is given in section 1.2. From this description and the assumptions of section 4.1, the finite element model of the Iron Butcher is developed. The following sections discuss in detail the method by which the various machine components and the fish–machine interactions are modeled.

4.2.1 The Table Surface

The table on the Iron Butcher measures approximately 1.80 m by 0.70 m and has three, 2.0 cm deep slots to house the chains which are part of the conveying system. The table is modeled by a single, 8–node brick element (refer to the ANSYS manual for a complete discription of the finite elements used) measuring 1.80 m by 0.70 m by 0.02 m, thereby providing a flat, horizontal and continuous surface on which the fish move (see Figure 4.1). The eight nodes which define this element are constrained to have zero displacement in the three coordinate directions. Because this element type has linear shape functions, constraining all the nodes of the element in this manner results in a perfectly rigid surface, regardless of any force or pressure loading applied to it.

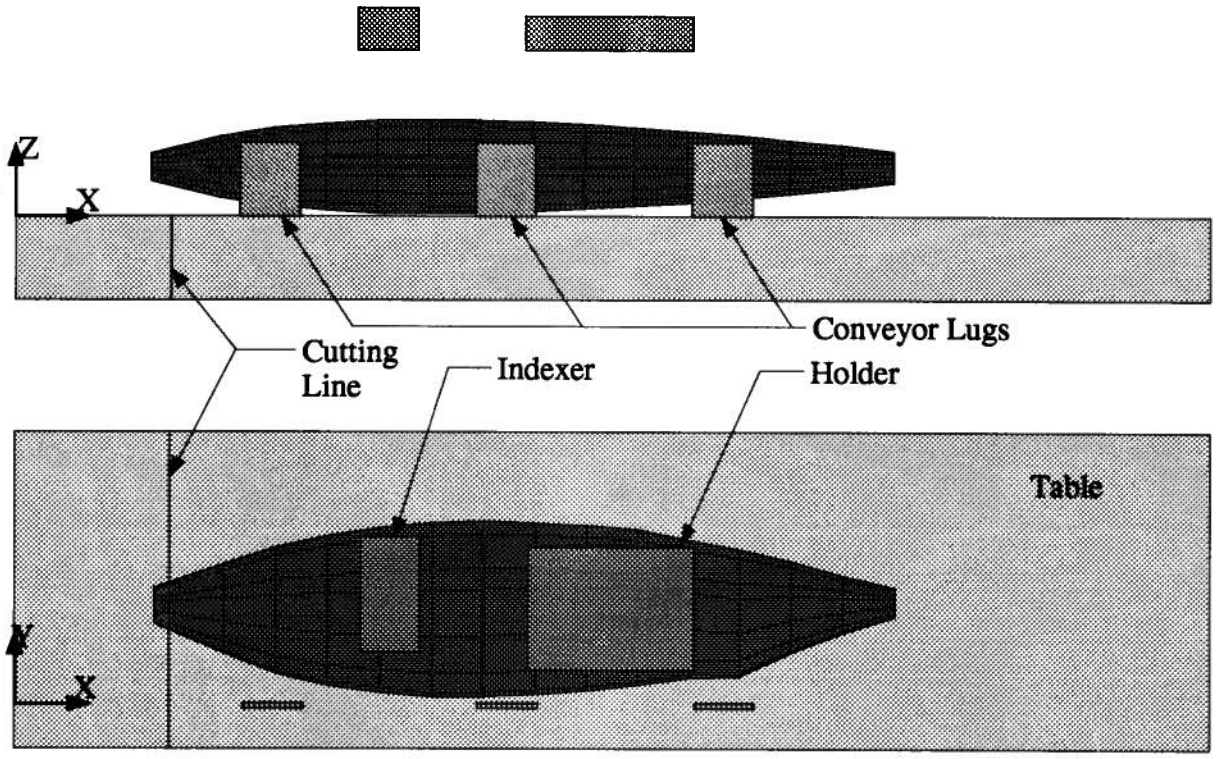

Figure 4.1: Two views showing the finite element model of the Iron Butcher.

4.2.2 The Conveying System

The conveying system on the Iron Butcher consists of the lugs and the chains; the lugs, which are attached to the chains, extend above the table surface and contact the fish, while the chains reside in the recessed slots of the table and transfer the locomotive power from the hydraulic drive to the lugs. The finite element model is simplified by combining the functions of both the chains and lugs into the lugs alone, and modeling them as motion sources. Each lug in the model is defined by one 8–node brick element (ANSYS SOLID45 element). The lugs may be positioned for straight conveying (i.e., the lugs form a straight line which is perpendicular to the conveyor motion) or staggered conveying (i.e., the lugs form a straight line at an angle to the conveyor motion) as shown in Figure 4.2.

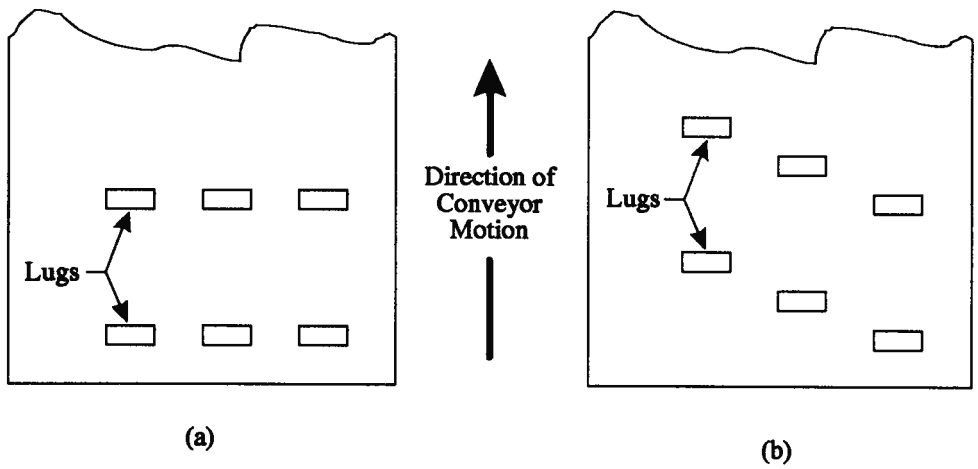

Figure 4.2: Orientation of the lugs for (a) straight conveying (b) staggered conveying.

Motion of the lugs is defined by specifying the displacement profiles of the type shown in Figure 4.3 to the lug nodes which define the surface which touches the fish. As these nodes on the contacting surface have displacement constraints imposed upon them, the surface will be rigid compared to the fish. Only a single set of three lugs, which touches the belly of the fish, is required for the model. The size and position of the lugs are initially taken to approximate those of the Iron Butcher. However, these parameters may be varied in subsequent simulations in order to improve the existing design.

4.2.3 The Holding Mechanism

The function of the holding mechanism is threefold: (1) to prevent fish from being pushed by the indexer before the latter is engaged with the collar–bone of the fish, (2) to prevent the fish from rotating away from the lugs during the indexing process, and (3) to hold the fish during the cutting process. To accomplish this, a pad measuring 10 cm by 7.5 cm by 2.0 cm and located between the two lugs furthest from the cutting line, applies a 8.4 N force to the fish. Although the pad and indexer are dropped onto the fish at the same

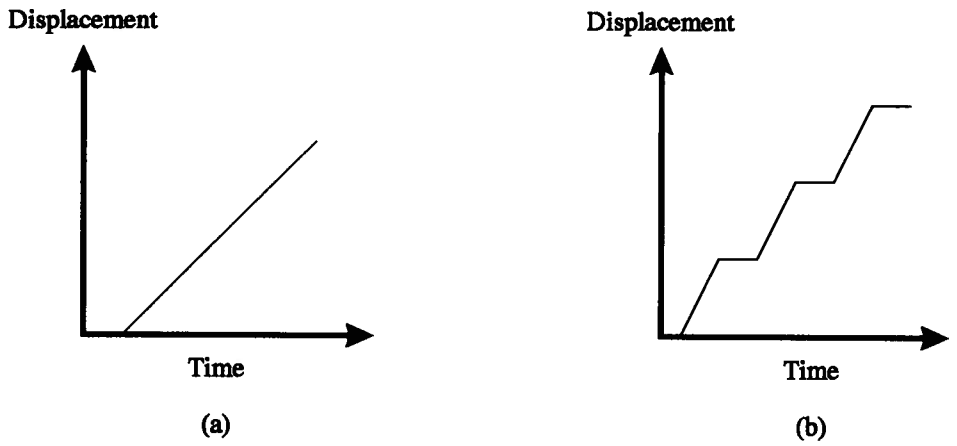

Figure 4.3: Displacement profiles (motion sources) that specify the motion of the lugs for (a) continuous conveying (b) pulsed conveying.

time, the exact instant of contact is determined by the initial distance between the fish and the holder. The pad is modeled by a single 8–node brick element (ANSYS SOLID45 element). The pad moves in the same direction and at the same rate as the conveyor, and in addition there is the vertical motion which causes contact between the fish and the pad. The displacement profiles defining the motion of the pad are applied to the nodes which form the contacting surface. The Young's modulus of the pad is two orders of magnitude larger than that of the fish muscle, so the pad appears to be rigid with respect to the fish. The location, size and magnitude of the holding force, as well as the number of holders, may be varied to establish the optimum method of holding the fish.

4.2.4 The Indexing System

The indexing system on the Iron Butcher is expected to properly align the collar–bone of the fish with the cutter. The system consists of the foot, which comes into contact with the fish, and associated mechanisms to move the foot, as necessary for the conveying process. For simplicity, the functions of these associated mechanisms are combined with

the finite element model of the foot. The foot is modeled by a single 8–node brick element (ANSYS SOLID45 element) with approximate dimensions of 7.5 cm by 3.6 cm by 2.5 cm and a mass of 0.85 kg. The size of the model of the indexer is slightly larger than the size of the actual indexer so that contact between the fish and indexer can be modeled while adding as few degrees of freedom as possible. The two perpendicular components of motion (i.e., the conveying motion and the indexing motion) of the foot are achieved by defining the displacement profiles of these motions at the nodes which form the two surfaces which come into contact with the fish. The vertical motion of the foot is unconstrained after the foot drops onto the fish, so that the weight of the foot alone will determine the vertical force between the foot and the fish. The Young's modulus of the indexer foot is chosen to be two orders of magnitude larger than that of the fish muscle, thereby approximating the relative rigidity of the foot.

4.2.5 The Fish–Machine Interface

In finite element analysis, a family of elements, known as contact elements, are used to represent contact and sliding between two surfaces or between nodes. In the case of contact between the fish and the Iron Butcher, the exact location of contact is not known beforehand, so it is not practical to define in the contact model all possibilities of node–to–node contact which may occur. Instead, the surfaces which may come into contact are specified, and a suitable contact element is defined to "link" these surfaces and model contact between these surfaces. The CONTAC49 element is selected as it represents contact and sliding between two surfaces in three dimensions.

To model contact between the fish and the table surface, the nodes on the side of the fish which may come in contact with the table are selected to define the first contact surface. Next, the nodes which represent the upper surface of the table are selected to define the second contact surface. CONTAC49 elements are then defined to "link" these

two surfaces, permitting contact and sliding to be modeled. The procedure is repeated to model fish–lug, fish–holder and fish–indexer contacts. Unless otherwise specified, $\mu = 0.1$ is used as the coefficient of friction between all surfaces.

If a finite element model can be separated into a linear part and a nonlinear part, a technique known as "substructuring" can sometimes be used to greatly reduce the CPU time required to run a simulation. Substructuring can be used only if the nonlinear solution options, such as plasticity, creep, swelling, stress stiffening and large deflection, are not used. In this instance, the elements which represent the fish and the components of the Iron Butcher (the table, lugs, holder, indexer and cutter) are linear, while the contact elements are nonlinear. Because the linear and nonlinear portions of the model can be separated, the linear elements are submodeled using the MATRIX50 element while the CONTAC49 elements are defined between the appropriate surfaces of the fish and machine components. In this work, the static analyses of section 3.5 do not use substructuring, as the large deflection option is used. However, in the simulations in Chapters 4 – 6, substructuring is used since the large deflection option is not used.

4.3 Verification of the Conveying Model

CONTAC49 elements are used to model contact and sliding between the fish and the machine components. When friction has to be introduced, CONTAC49 elements are capable of modeling either rigid friction or elastic friction, which are defined by the characteristic curves in Figure 4.4. Although rigid friction closely approximates the friction in the real world, elastic friction has the advantage of allowing the solution to converge more easily than if the rigid friction option is used. However, if K_s, the parameter for the elastic friction option, is not properly evaluated, large errors can be introduced into the simulation results. For the case of an object with an initial velocity,

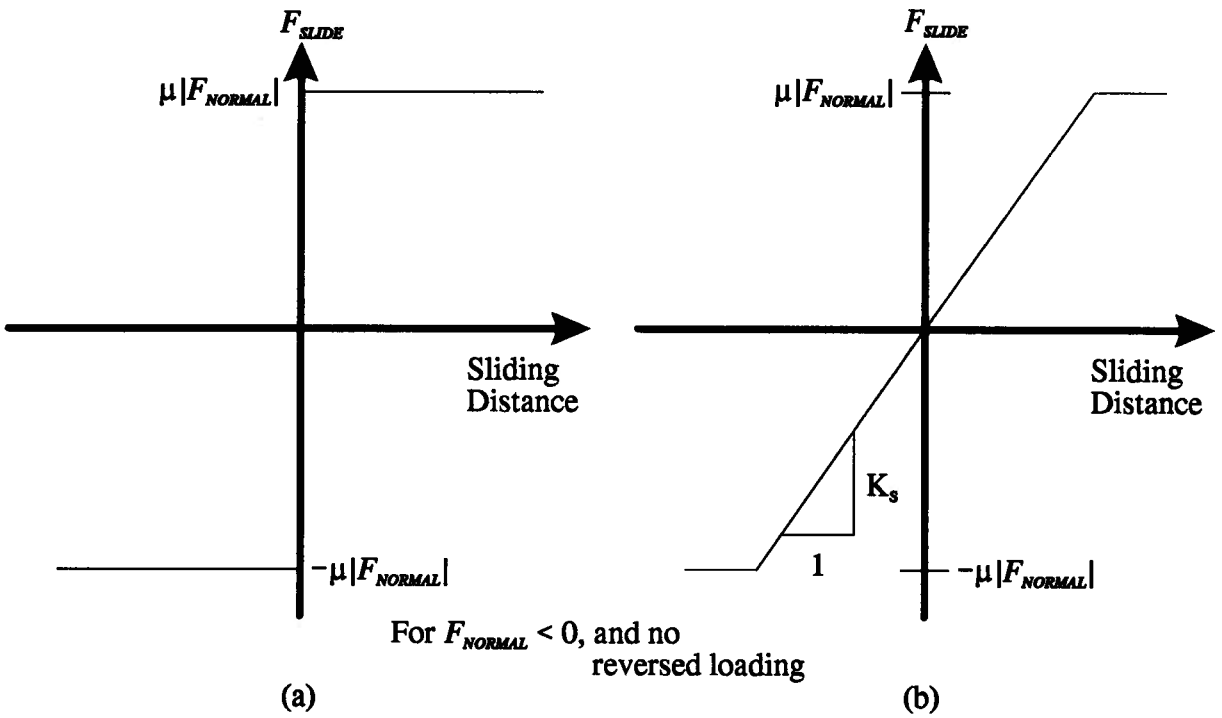

Figure 4.4: The force–deflection relationships for a CONTACT49 element specified with (a) rigid friction (b) elastic friction.

sliding on a flat surface with a coefficient of friction μ, the object will exhibit oscillations about its steady–state resting position if the elastic friction option is used. The amplitude of the oscillation is inversely related to the value of the elastic friction parameter, so care has to be exercised in choosing this value.

Verification is required to ensure that the assumptions for the Iron Butcher are valid, that the finite element model is properly defined, and that the use of elastic friction does not adversely affect the simulation results.

4.3.1 Order of Magnitude Calculation

Consider an object which is characterized by a mass m, damping constant c and stiffness k, which is free to slide over a flat, horizontal surface. A coefficient of friction, μ, exists

between the surface and the object. Motion of the object over the surface can be described by equation (4.1), where $\ddot{x}$, $\dot{x}$, and x are the acceleration, speed and position of the object, respectively, and f is the sum of the applied forces.

$$m\,\ddot{x} + c\,\dot{x} + kx = -f \tag{4.1}$$

If the only forces acting on the object are gravity and friction, then

$$c\,\dot{x} = kx = 0 \tag{4.2}$$

and equation (4.1) reduces to

$$\ddot{x} = -\mu g \tag{4.3}$$

By successively integrating equation (4.3) we get

$$\dot{x} = -\mu g t + c_1 \tag{4.4}$$

and

$$x = \frac{-\mu g t^2}{2} + c_1 t + c_2 \tag{4.5}$$

Equations (4.4) and (4.5) require initial conditions to solve for c_1 and c_2. For example, if at time $t = 0$ seconds the object is moving at 0.5 m/s (the conveying speed on the Iron Butcher), and the corresponding instantaneous location of the object is taken as the reference point, then

$$\dot{x}\,(0) = 0.5\ m/s \qquad x(0) = 0.0\ m \tag{4.6}$$

The initial conditions given by equation (4.6) are used to solve for the constants in equation (4.4) and (4.5). This results in

$$\dot{x} = -\mu g t + 0.5 \tag{4.7}$$

$$x = \frac{-\mu g t^2}{2} + 0.5t \tag{4.8}$$

By solving equation (4.7) for the time at which the object has zero speed, we get

$$t_1 = \frac{0.5}{\mu g} \; seconds \tag{4.9}$$

By substituting t_1 into equation (4.8) we can determine the distance the object travels before coming to a stop, as

$$x(t_1) = \frac{0.125}{\mu g} \tag{4.10}$$

Equation (4.10) approximates the distance the center of mass of a fish having an initial velocity of 0.5 m/s will travel while sliding on the table of the Iron Butcher. With a coefficient of friction $\mu = 0.3$, this distance is computed to be $x(t_1) = 0.0425$ meters.

4.3.2 Simulation Results

Nonlinear, transient, dynamic simulations are run to verify the conveying model for firm and soft fish. In these simulations, a fish starts from rest on the table of the Iron Butcher with the lugs located just 4 mm away from the fish belly. The lugs move 0.10 m at the rate of 0.5 m/s, pushing and accelerating the fish. The lugs then instantaneously stop moving, freeing the fish to slide on the table surface. Figure 4.5 shows the location of the fish mass center as a function of time. The mass center overshoots the steady–state resting position and oscillates about this point before coming to rest. The actual overshoot and the steady–state resting position of the fish mass center for the simulations of conveying firm and soft fish are listed in Table 4.1. Overshoot is defined as the difference between the maximum position and the final resting position of the mass center, while the steady–state position is the difference in the mass center location between the final resting position and the position when the lugs stopped moving (time = 1.2 seconds).

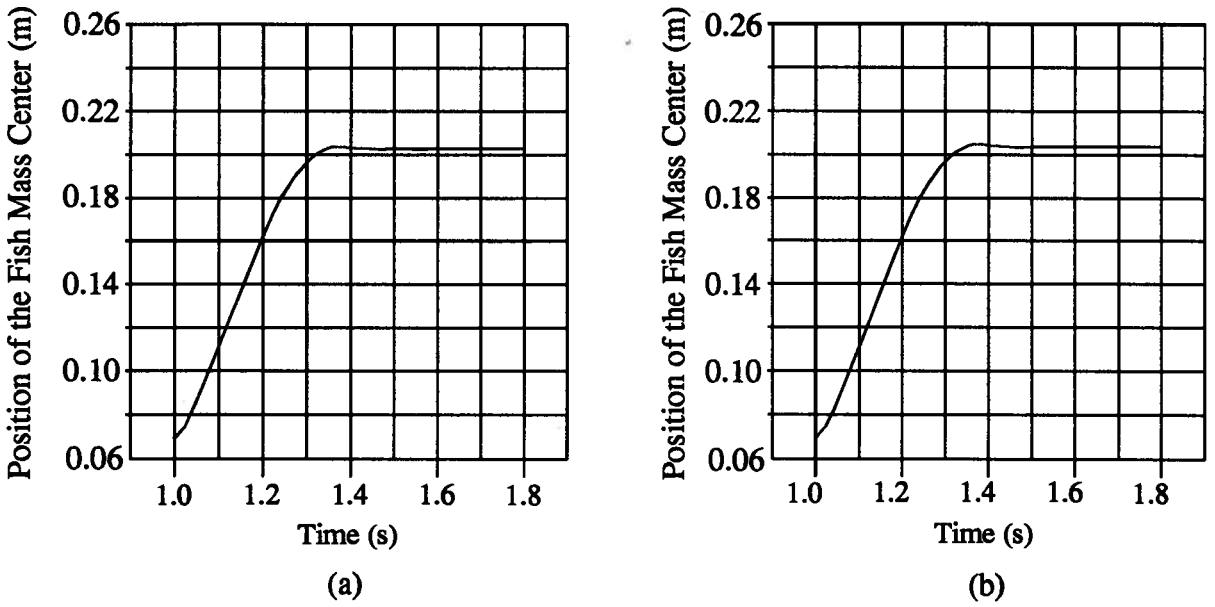

Figure 4.5: Position of the fish mass center for the simulation of the conveying of (a) firm fish (b) soft fish.

Table 4.1: Overshoot and steady–state resting position for the simulations of conveying firm and soft fish.

Simulation	Overshoot (m)	Steady–state position (m)
Firm fish	0.000860	0.041990
Soft fish	0.001033	0.042155

4.3.3 Discussion of Results

The simulation results are in close agreement with the order of magnitude calculations, with a 3.1% error for the conveying of firm fish and a 0.81% error for the conveying of soft fish. Because the order of magnitude calculation is, at best, only an estimate of where the fish should come to rest, these error values cannot be interpreted as the actual error in the conveying model. These errors only indicate that the simulation results are intuitively correct.

The simulation results indicate that the use of elastic friction with the proper values

for the elastic friction parameter, does not produce large errors. The maximum overshoot observed in the simulation is 0.001 m, which is acceptable considering the scale of the fish and Iron Butcher, and the motions involved.

The close agreement between the order of magnitude calculations and the simulation results indicates that the assumptions pertaining to the conveying system of the Iron Butcher are valid, the conveying model is properly defined, and the values of the elastic friction parameters are correctly chosen.

4.4 Verification of the Indexing and Holding Model

Contact of the fish, with both the indexer and the holder is modeled using CONTAC49 elements. As was explained in section 4.3, the value of the elastic friction parameter K_s has to be carefully selected to ensure that the error in the simulation resulting from the use of the elastic friction model is acceptable. Verification of the indexing and holding model is also required in order to determine if the assumptions pertaining to the holding and indexing system of the Iron Butcher are valid, and if the finite element model is properly defined.

4.4.1 Operation of the Iron Butcher

From the spatial measurements of the Iron Butcher and by observing recorded video–tape images of the indexing and holding process, the motion and timing of the indexer and holder are determined. This information forms the basis upon which the finite element model of indexing and holding is evaluated.

The initial location of the holder and indexer are described in sections 4.2.3 and 4.2.4 respectively. After the lugs, along with the indexer and the holder move down the table through 0.35 m, both the indexer and the holder are released and dropped onto the fish

body. At this instant, the indexer also starts to move laterally to position the fish for the head cut. The lugs, the indexer and the holder move through 0.30 m down the table as the indexer moves through 0.09 m laterally. When the indexer completes its lateral motion, it is lifted off the fish so that the head cut can be made. Now the fish should be positioned with its collar–bone on the cutting line and the belly resting firmly against the lugs. This entire process takes approximately 1.3 seconds. Figure 4.6 is a schematic representation showing the motion of the lugs, indexer and holder.

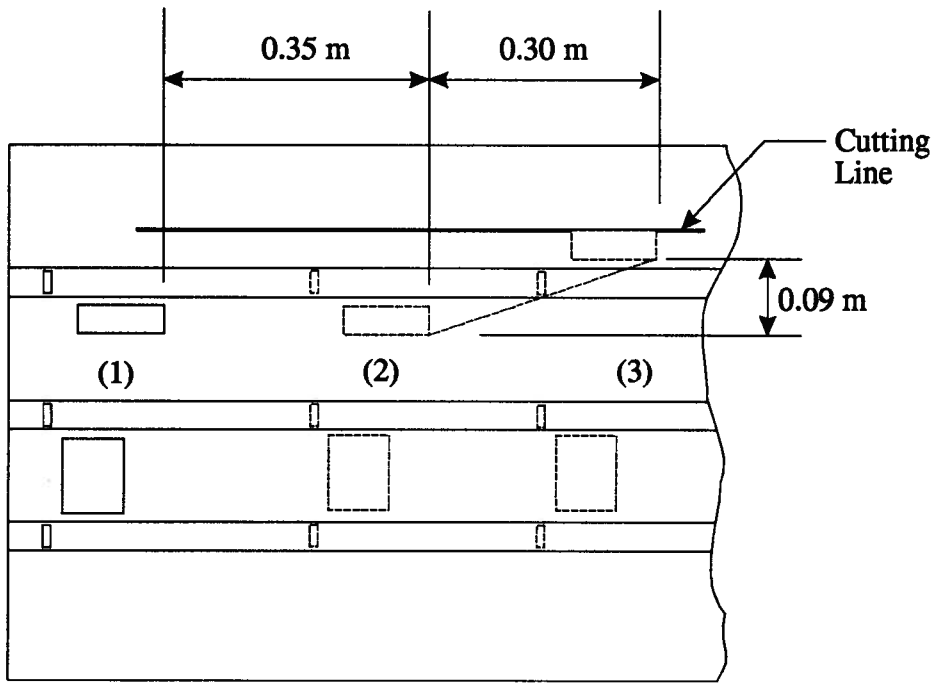

Figure 4.6: Schematic representation of the Iron Butcher showing the location and motion of the lugs, indexer and holder during the indexing and holding process. (1) Initial position (2) Position when the indexer and holder drop onto the fish (3) Final position when indexing is completed.

4.4.2 Simulation Results

A nonlinear, transient, dynamic analysis of the indexing and holding process is carried out for both a small and a large salmon. The small salmon has a length and mass of

0.442 m and 1.48 kg respectively, while the large salmon has a length of 0.645 m and a mass of 4.59 kg. The coefficient of friction, μ, between all surfaces is taken as 0.10. The fish are initially located on the Iron Butcher such that the collar–bone is in–line with the lug nearest the cutter. To reduce the solution CPU time, the lugs, indexer and holder are made to move just 0.05 m before the indexer and holder drop onto the fish, and furthermore, the indexer is not lifted off the salmon after indexing is complete. These are the only differences between the operation of the actual Iron Butcher and the simulation.

Figures 4.7 and 4.8 show the simulation results, for the small and large salmon respectively, at discrete points in time. Time = 0.01 s, Time = 0.11 s and Time = 0.71 s correspond to stages (1), (2) and (3), respectively, in Figure 4.6. In both simulations the fish deforms from the weight of the indexer and holder when contact occurs. In addition, the location of contact between the fish and these components changes; the indexer slides over the fish toward the gill cover before engaging with the gill cover, and the location of contact between the fish and holder changes after the indexer engages with the gill cover and positions the fish. In both cases the fish are ultimately positioned with the collar–bone at the cutting line.

4.4.3 Discussion of Results

Comparison of the simulation results with the actual operation of the Iron Butcher yields favorable results. Motion of the holder and indexer mirror those of the actual Iron Butcher. Contact and sliding motion between the fish, and both the holder and the indexer, is realistic. The indexer also correctly engages with the gill cover while indexing and the fish is correctly positioned for the head cut. These results indicate that the elastic friction coefficient, K_s, is properly chosen, the assumptions pertaining to the holding and indexing system are valid, and the finite element model is properly defined.

4.5 Limitations of the Model

Limitations on the finite element model of fish processing can be attributed to the conflict between the opposing goals of accuracy and computing time. Although high solution accuracy is desired, it comes only at the cost of excessive computing time.

The conflicting goals of simulation accuracy versus computational load must somehow be balanced. This balance is achieved in section 3.5.2 when the mesh density for the finite element model of the fish is established. However, the trade–off between accuracy and computing time imposes limitations on the development of the model of the processing machine.

The chosen mesh density for the fish is characterized by an x–direction spacing of the cross–sections which is 6% of the fish length. As it is the case that, all other things being equal, the larger the number of finite elements in a model the greater the computing time required to obtain a solution, every effort is made to reduce the number of elements used. Thus, given the mesh density of the fish model, the least computationally expensive way to model contact between the fish and the machine components requires the machine components to have an x–direction length greater than 6% of the fish length. This requirement specifies chain lugs and an indexer to have x–direction dimensions which are larger than those of the actual machine (see Table 4.2).

Table 4.2: A comparison of the actual size of the machine components and the corresponding component size in the finite element models.

Component	Actual size (m)	Finite element size (m)	
		Small Fish Model	Large Fish Model
lug	0.025 x 0.0032 x 0.045	0.036 x 0.0032 x 0.045	0.053 x 0.0032 x 0.070
indexer	0.025 x 0.075 x 0.025	0.036 x 0.075 x 0.025	0.053 x 0.075 x 0.025
holder	0.10 x 0.075 x 0.02	0.10 x 0.075 x 0.02	0.10 x 0.075 x 0.02

Furthermore, for contact to occur, a node on the fish (which only exists at a cross–section) must lie within the bounds of a machine component. If nodes on adjacent cross–sections come in contact with the same component simultaneously, the modeled contact will closely approximate the actual contact on the machine. But if nodes on only one cross–section touches a component, then the contact occurs at only one point, so the results do not closely approximate the actual contact.

Although this technique of modeling contact may seem to have a large detrimental effect on the simulation results, it in fact does not. Actual contact can be closely approximated by summing the contact forces and applying them at a single point. The simulation error which results due to contacts can be attributed to the difference between the location of the resulting contact force and the location of where the resulting contact force should be applied.

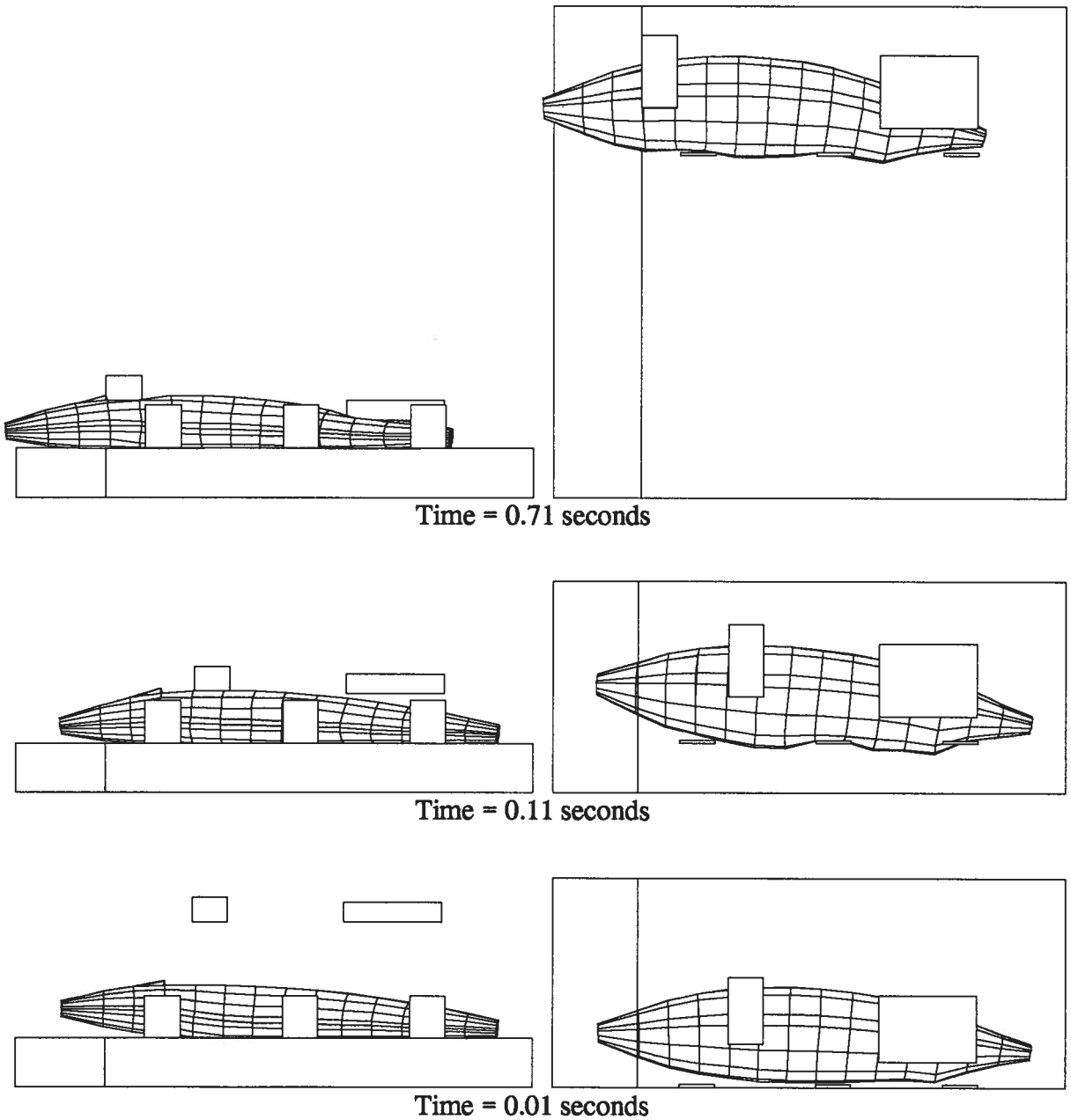

Figure 4.7: Simulation results for the validation of indexing and holding processes of small fish.

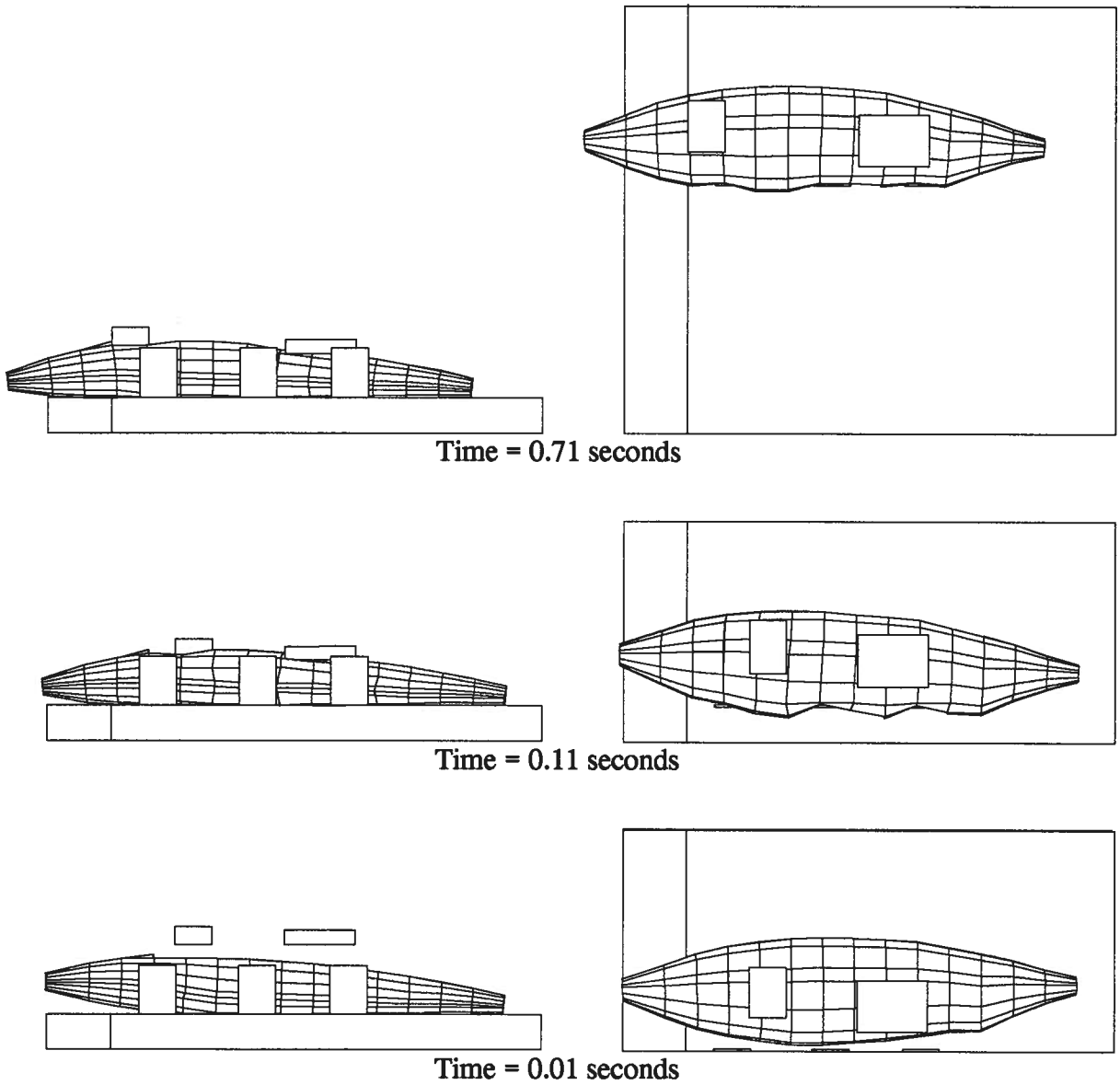

Figure 4.8: Simulation results for the validation of indexing and holding processes of large fish.

Chapter 5

Finite Element Simulation of Conveying

The development and validation of the finite element models of the fish and the processing machine were presented in chapters 3 and 4. With these models it is possible to investigate the operation of the Iron Butcher in its present configuration, or in some modified configuration, without having to physically modify the machine. Since the current Iron Butcher cannot automatically compensate for errors in the position and orientation of the fish introduced during conveying, the fish must be reliably transported from one stage of processing to the next in such a manner that the error in its final position and orientation is minimal.

The conveying process of the Iron Butcher in it present configuration is investigated in section 5.1, to determine if the machine can accurately and reliably convey fish of different sizes and firmness. Section 5.2 then presents the investigation of conveying when the configuration of the Iron Butcher is altered. Recommendations for the design of the conveying system are listed in section 5.3.

5.1 Conventional Conveying

In this section, the performance of the conventional Iron Butcher, during the conveying process, is investigated. The simulations will address the question of whether or not the Iron Butcher, in its present configuration, can reliably convey fish of different sizes and muscle firmness.

Nonlinear, transient, dynamic analyses are performed for four types of fish: small fish

with soft muscle, small fish with firm muscle, large fish with soft muscle and large fish with firm muscle. In each case, both the fish and the chain lugs are initially at rest. The lugs move through 1.0 m in 2.0 s at a constant speed of 0.5 m/s. The coefficient of friction at both the fish–table interface and the fish–lug interface is set at 0.10.

The simulation results are shown in Figures 5.1 – 5.4. In each case, a similar pattern of motion is observed, which is characterized by an initial transient phase followed by a steady–state phase. Initially, the fish comes in contact with all three lugs. Then the contact between the fish and the left–most lug is lost as the fish rotates clockwise. At some point, the fish reverses its direction of rotation so that the gap between the fish and the left–most lug is closed. Fish with soft muscle stop this "rocking" motion when the fish touches the left–most lug, so that from this point on the relative position of the fish with respect to the lugs remains fixed. The "rocking"continues for the firm fish until the contact between the fish and the right–most lug is broken and then re–established. The duration of the transient (rocking) period varies from approximately 0.6 s for the conveying of small, soft fish to 1.60 s for the conveying of large, firm fish.

These results indicate that the Iron Butcher, in its present configuration, can reliably convey fish of different sizes and muscle firmness. Furthermore, the fish should be conveyed through 0.8 m before the next stage of processing is started so that the transient "rocking" motion can be sufficiently settled.

5.2 Modified Iron Butcher Conveying

Prior to cutting the fish, the fish and cutter must be properly aligned. To accomplish this, either the fish can be manipulated, the cutter can be manipulated, or both the fish and the cutter can be repositioned so that they are properly aligned for the head cut. In the current Iron Butcher design, the fish is moved to the cutter. However, because

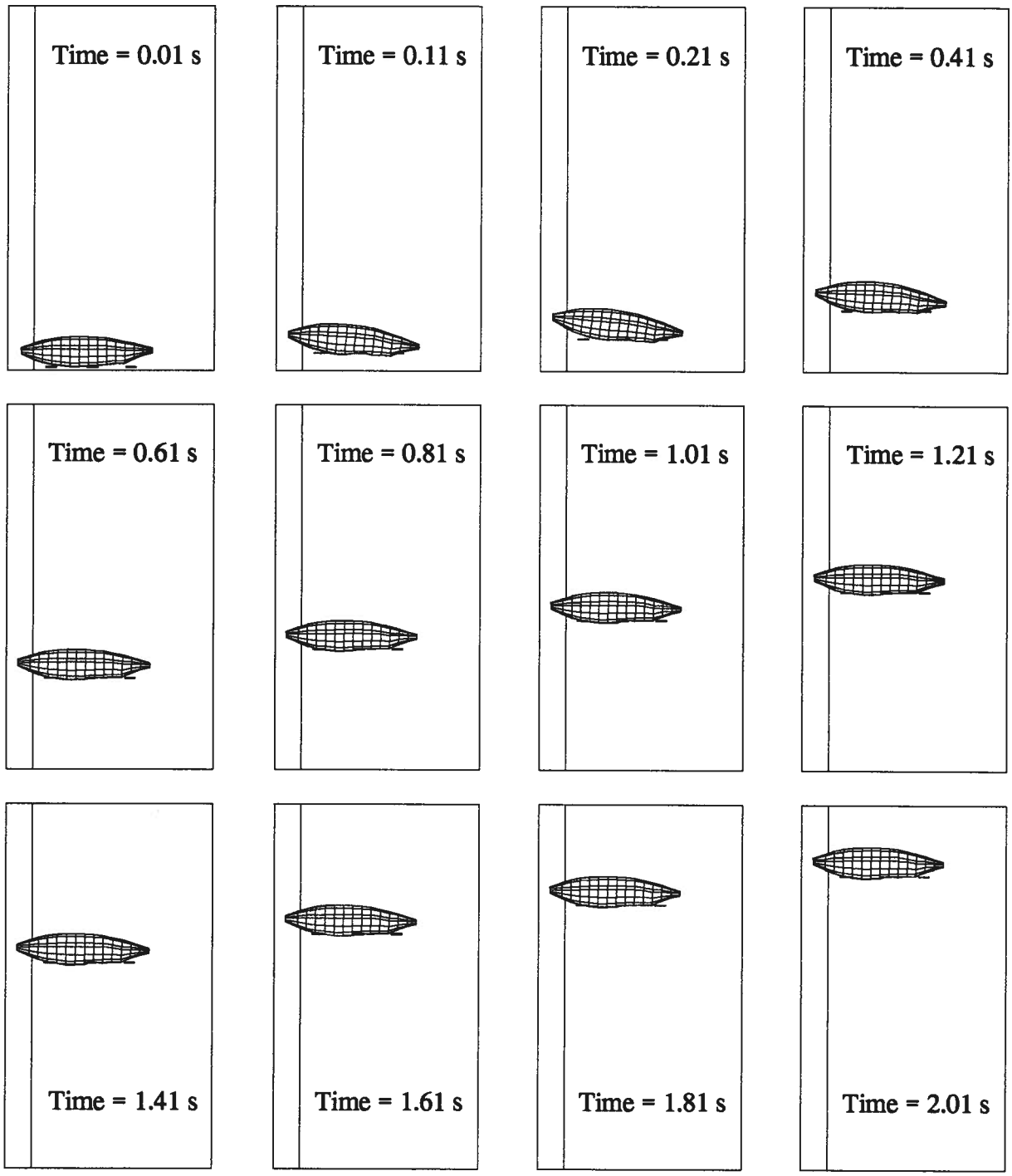

Figure 5.1: Constant speed conveying of small, soft fish using the existing configuration of the Iron Butcher. The transient "rocking" motion is sufficiently settled at Time = 0.61 s.

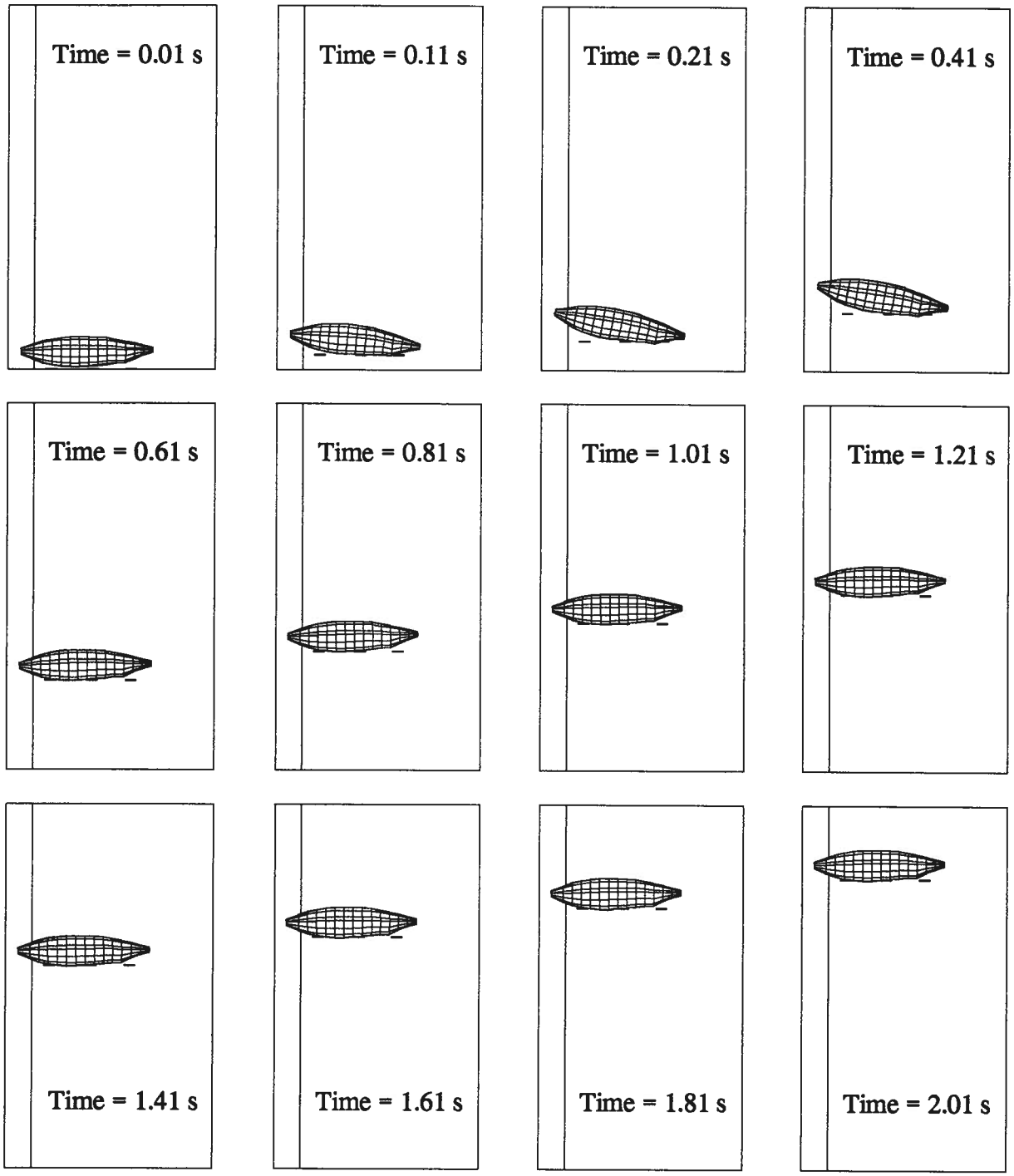

Figure 5.2: Constant speed conveying of small, firm fish using the existing configuration of the Iron Butcher. The transient "rocking" motion is sufficiently settled at Time = 1.01 s.

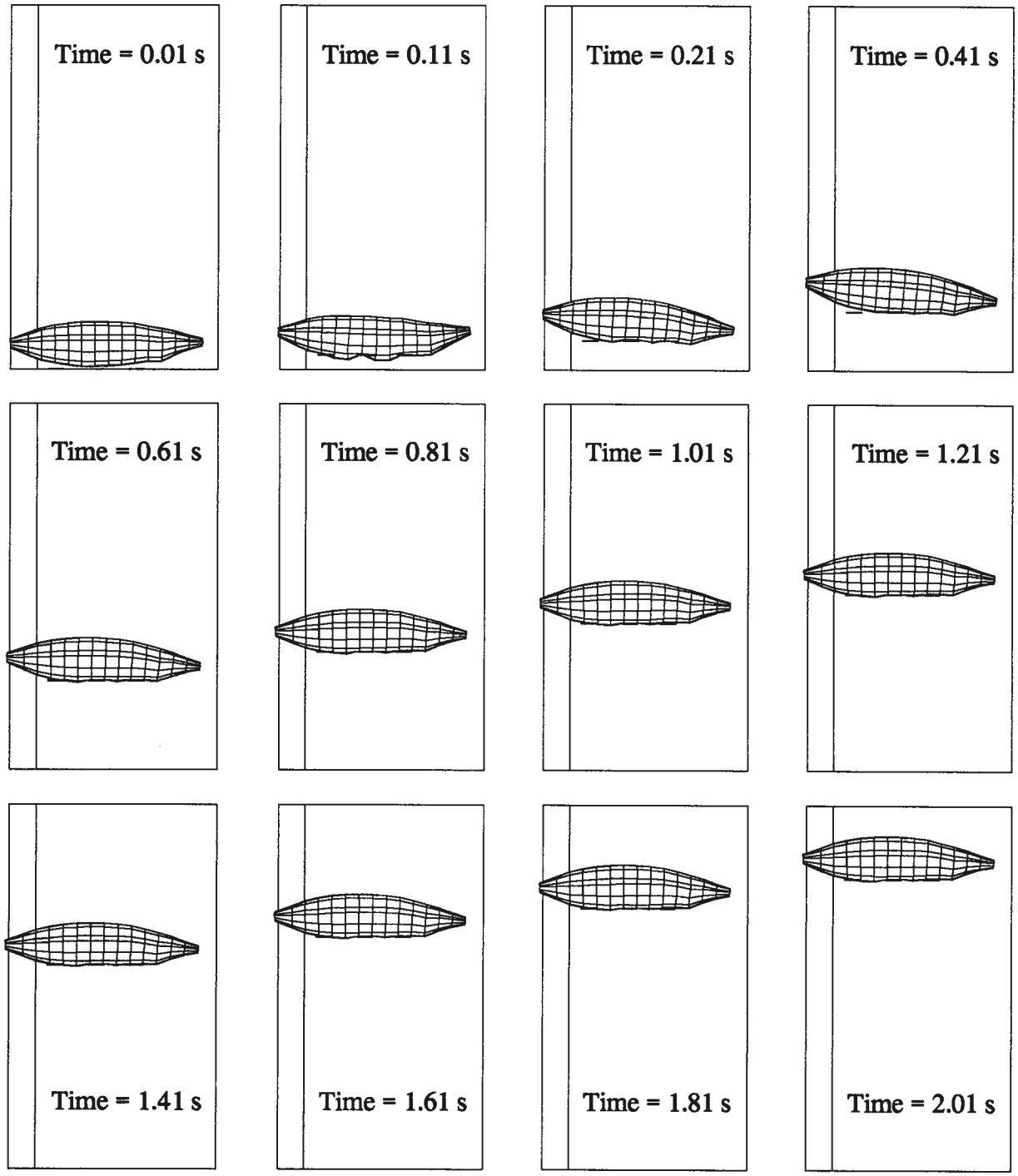

Figure 5.3: Constant speed conveying of large, soft fish using the existing configuration of the Iron Butcher. The transient "rocking" motion is sufficiently settled at Time = 0.81 s.

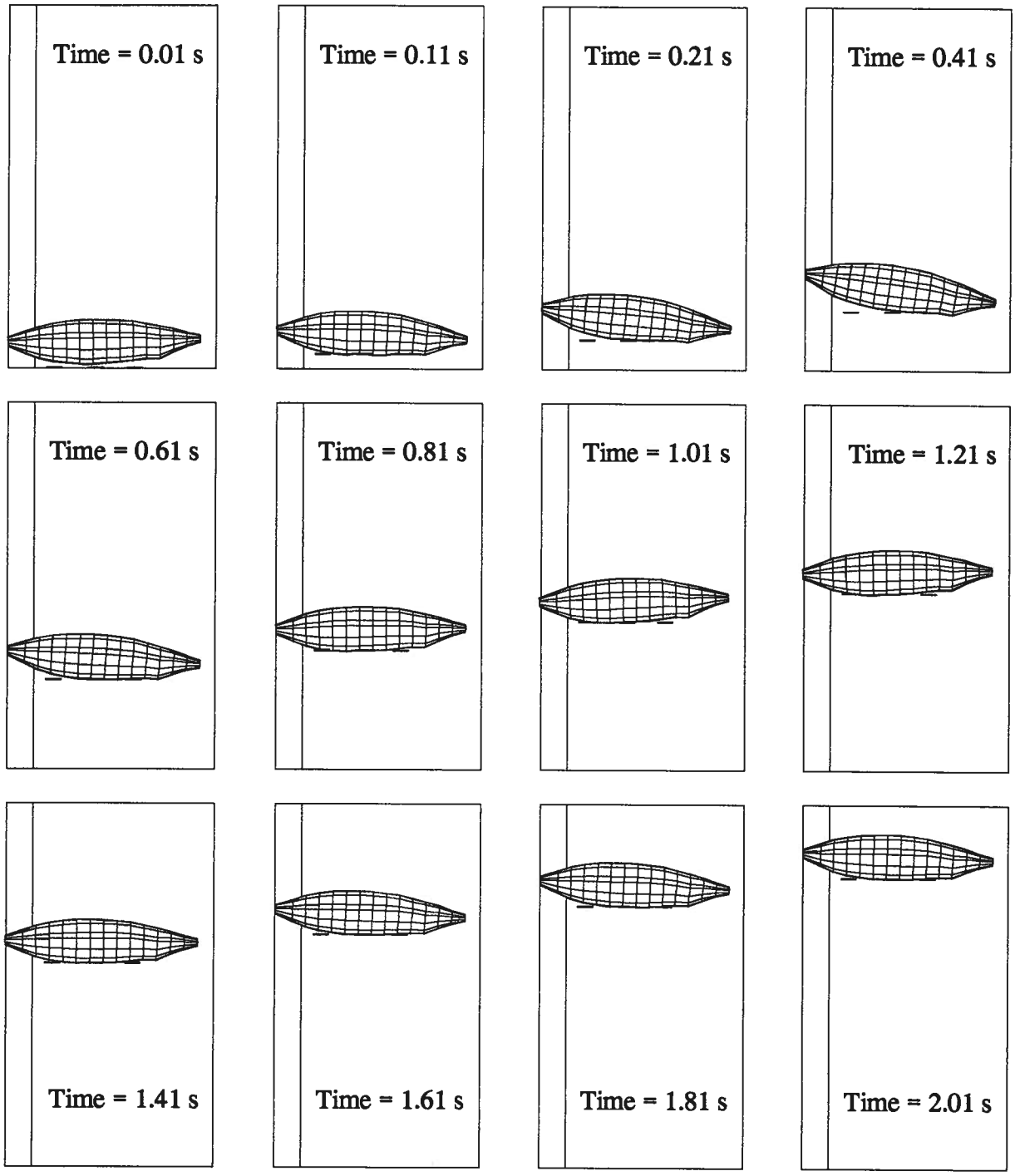

Figure 5.4: Constant speed conveying of large, firm fish using the existing configuration of the Iron Butcher. The transient "rocking" motion is sufficiently settled at Time = 1.61 s.

the fish is a flexible body whose exact shape, material properties and dynamic response are not exactly known, it may be easier to position the cutter and not move the fish in the final stages of "fine manipulation". The appeal of this method arises from the fact that the control of robots and similarly controlled mechanical linkages, which the cutter may be considered as a special case, is more widely researched and implemented than is the control of flexible bodies. If the decision is made to move the cutter, then sensing is required to locate the position on the fish body to which the cutter should be moved for performing the head cut. De Silva and Riahi [31] have shown that computer vision can be used to successfully determine the location on a fish where the head cut should be made. Recording the image of the fish is simplified and the accuracy is improved if the fish is stationary during imaging. Furthermore, the cutter design can be simplified and the accuracy of cut will be higher if the fish is stationary during cutting. For these reasons, the results of pulsed (intermittent) conveying using the current configuration of the Iron Butcher is investigated in section 5.2.1.

Gamage [32] has shown that the maximum yield for a straight cutter used for the removal of salmon heads will occur if the fish is rotated clockwise through 30°. For this reason, staggered conveying in which the fish is rotated clockwise through 30° is investigated in section 5.2.2. The use of pans to hold and transport the fish may be a viable alternative to the present system of chain lugs, and is investigated in section 5.2.3.

5.2.1 Pulsed Conveyor Motion of the Current Iron Butcher

If conveying on the current Iron Butcher is changed from a constant speed to a pulsed motion without making additional changes to the Iron Butcher, it is obvious that problems will occur during the conveying process. First, if a holding mechanism is not added for the conveying process, then the fish will remain unconstrained when the conveyor stops, so the momentum of the fish will cause it to continue moving until it collides with

the leading set of chain lugs. Second, the lack of a proper holder may allow the fish to move laterally during the cycling of the conveyor motion, which would result in a poorly located head cut.

The results from a nonlinear, transient, dynamic analysis, in which the conveyor motion of the conventional Iron Butcher is modified from a continuous motion to a pulsed (intermittent) motion, shows that an error of 0.01 m in the lateral position of the fish occurs after the fish is conveyed through just two cycles (see Figure 5.5). In the simulation, the coefficient of friction at both the fish–table and at the fish–lug interface is set at 0.10. The conveying cycle is one second in length, consisting of a constant conveying speed of 0.5 m/s for the first half–second, followed by a stationary period of a half–second. These results illustrate the need for a holder that will securely hold the fish if a pulsed motion is used for its conveying.

Two general types of holders are investigated to determine their effectiveness in holding the salmon during the pulsed conveying on the conventional Iron Butcher. The bottom surface (i.e., the surface that is in contact with the salmon) of the first holder is parallel to the table surface, while the bottom surface of the second holder makes a 7.6° angle with the table surface, with the edge of the holder that is away from the lugs being inclined towards the table top. The first type of holder is referred to as a parallel holder, since the surface touching the fish is parallel to the table top, while the second type of holder is referred to as a slanted holder because the surface which touches the fish is inclined towards the table top. The effectiveness of both a single holder and a pair of holders of the same type is determined. All simulations are nonlinear, transient, dynamic analyses of conveying. Again, the coefficient of friction at the fish–table and fish–lug interfaces are set at 0.10, while the coefficient of friction at the fish–holder interface is set at 0.40. To maintain a processing rate of two fish per second, the period of conveying is made to equal 0.5 s, which consists of a conveyor motion of 0.8 m/s for

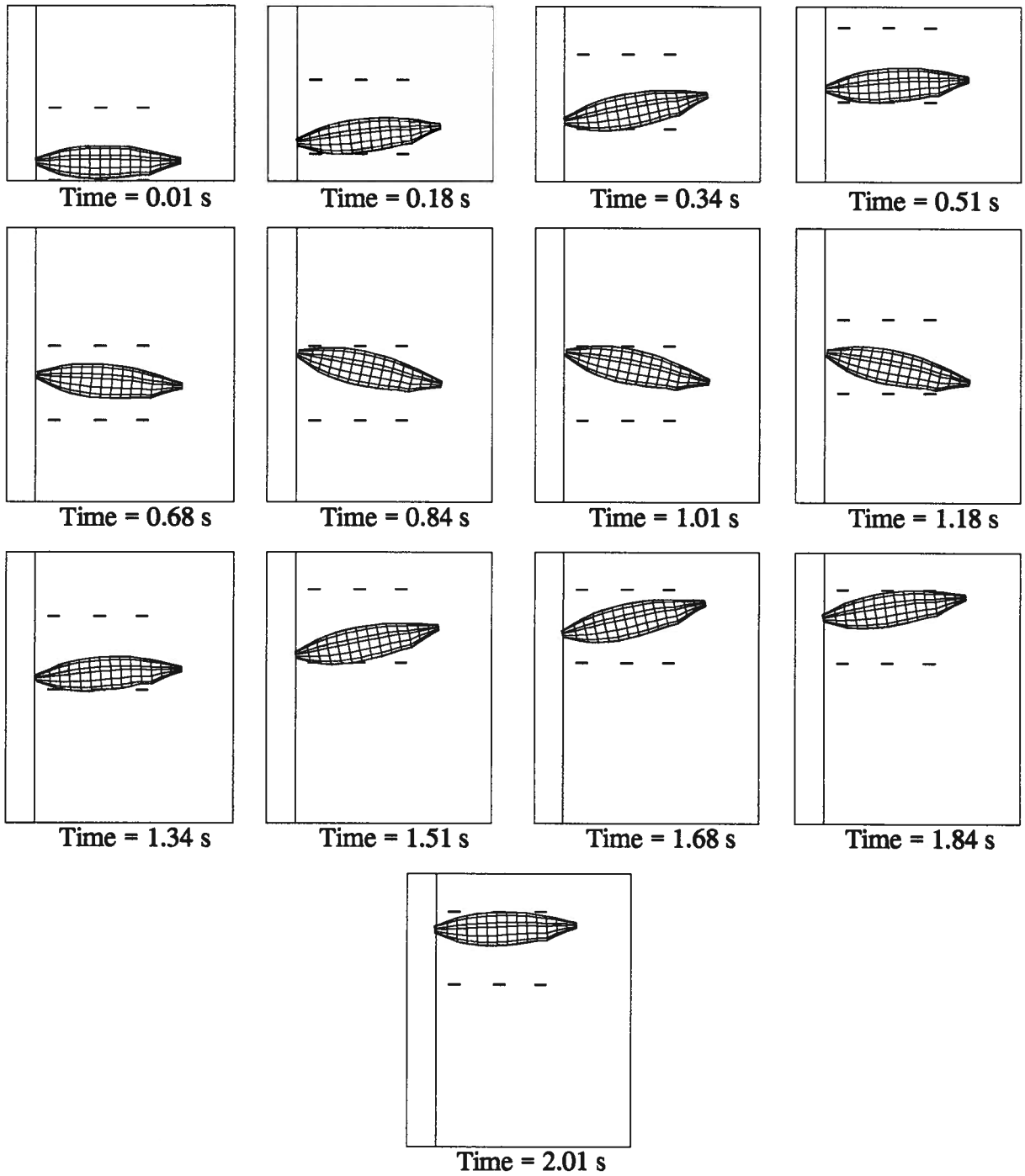

Figure 5.5: Pulsed conveying of a small, soft fish using the existing configuration of the Iron Butcher shows that an error in the lateral position of the fish is introduced after only two cycles of the conveyor motion.

the first 0.25 s, followed by a pause in the conveyor motion for the final 0.25 s. All simulations are carried out through two conveying cycles to determine if a successful hold is achieved. A successful hold for these simulations is defined as a hold which maintains contact between the fish and at least one chain lug throughout the conveying process.

The first simulation tests the effectiveness of a single parallel holder. The simulation results indicate that a single parallel holder cannot achieve a successful hold using the parameters defined above (see Figure 5.6). However, if a pair of parallel holders are used, a successful hold can be achieved (see Figure 5.7). Although this hold satisfies the definition of a successful hold, the holding forces and the resulting deformation of the fish are so large that a great deal of bruising and mutilation of the fish muscle would result (see Figure 5.8). For these reasons, parallel holders cannot be used here.

Successful holds are achieved for a single, slanted holder and for a pair of slanted holders (see Figures 5.9 – 5.10). The magnitude of the holding forces and the resulting deformation of the fish that are required to obtain a successful hold with slanted holders are much smaller than those experienced when parallel holders are used (see Figures 5.11 – 5.12). Slanted holders will produce minimal bruising of the fish muscle and will not mutilate the fish at all. The use of a pair of slanted holders is preferred to a single, slanted holder for this holding task because the holding force is smaller in the former case, where the motion of the fish head and tail is also smaller during the pause in the conveyor motion.

5.2.2 Conveying Using Staggered Lugs

As was previously noted, aligning the lugs to form a line at an angle of 30° to the cutter blade will maximize the yield of useful meat when a straight cutter is used at the head cut. In this section, the conditions which must exist for a fish to slide along the staggered lugs during constant speed conveying are first estimated. Next, a suitable

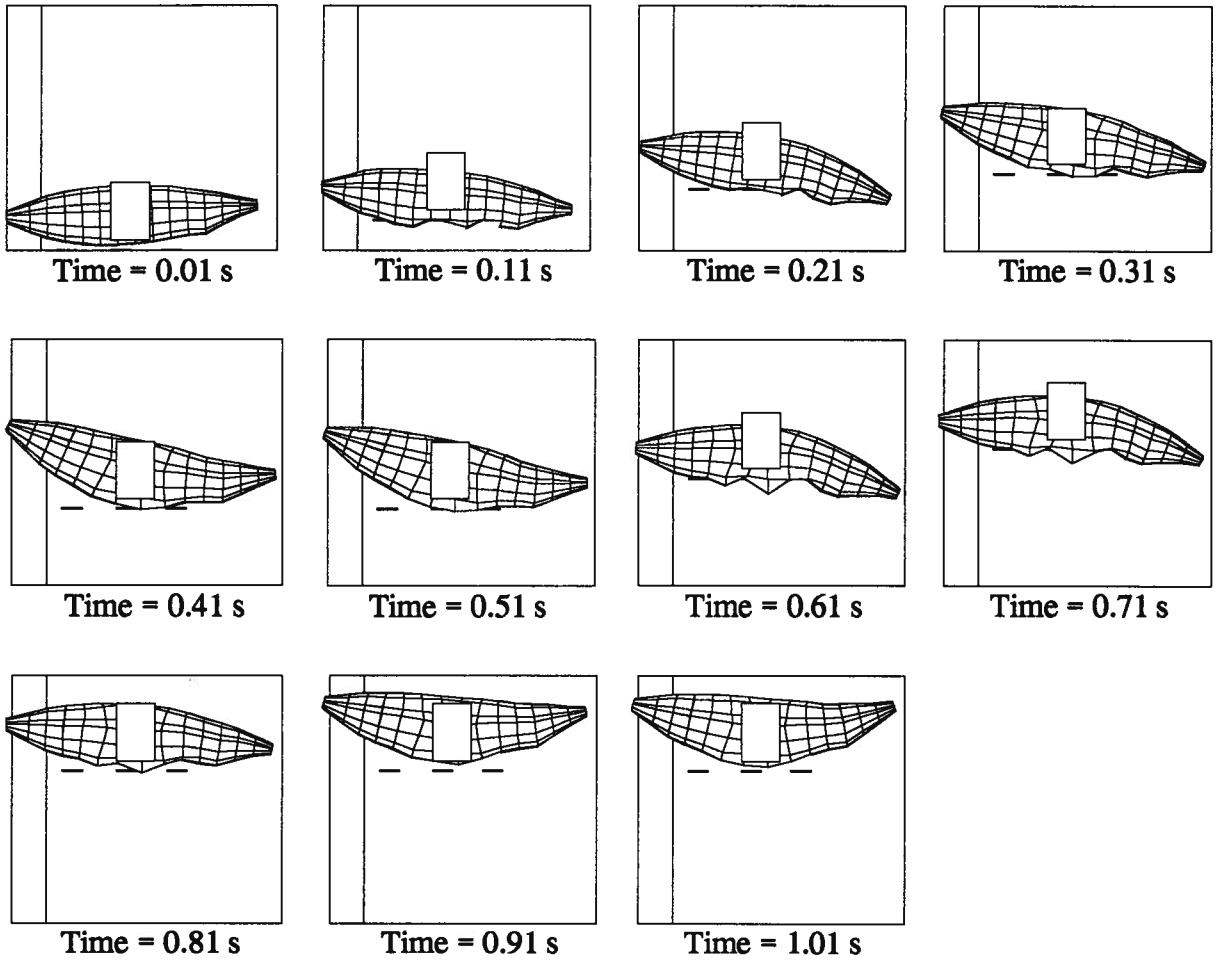

Figure 5.6: Simulation results for the pulsed conveying of a large, soft salmon with a single parallel holder show that a successful hold is not achieved.

holder is determined for the case of pulsed conveying, with staggered chain lugs.

The conditions which must exist for a fish to slide along the staggered lugs during constant speed conveying are estimated from a kinematic analysis of the idealized process. First, the three lugs are replaced by a rigid, rectangular pusher, and the fish is similarly substituted by a rigid rectangular block. The pusher is rotated clockwise through 30°. The approximate model and the free–body diagram for the pusher are shown in Figure 5.13. In this figure, F_1 is the frictional force opposing the motion u of the fish over

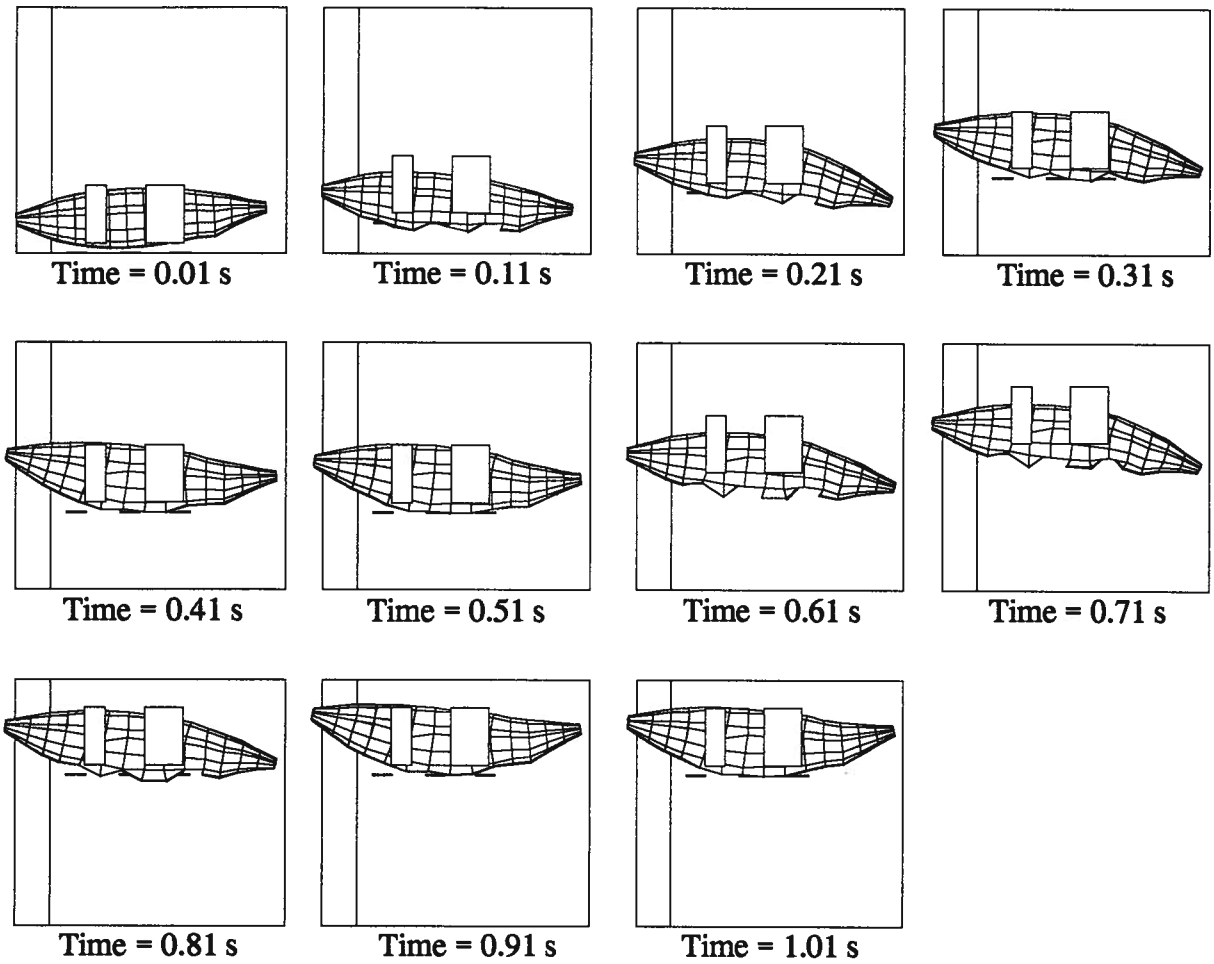

Figure 5.7: Simulation results for the pulsed conveying of a large, soft salmon with two parallel holders show that a successful hold is possible.

the table surface, while F_2 and F_3 are the components of F_1 parallel and perpendicular to the pusher surface. Assuming Coulomb friction between the fish and table,

$$F_1 = \mu_1 \, m_{fish} \, g \tag{5.1}$$

where μ_1 is the coefficient of friction between the table and the fish. From the geometry,

$$F_2 = \mu_1 \, m_{fish} \, g \, sin\theta \tag{5.2}$$

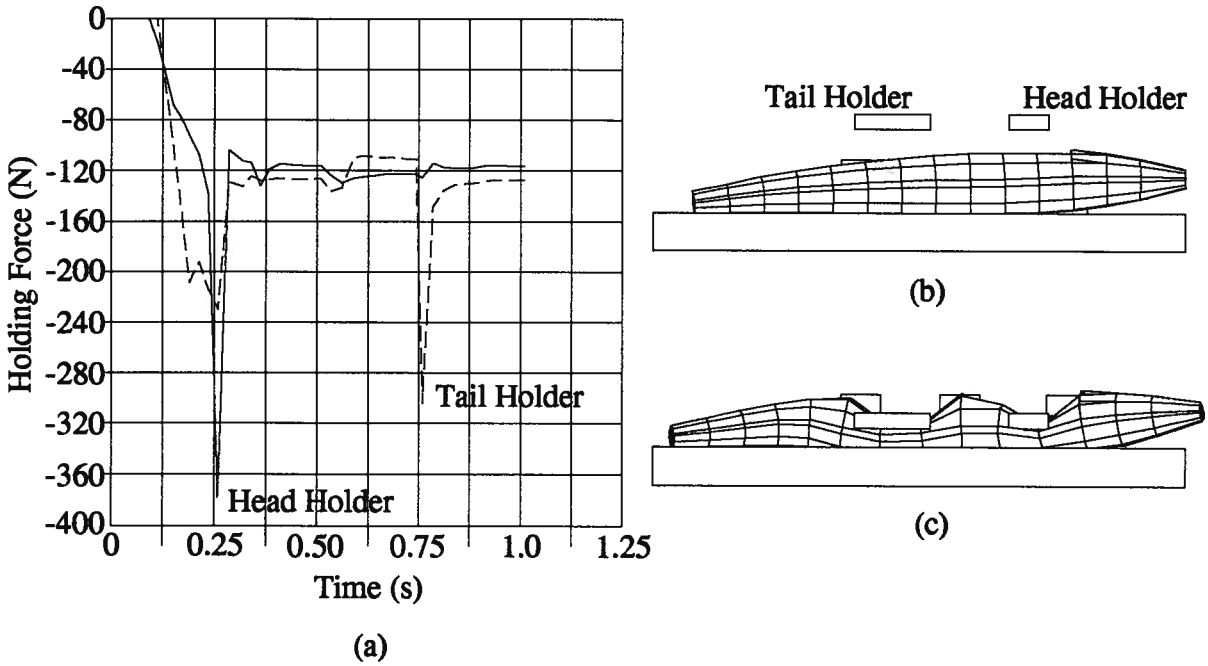

Figure 5.8: Simulation results for the pulsed conveying of a large, soft salmon when two parallel holders are used: (a) the holding forces, (b) the undeformed state of the fish prior to starting the holding process and (c) the deformed state of the fish during the holding process.

For the fish to slide along the pusher,

$$F_2 \geq \mu_2 \, m_{fish} \, g \tag{5.3}$$

where μ_2 is the coefficient of friction between the fish and pusher. Substituting equation (5.2) into (5.3) and simplifying the result gives,

$$sin\theta \geq \frac{\mu_2}{\mu_1} \tag{5.4}$$

With $\theta = 30°$, sliding will occur if and only if

$$\mu_1 \geq 2\mu_2 \tag{5.5}$$

In the present design of the Iron Butcher, $\mu_1 = \mu_2$, so the fish will not slide along the staggered chain lugs during the conveying process.

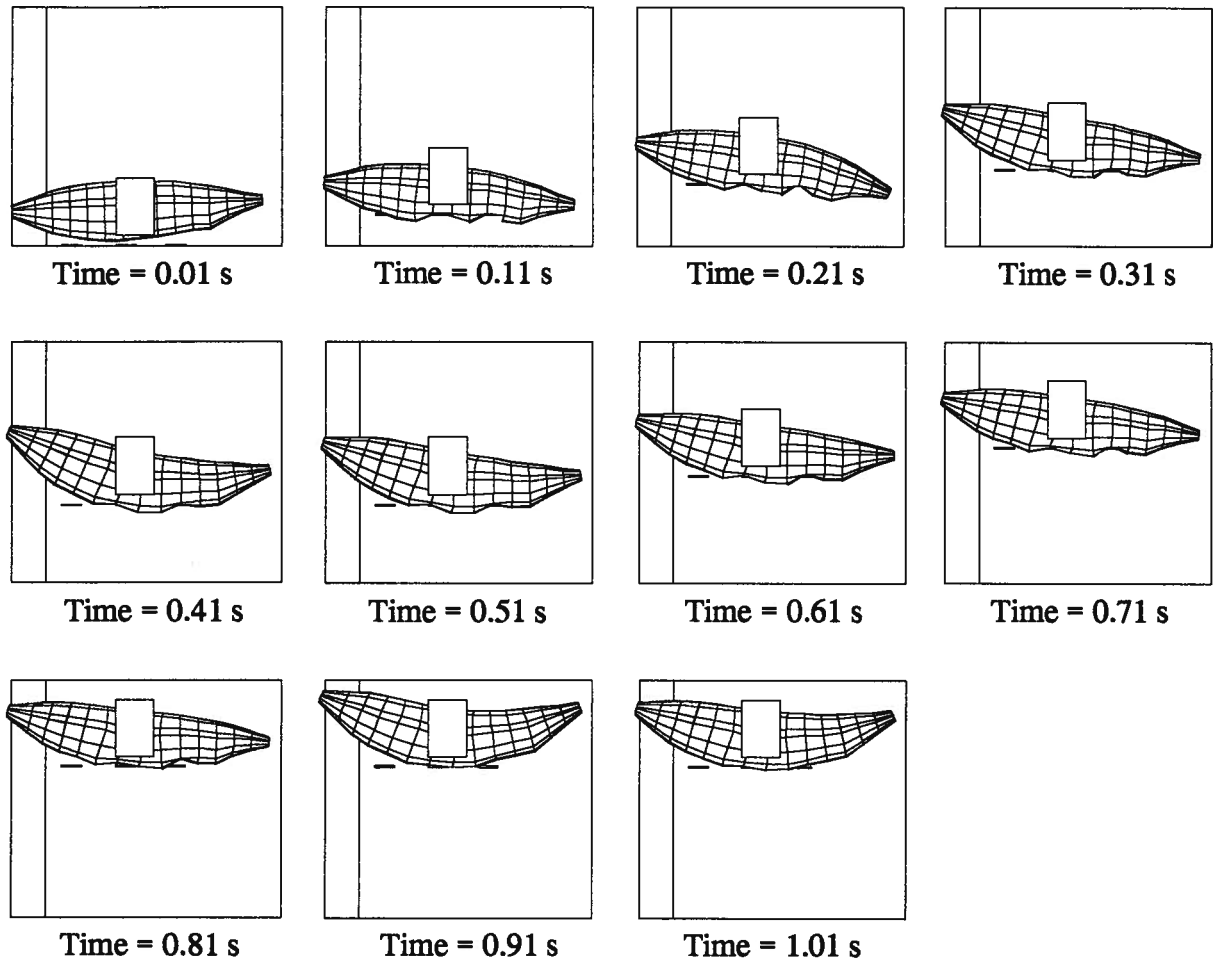

Figure 5.9: Simulation results for the pulsed conveying of a large, soft salmon when one slanted holder is used, show that a successful hold is possible.

Results from a nonlinear, transient, dynamic simulation for the staggered lug, constant speed conveying of a large, firm fish are in agreement with this kinematic analysis, as the fish does not slide along the lugs (see Figure 5.14). In this simulation the conveying speed is set at 0.5 m/s, while the coefficient of friction between the fish–table and fish–lug surfaces is assigned the value 0.1.

Having shown that the fish will not slide along the lugs during constant speed conveying using staggered chain lugs, we shall proceed to develop suitable holders for pulsed

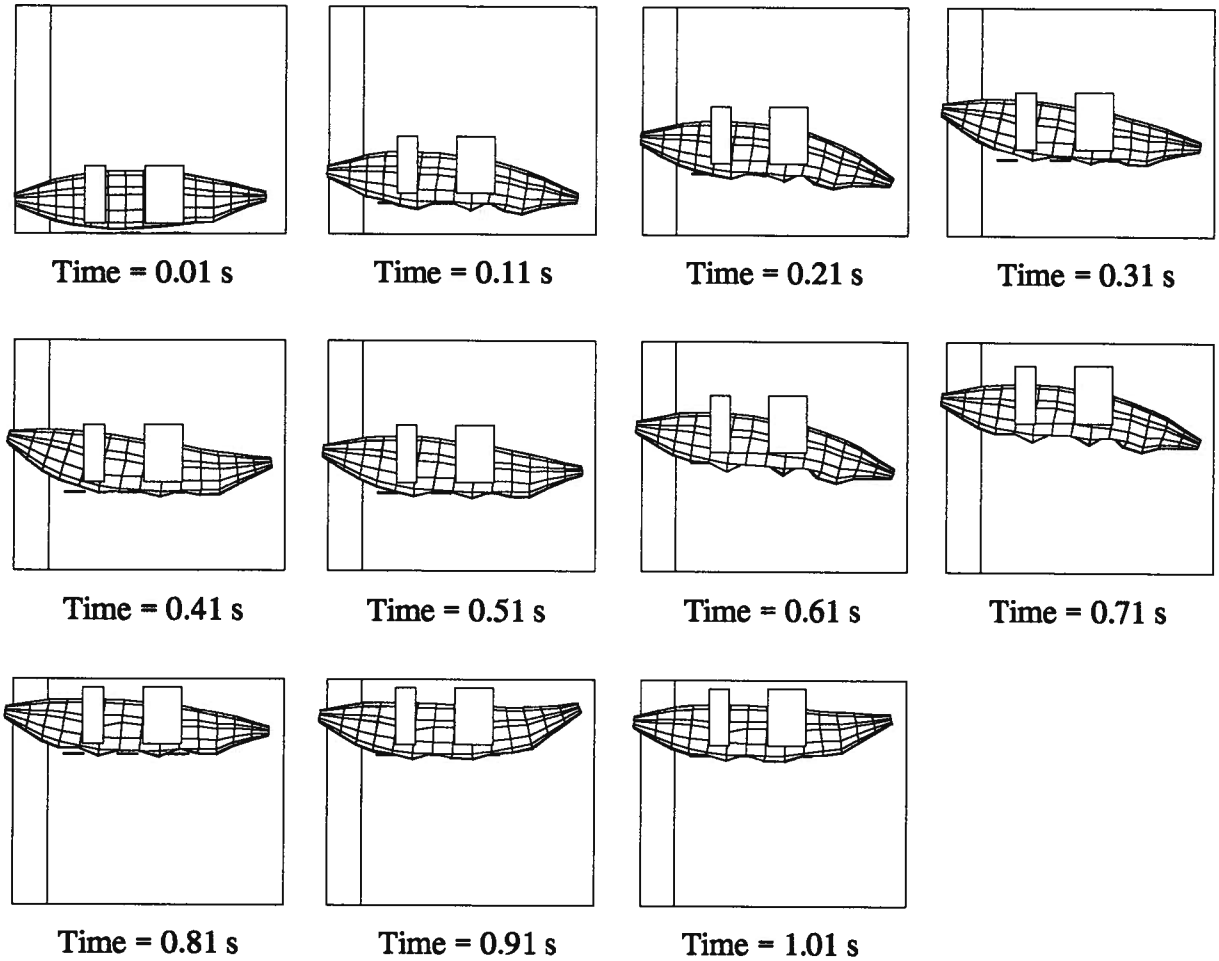

Figure 5.10: Simulation results for the pulsed conveying of a large, soft salmon when two slanted holders are used, show that a successful hold is possible.

conveying, again using staggered chain lugs. Nonlinear, transient, dynamic simulations are run to determine a suitable design for the holders. Drawing on the simulation results of section 5.2.1, only the case of two slanted holders is investigated. The conveying speed is 0.8 m/s and the period of the conveying cycle is 0.5 s. The coefficient of friction at the fish–table and the fish–lug surfaces is 0.10, while the coefficient of friction at the fish–holder surface is 0.40. The orientation of the holders, with respect to the lugs, is varied to determine its effect on the quality of hold. When the holders are rotated so that

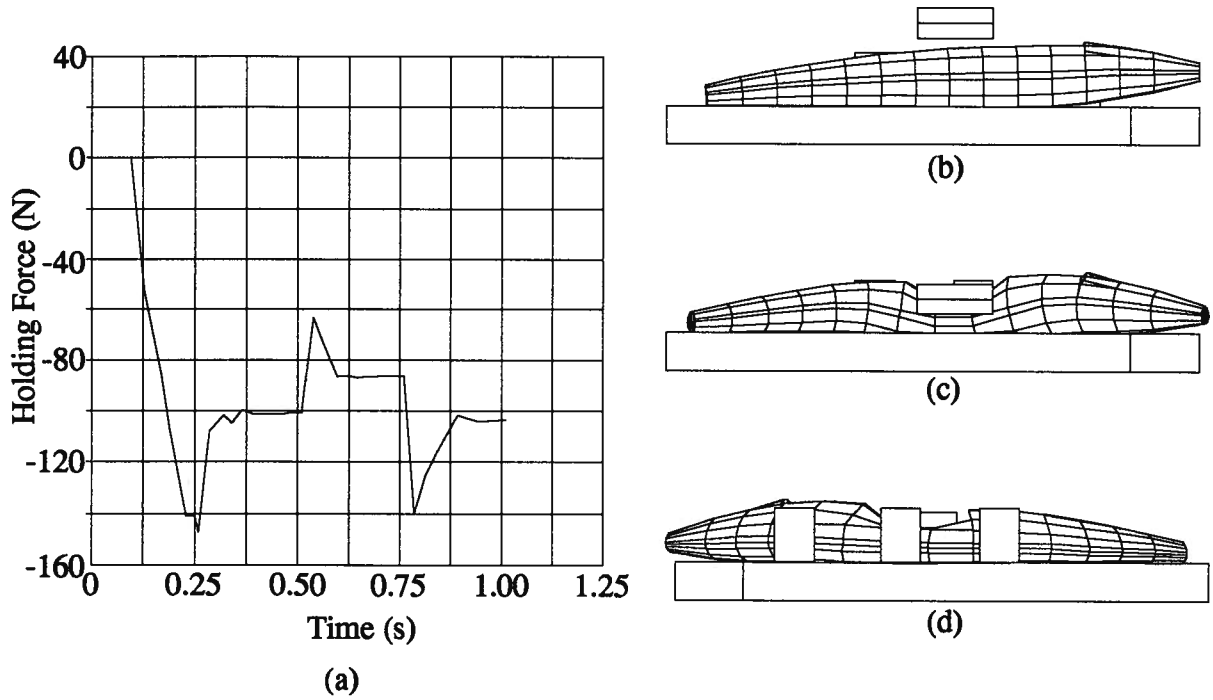

Figure 5.11: Simulation results for the pulsed conveying of a large, soft salmon when one slanted holder is used: (a) the holding force, (b) the undeformed state of the fish prior to starting the holding process and the deformed state of the fish (c) viewed from the dorsal (back) side of the fish (d) viewed from the ventral (belly) side of the fish.

they are perpendicular to the line created by the lugs, the fish is held so that it maintains contact with the lugs. Unfortunately, the fish is squeezed forward as the holding force is increased, thereby introducing an error in the position of the gill cover of the fish (see Figure 5.15). However, if the holders are oriented such that the sides of the holders are parallel to the corresponding sides of the table, the fish maintains contact with the lugs without introducing any error in the lateral position of the fish (see Figure 5.16). Therefore, two slanted holders, oriented as shown in Figure 5.16, are suitable for holding the fish during pulsed conveying, using staggered chain lugs.

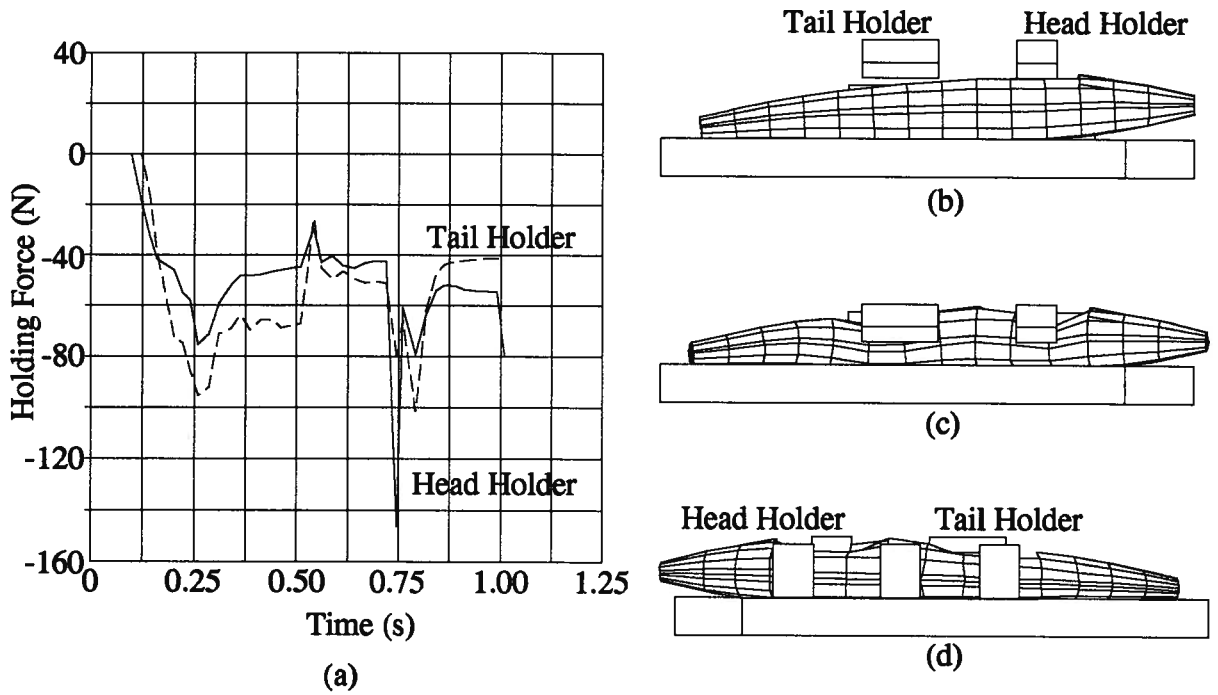

Figure 5.12: Simulation results for the pulsed conveying of a large, soft salmon when two slanted holders are used to hold the fish: (a) the holding force, (b) the undeformed state of the fish prior to starting the holding process and the deformed state of the fish (c) viewed from the dorsal (back) side of the fish (d) viewed from the ventral (belly) side of the fish.

5.2.3 Conveying Using Holding Pans

The investigation of pulsed conveying with straight or staggered lugs in sections 5.2.1 and 5.2.2 shows that although a successful hold, as defined in those sections, can be achieved, the motion of the head and tail of the fish is still quite large. The motion of the tail is not a problem since this region of the fish is not processed here. However, the large head motion during the pulsed conveying cycle will introduce positional errors in the location of the collar–bone, which will adversely affect the yield of useful meat at the head cut. In this section, the use of a simple holding pan with holders is investigated to determine if a more reliable hold, with less undesirable motion of the fish head and tail, can be achieved.

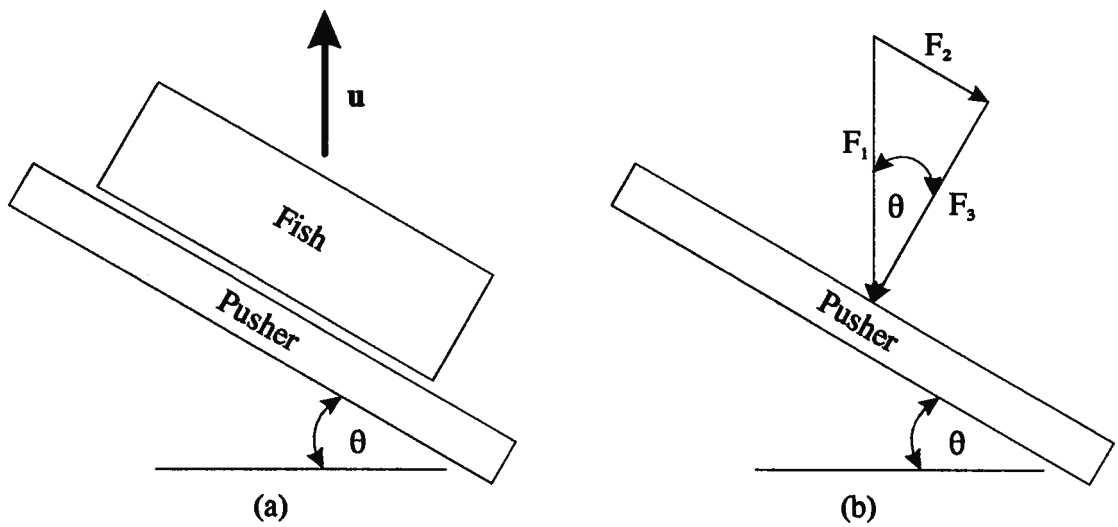

Figure 5.13: (a) The approximate model for the staggered–lug conveying process and (b) the resulting free–body diagram for the pusher.

The pan which is used in the simulations is shown in Figure 5.17. The pan is divided into two sections which are separated by 0.04 m to give adequate clearance for the cutter. The finite element model of the pan is developed in the same manner as that of the table and the fish–table contact. Nonlinear, transient, dynamic analyses of pulsed conveying are carried out with both the parallel holder and the slanted holder. For all cases, the coefficients of friction are maintained at the same values, with $\mu_{fish-pan} = 0.1$ and $\mu_{fish-holder} = 0.4$. The simulations proceed through two conveying cycles, with the period of each conveying cycle being 0.5 s in length and with a conveyor speed of 0.8 m/s.

The simulation results show that a more reliable hold is achieved when the lug–holder configuration is replaced by the pan–holder configuration (see Figures 5.18 – 5.19). The motion of the head and tail is greatly reduced and the magnitude of the holding forces are less (see Figure 5.20) when the pan–holder configuration is used. There is no difference in the motion of the fish whether a pair of parallel holders or a pair of slanted holders are used, however, the magnitude of the holding forces is slightly less for the pair of slanted

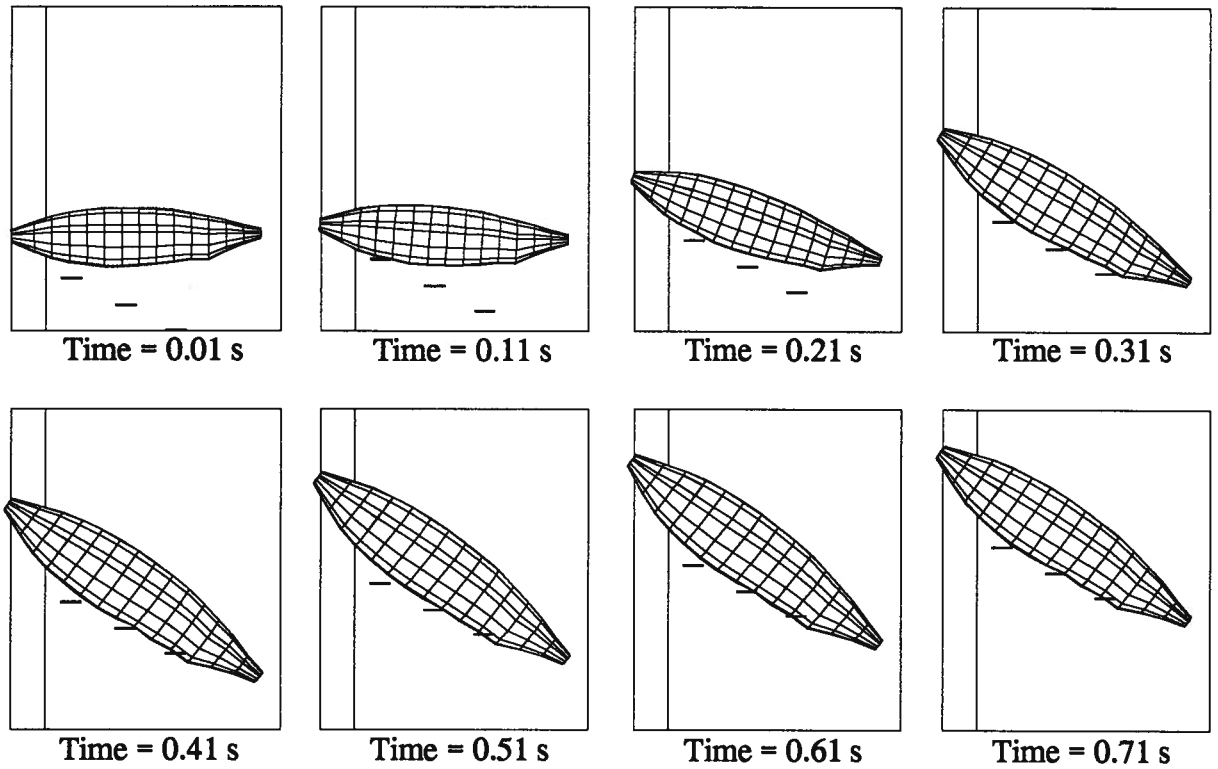

Figure 5.14: Constant speed conveying of a large, firm fish, using staggered lugs.

holders. When the holding pan is rotated clockwise through 30°, as in Figure 5.21, the new configuration of the pan and holder convey the fish without the large, undesirable motion of the head and tail which is present when the lug–holder configuration is used during pulsed conveying.

5.3 Summary of Results and Design Recommendations

The Results of this chapter are summarized below.

5.1 When using lugs to convey at a constant speed, the "rocking" motion sufficiently settles down after the fish are conveyed through 0.8 m.

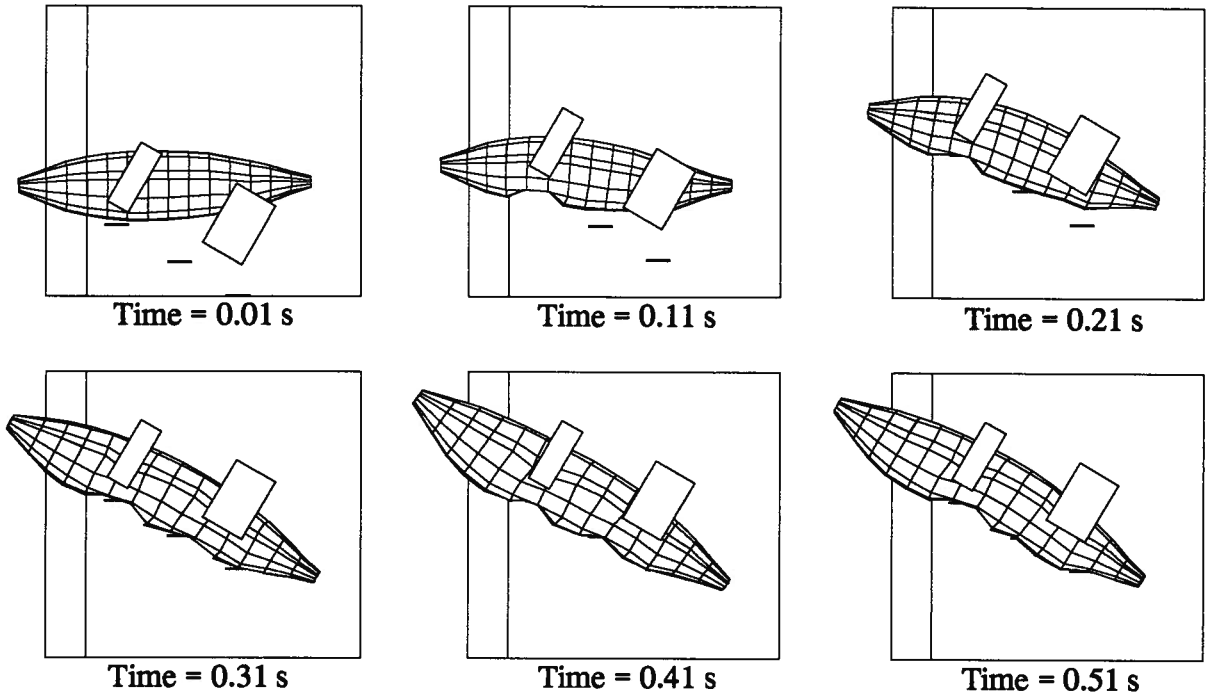

Figure 5.15: Pulsed conveying of a large, soft fish using staggered chain lugs, with the holders oriented perpendicular to the line created by the lugs.

5.2.1 When straight lugs are used with a pulsed conveying motion, a pair of holders are required to hold the fish. In addition, slanted holders provide a better hold with a lower holding force than parallel holders.

5.2.2 When staggered lugs convey fish at a constant speed and holders are not used, the fish will not slide along the lugs provided $\mu_{fish-table} < 2\mu_{fish-lugs}$. When staggered lugs follow a pulsed motion, two holders are required to hold the fish. The holders should be slanted to provide a better hold with a lower holding force, and the sides of the holders should be parallel to the sides of the table.

5.2.3 Holding pans convey fish so that the undesirable motion of the head and tail is greatly reduced from that seen when chain lugs are used for conveying. Slanted holders and parallel holders are equally satisfactory at restraining the fish, but the

holding force of the slanted holders is approximately 10–20% lower than that of the parallel holders.

The following recommendations are made to improve the conveying system of the Iron Butcher:

1. **Replace the chain lugs with holding pans.** By using holding pans instead of chain lugs to convey the fish, the unwanted motion of the head and tail is greatly reduced, whether conveying is at continuous speed or intermittent (pulsed). This improved positional accuracy will directly translate into less waste at the head cut. If constant speed conveying is desired, then the fish need be conveyed only through 0.1 m (as compared to 0.8 m for chain lugs) before progressing to the next stage of processing, as the holding pans help settle the transient motion more quickly than is possible with the lugs. This benefit means that a more compact machine can be built, thus saving valuable work space and will have a lower cost since fewer resources go into producing the machine. Finally, even a simple design for the holding pan, as was used in the simulations, produces significantly improved conveying results. Stainless steel or aluminum would be a suitable material for the holding pans for reasons of hygiene (easy to clean and disinfect) and manufacturability.

2. **Use contoured holders to hold the fish.** Slanted holders are shown to be superior to parallel holders, yet slanted holders provide improved restraint only when the conveyor pauses in pulsed conveying. If the holders are contoured to approximate the contour of the fish, then the fish would be better restrained when the conveyor starts to move as well as when the conveyor pauses. The motion of the head would be smaller, so the waste at the head cut, as a result of this extraneous motion of the head, would be reduced. The contour should conform with a range of fish, at least in an average sense, however.

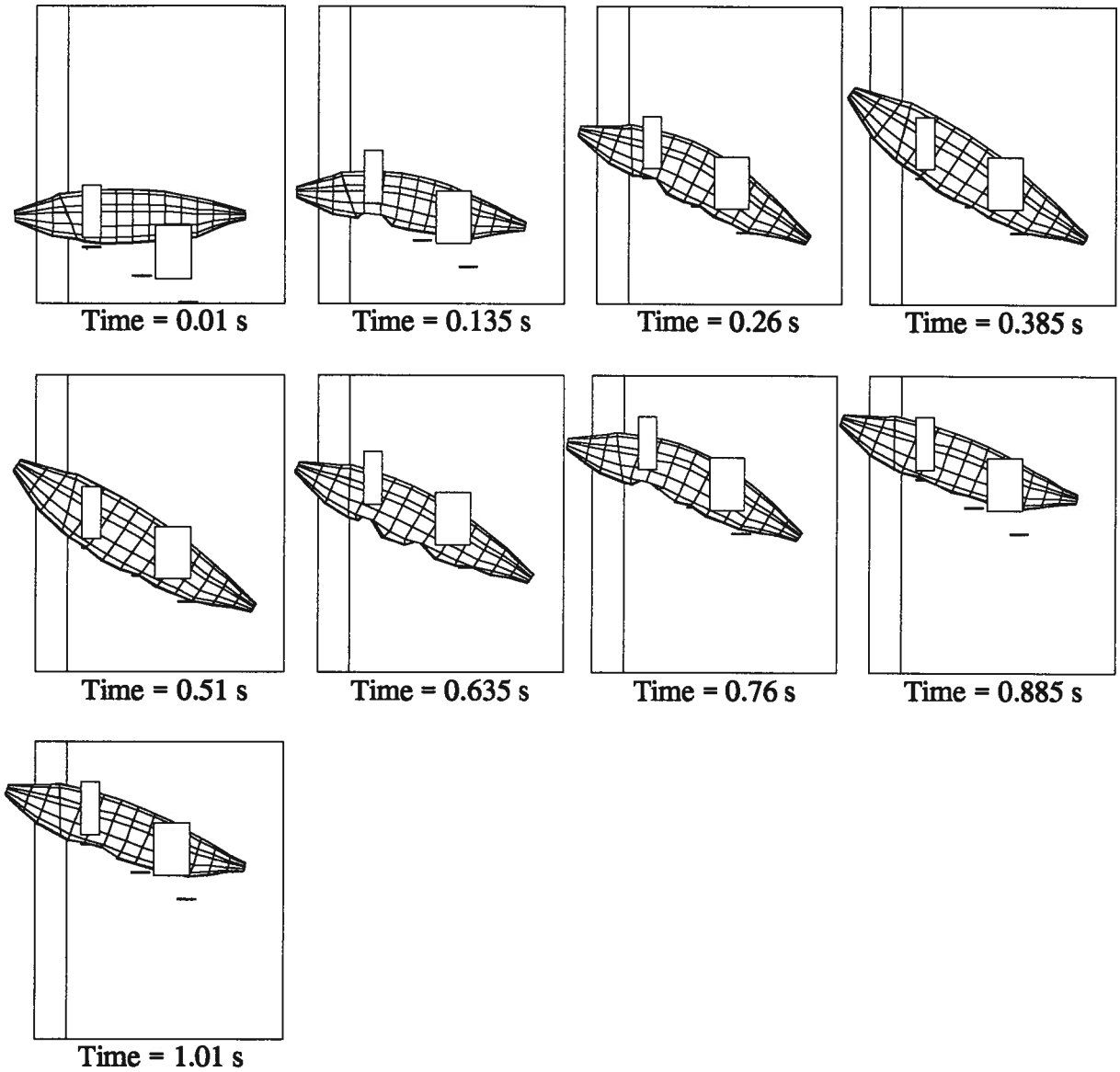

Figure 5.16: Pulsed conveying of a large, soft fish using staggered chain lugs with the edges of the holders parallel to the corresponding sides of the table.

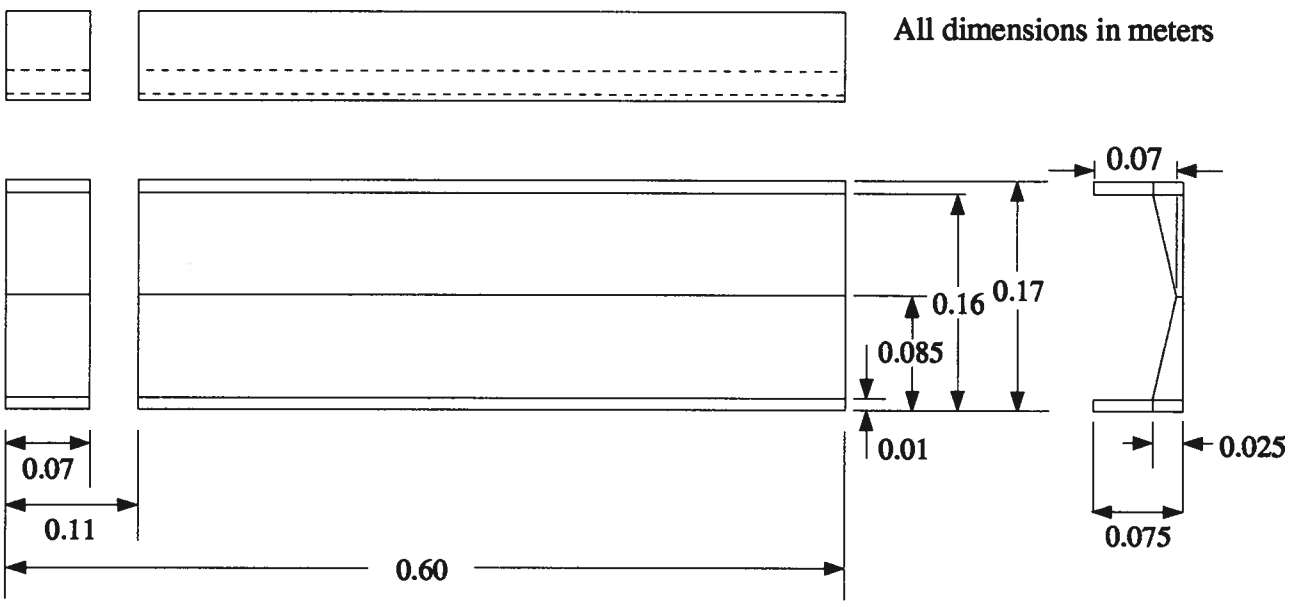

Figure 5.17: A sketch of the holding pan used in the simulations.

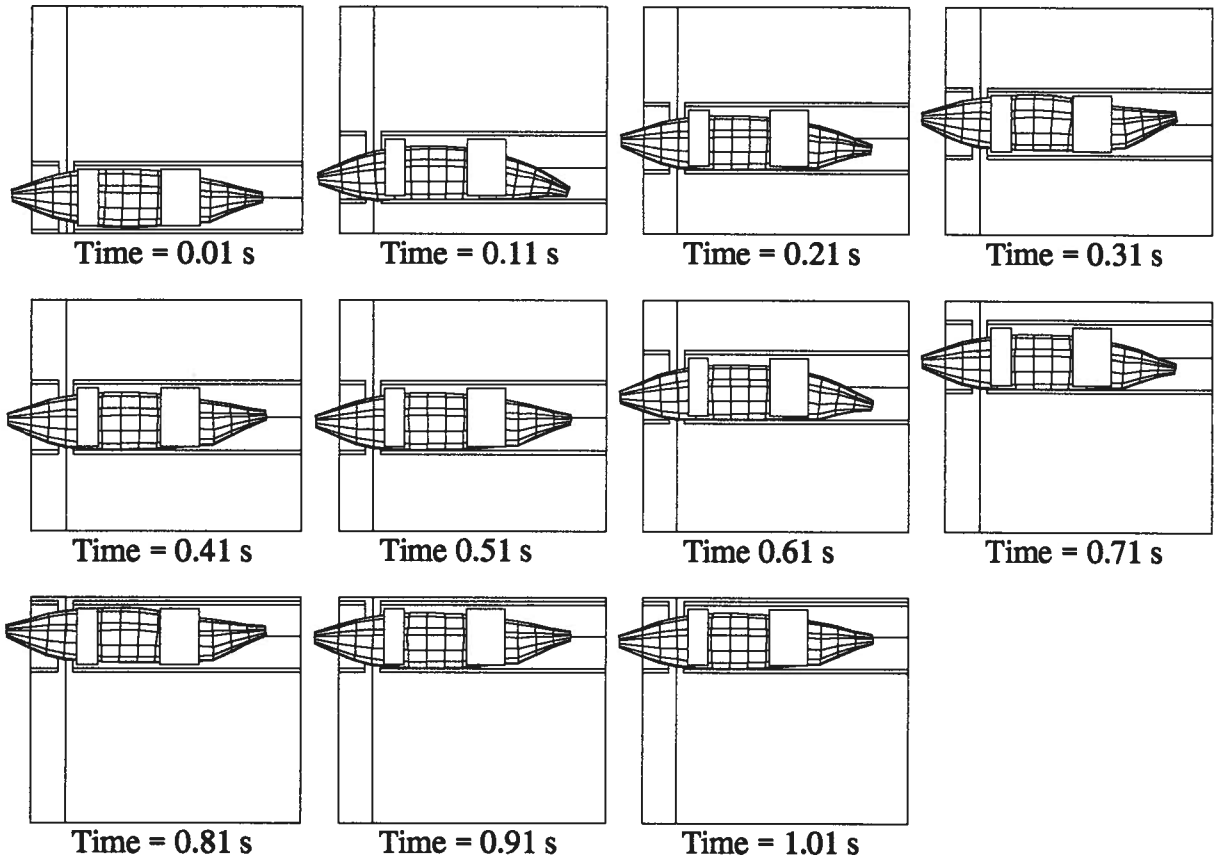

Figure 5.18: Pulsed conveying of a large, soft fish using a pan and parallel holders.

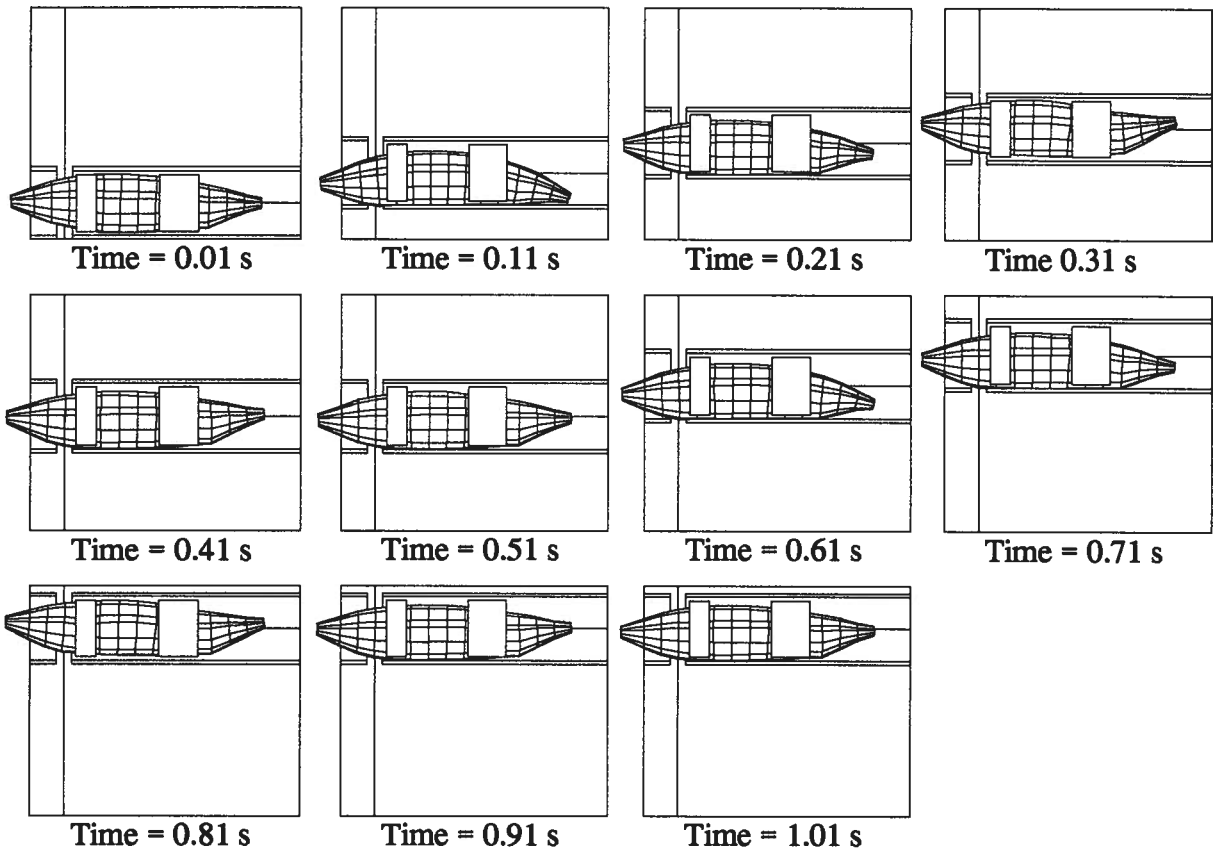

Figure 5.19: Pulsed conveying of a large, soft fish using a pan and slanted holders.

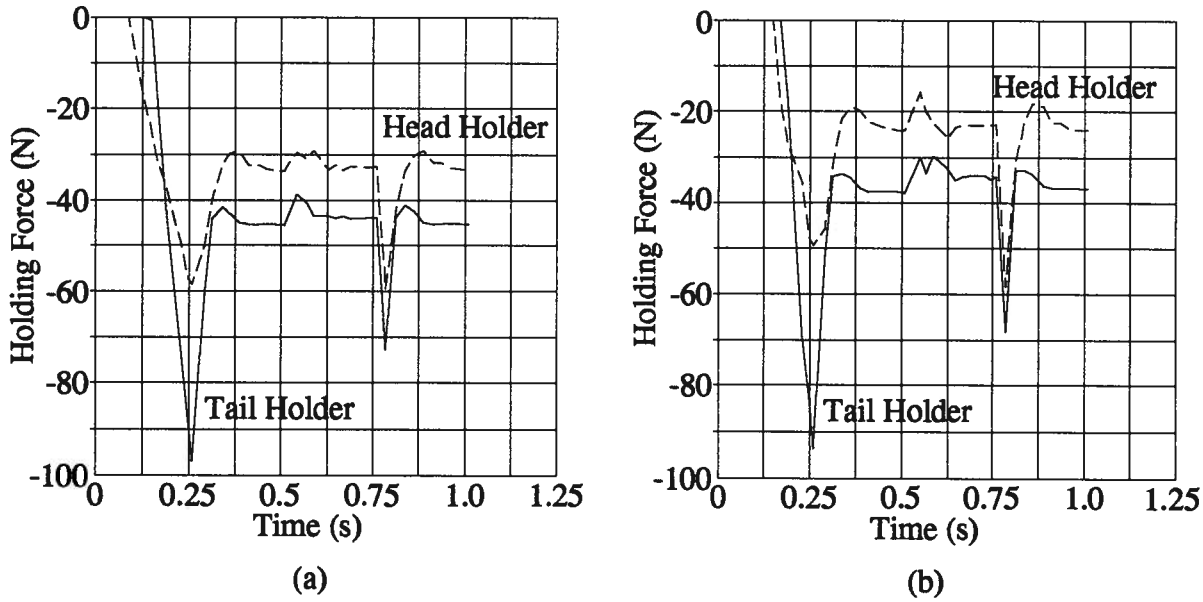

Figure 5.20: Holding forces for the pulsed conveying of a large, soft fish using a holding pan with (a) parallel holders (b) slanted holders.

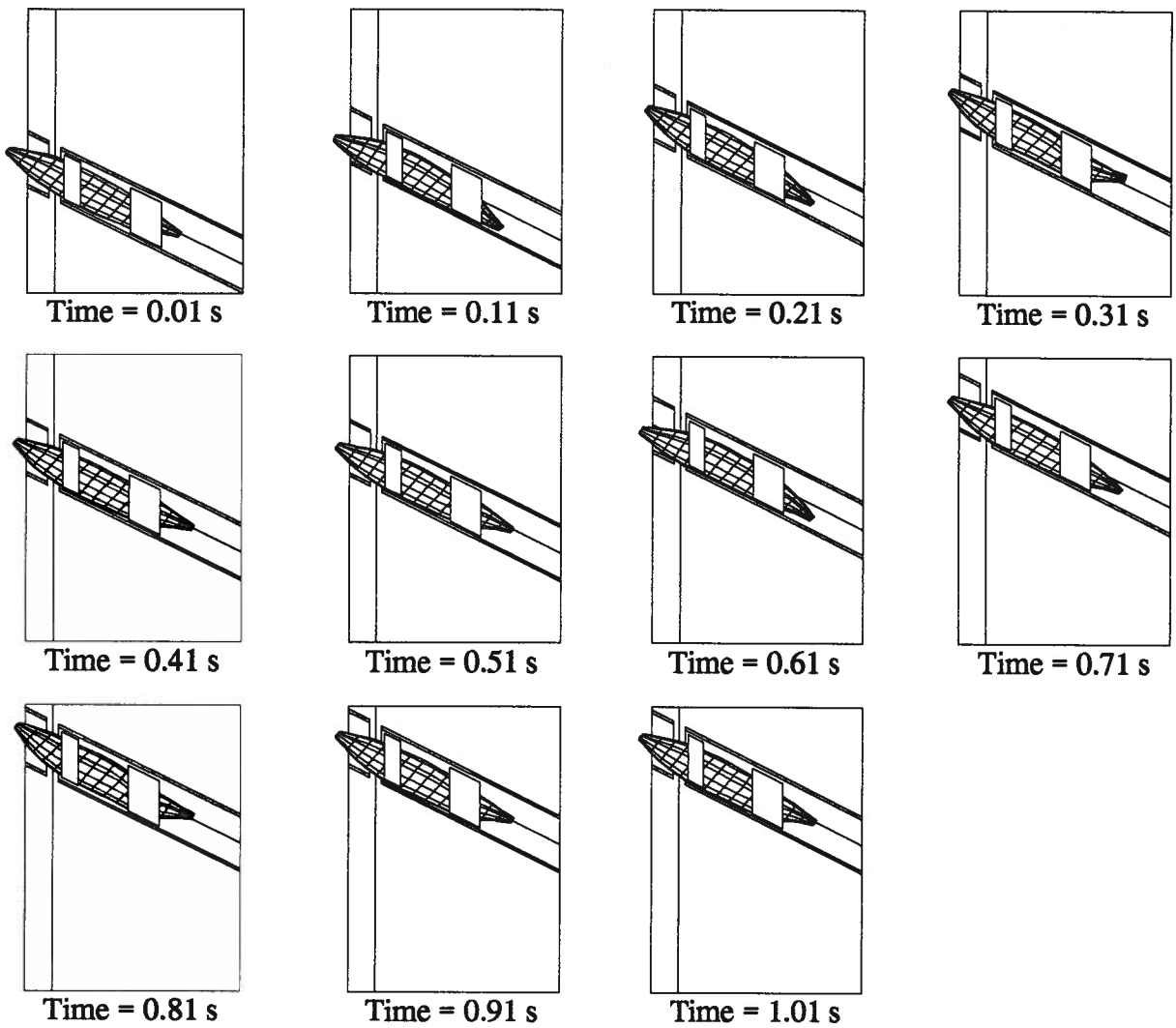

Figure 5.21: Pulsed conveying of a large, soft fish using a rotated pan and slanted holders.

Chapter 6

Investigation of Indexing Errors

On the present Iron Butcher, the wastage at the head cut results primarily from the improper indexing of the fish. The extreme cases of indexing error, underfeed and overfeed, are examined in this chapter. The possible mechanisms which cause these errors are studied through simulation. Design improvements are then proposed and tested to determine their effectiveness in preventing these errors from occuring. Recommendations for the redesign of the machine to reduce the frequency of underfeed and overfeed errors are then made.

6.1 Investigation of Underfeed Error

Underfeed error occurs when the indexer does not engage with the collar–bone and gill cover, but instead slips past both these structures and continues to move toward the cutting line without indexing the fish. Two explanations are available to describe why the indexer does not properly engage with the gill cover and collar–bone.

1. **The gill cover is pushed into the gill cavity**. During handling, the gill cover is sometimes pushed into the gill cavity. When this happens, the gill cover is below the surface of the fish, so it is impossible for the indexer to engage the gill cover. With frozen and thawed fish, the gill cover could be stuck in this manner.

2. **The gap between the gill cover and the side of the fish is not large enough for the indexer to engage with the gill cover**. The fish–gill cover

gap is illustrated in Figure 6.1.

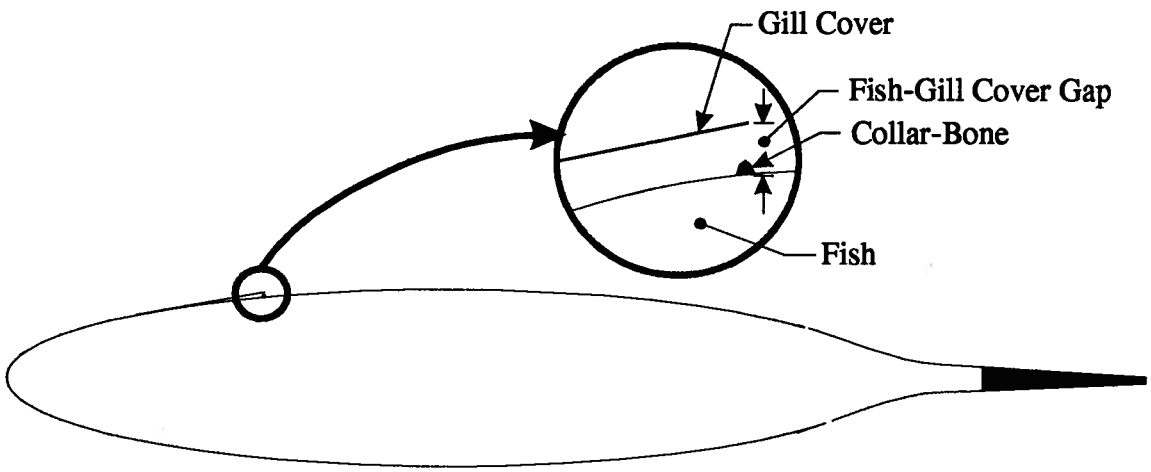

Figure 6.1: The fish–gill cover gap.

If the gill cover is pushed into the gill cavity, the gill cover should be freed from the gill cavity before the fish is placed on the Iron Butcher. If this is not done, the indexing process will be more likely to fail, since the indexer cannot engage with the gill cover. It is expected that a minimum gap size is required for the indexer to engage with the gill cover for indexing, but it is not known if this minimum gap size varies with the location of the gill cover relative to the collar–bone. Estimating the minimum gap size for successful indexing, and how this gap size varies with the position of the gill cover, is determined through computer simulation.

Nonlinear, transient, dynamic analysis of the indexing process is performed to determine the minimum gill cover–fish gap size for successful indexing. The model for a large, firm fish is used, with the coefficients $\mu_{fish-indexer}$, $\mu_{fish-holder}$ and $\mu_{fish-lugs}$ all set to 0.1. An initial static load step is used to specify the simulation initial conditions, which are zero velocity and acceleration for the fish, and the fish lying flat on the table under gravity loading. The time at the end of this static load step is 0.01 s.

Table 6.1: Variation in the minimum gill cover–fish gap size for successful indexing using the current design of the Iron Butcher.

Distance the gill cover is posterior of the collar–bone (m)	Minimum initial gill cover–fish gap size (m)
0.000	0.002
0.0025	0.0009
0.005	0.0007

The location of the end of the gill cover, which is engaged by the indexer, is not fixed. As can be expected of a natural resource, there is some variation in the location of this feature, but this feature will not normally be superior of the collar–bone and will be up to 0.005 m posterior of the collar–bone. For positions within this range of possible locations of the end of the gill cover, the gill cover–fish gap size is varied until the minimum gap size for successful indexing is obtained. The results of the simulations are summarized in Table 6.1. The results show that the minimum gap size for successful indexing increases as the location of the gill cover approaches the collar–bone. This trend can be explained by the fact that while the fish muscle deforms under the weight of the indexer, the collar–bone does not deform under this weight. Since the fish muscle immediately adjacent to the collar–bone is attached to the collar–bone, this muscle would deform less than muscle tissue further from the collar–bone when the same loading is applied to each. If the tissue below the indexer deforms more due to the weight of the indexer, then the initial gill cover–fish gap size (i.e., the gill cover–fish gap size before the fish muscle deforms under the weight of the indexer) can be smaller for successful indexing to occur.

From the above results, it is apparent that increasing the gill cover–fish gap size so that it exceeds the minimum gap size for successful indexing, will significantly reduce or altogether eliminate underfeed error. In order to increase the gill cover–fish gap size for each fish that is processed on the Iron Butcher, a mechanism to push the fish head

down, and as a result increase the gill cover–fish gap size, is proposed. The push–down mechanism in Figure 6.2 consists of a flat plate with a mass of 0.85 kg and measures 0.06 m x 0.15 m x 0.01 m. This plate can drop onto the nose of the fish and move with

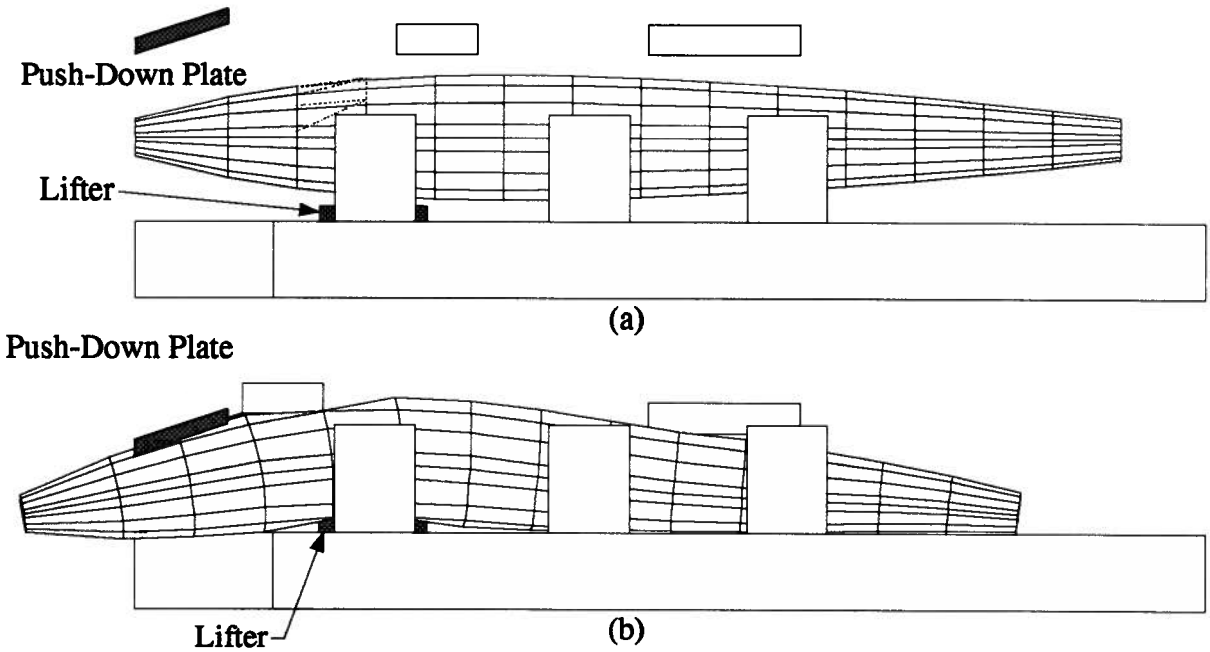

Figure 6.2: Components of the push–down mechanism: (a) the finite element model and (b) simulation result for indexing.

the conveyor, or it can remain stationary and be hinged to allow the fish head to pass below it as the fish is conveyed toward the cutter. In addition to this plate, a 0.01 m high bar is added to the surface of the table and runs the length of the table. The fish head is lifted by the bar to increase the clearance between the fish head and the table so that the plate can push the nose of the fish down and increase the gill cover–fish gap size.

Nonlinear, transient, dynamic analyses are performed to determine the effectiveness of the push–down mechanism in preventing underfeed error. The simulations use the model of a large, firm fish, and the coefficients of friction $\mu_{fish-table}$, $\mu_{fish-lugs}$, $\mu_{fish-indexer}$,

Table 6.2: Variation in the minimum gill cover–fish gap size for successful indexing when the nose push–down device is added to the Iron Butcher.

Distance the gill cover is posterior of the collar–bone (m)	Minimum initial gill cover–fish gap size (m)
0.000	0.001
0.0025	0.0001
0.005	0.0003

$\mu_{fish-holder}$, $\mu_{fish-pushdownplate}$ and $\mu_{fish-lifter}$ are all assigned a value of 0.1. For the simulations, the push–down plate drops onto the fish head and moves with the fish as it is conveyed. The simulation results for the minimum initial gill cover–fish gap size for successful indexing are summarized in Table 6.2. These results indicate that the push–down mechanism successfully increases the size of the gap from its initial value to a larger value that is required for successful indexing to occur, without adversely affecting the conveying or indexing processes.

6.2 Investigation of Overfeed Error

Four possible causes for overfeed error have been identified. These are:

1. Friction between the fish and indexer, and/or between the fish and the table surface.

2. Structural deformities on the fish. Examples of these are cuts or gouges in the fish flesh, permanent crease lines caused by nets during fishing or caused during transport or storage, or the absence of scales in a region of the fish.

3. The design and/or configuration of the machine components.

4. Softness of the fish muscle.

There is some inter–relationship between these suspected causes of overfeed error. For example, a cut may be modeled as a structural deformity, but the absence of fish scales from a region of the fish, although classified as a structural deformity, may be better modeled as a change in the coefficient of friction between the fish and indexer in that region. The following simulations of indexing terminate prior to the indexer engaging with the gill cover. As a result, the motion of the fish can be attributed to mechanisms which cause overfeed error.

6.2.1 The Role of Friction in Overfeed Error

In order to determine if friction plays an active role in the occurrence of overfeed error, a series of simulations are performed. The purpose of the first simulation is to determine the motion of the fish when the fish comes into contact and conforms to the table surface under gravity loading. The second set of simulations determine the motion of the fish as the fish–indexer and fish–table coefficients of friction are varied. The third set of simulations determine if the holder has any affect on overfeed error. The last set of simulations determine if repositioning the holder has a positive effect in reducing the likelihood of overfeed error occuring. All simulations have an initial static load step to permit the fish to come into contact and conform to the table surface, after which point dynamic load steps simulate various combinations of holding and motion of the indexer sliding over the fish.

Motion of the Fish Under Gravity Loading

In all the finite element simulations, the fish is initially located slightly above the table of the Iron Butcher. A static load step is first performed to permit the fish to contact and conform to the table surface under gravity loading. After this static load step, the fish is at rest on the table surface and dynamic load steps are then performed to model

various stages of processing. The coefficient of friction at the fish–table interface is 0.1, and the model of a large, soft fish is used. Figure 6.3 shows the x–direction motion of the fish as the fish comes into contact with and conforms to the table surface. It should be noted that in the simulations, indexing occurs in the negative x–direction of the global coordinate system. These results indicate that the fish moves through approximately 0.005 m in the negative x–direction when it conforms to the table surface. Any motion in the the global x–direction in excess of -0.005 m in the following simulations can be considered to be indexing error.

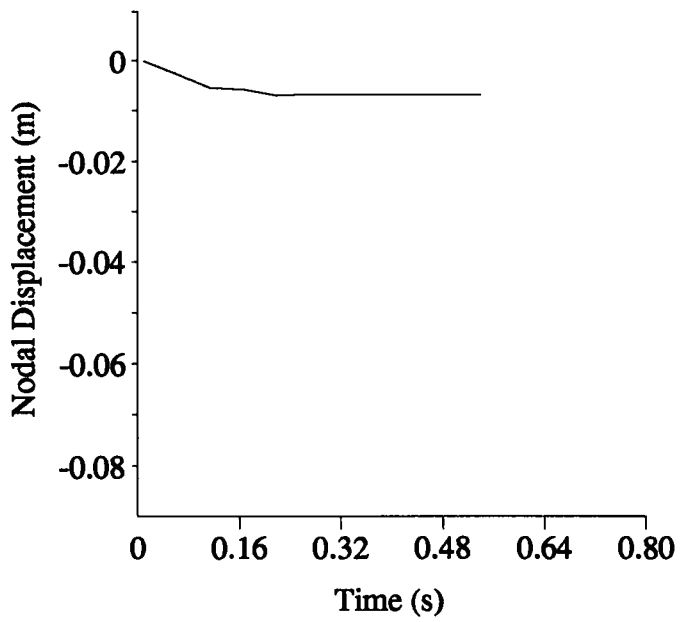

Figure 6.3: Overfeed motion (in the x–direction) of the fish when the fish conforms to the table surface under gravity loading ($\mu_{fish-table} = 0.1$).

Overfeed Error as a Function of the Coefficients of Friction

A series of simulations are performed to determine how the x–direction motion of the fish changes as the coefficient of friction between the fish and indexer changes. Simulations are performed for a large, firm fish and a large, soft fish. The coefficient of friction for

the other surfaces are $\mu_{fish-table} = \mu_{fish-holder} = 0.1$. The results of the simulations are summarized in Figure 6.4. These curves show the x–direction motion of the fish for different values of $\mu_{fish-indexer}$. The motion of the indexer is also shown so that the results can be interpreted relative to that motion.

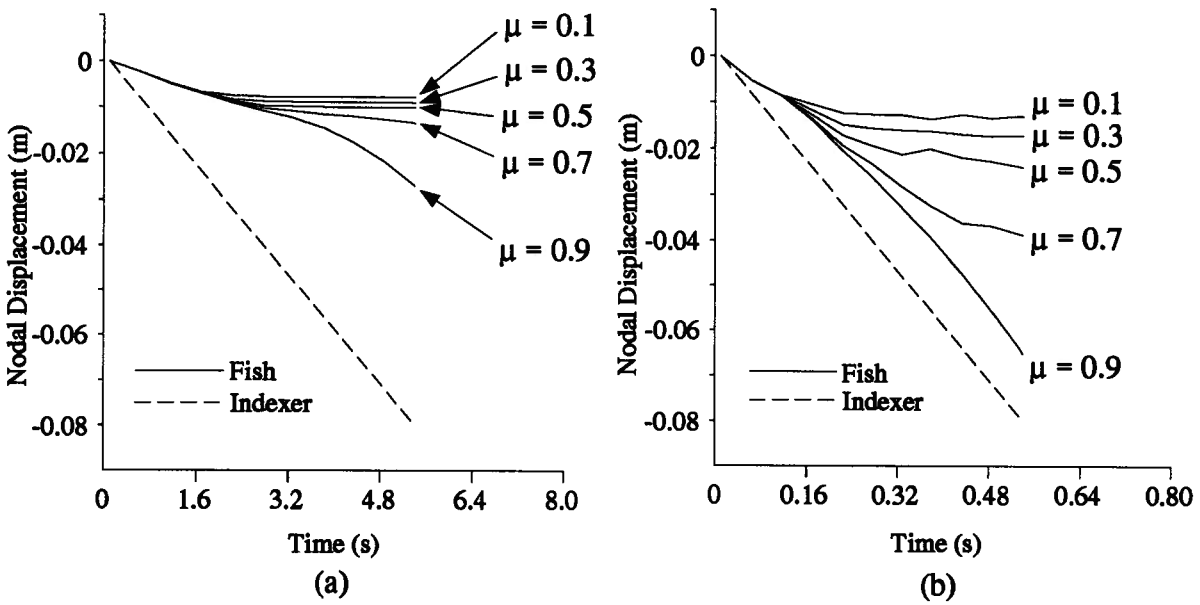

Figure 6.4: Overfeed motion (x–direction) of the fish as a function of the coefficient of friction between the fish and indexer ($\mu_{fish-table} = 0.1$). Simulation results for indexing large fish with (a) firm muscle (b) soft muscle.

In addition to the effect the fish–indexer coefficient of friction has on overfeed, intuitively, reducing the fish–table coefficient of friction should increase the possibility of overfeed. A series of simulations are carried out to determine the effect of the fish–table coefficient of friction on overfeed error. In these simulations, the coefficient of friction $\mu_{fish-table}$ is set to 0.05, instead of 0.10 as in the above simulations. Figure 6.5 shows the results of these simulations.

A comparison of the curves in Figure 6.4 with those in Figure 6.5 immediately provides four general results. First, friction between the fish and indexer is a possible mechanism causing overfeed error. Second, overfeed error increases with increasing $\mu_{fish-indexer}$.

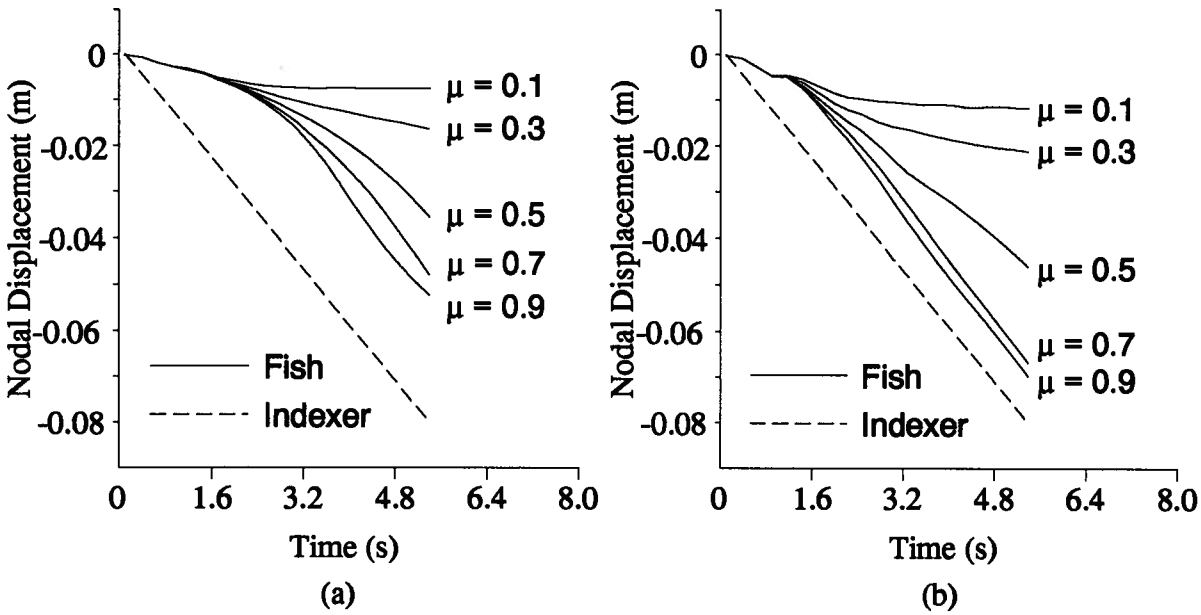

Figure 6.5: Overfeed motion (x–direction) of the fish as a function of the coefficient of friction between the fish and indexer ($\mu_{fish-table} = 0.05$). Simulation results for indexing large fish with (a) firm muscle (b) soft muscle.

Third, overfeed is more likely to occur as $\mu_{fish-table}$ decreases. Fourth, overfeed error is more likely to occur, and is larger, for soft fish than it is for firm fish.

Closer examination of the curves in Figure 6.4(b) provides further information as to the behaviour of the interactions as the indexer slides across the fish. The curves for $0.1 \leq \mu_{fish-indexer} \leq 0.7$ all have an instantaneous slope that is smaller in magnitude than the slope of the line denoting the motion of the indexer. For these cases, even though the fish is being pushed laterally, there is slip between the indexer and fish, with the indexer moving at a higher rate than the fish. For the case of $\mu_{fish-indexer} = 0.9$, the same holds true during the period of 0.0 s to 0.46 s. However, after 0.46 s, the instantaneous slope of the curve is greater in magnitude than the slope of the line denoting the motion of the indexer. After 0.46 s, the fish is moving faster than the indexer, so another mechanism must be working to introduce the overfeed error.

Effect of the Holder

Since it has been determined that another mechanism, in addition to friction, is responsible for overfeed error, a simulation is run that does not include a holder. These simulation results will indicate if the holder contributes to overfeed error. A large, soft fish is modeled with $\mu_{fish-table} = 0.1$ and $\mu_{fish-indexer} = 0.3$. Figure 6.6 shows that the fish moves approximately 0.002 m in the negative x–direction when the holder is not used during the indexing process. From Figure 6.4(b), the movement of the fish is approximately 0.015 m when the holder is used during indexing. The holder contributes to the overfeed error because as it presses down on the fish there is also a component of the force that causes the fish to slide in the negative x–direction. From this result, it can be concluded that the interaction of the fish with the holder is a mechanism in overfeed error.

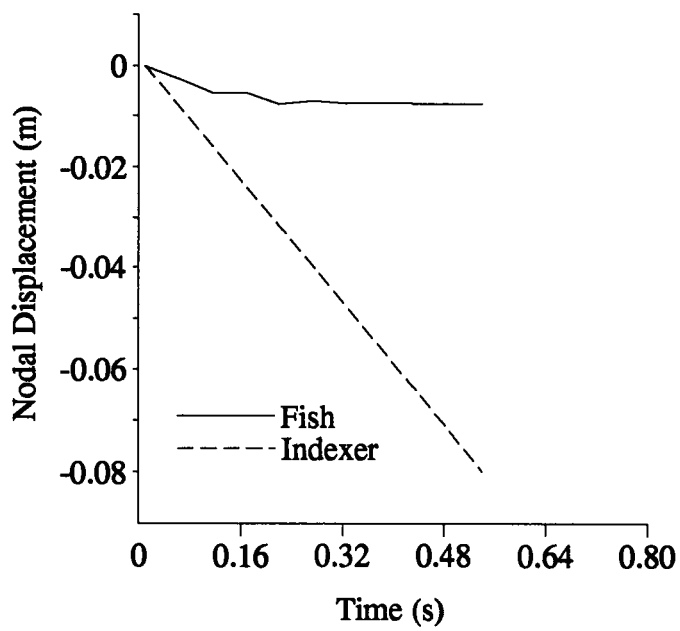

Figure 6.6: Overfeed motion (x–direction) of a large, soft fish when the holder is not used ($\mu_{fish-table} = 0.1$).

Redesign of the Indexing System

To minimize the component of the holding force which causes overfeed, the holder is moved so that it is located over the thickest part of the fish. A series of simulations are then carried out for a range of values of the coefficient of friction $\mu_{fish-indexer}$ to see if the overfeed error is reduced. The results are given in Figure 6.7. By comparing these curves with those of Figure 6.4(b), it is seen that for a large, soft fish, the contribution that the holder makes to overfeed error is significantly reduced when the holder is positioned over the thickest part of the fish. Furthermore, when the holder is positioned over the thickest part of the fish, overfeed will likely occur only if $\mu_{fish-indexer} > 0.5$.

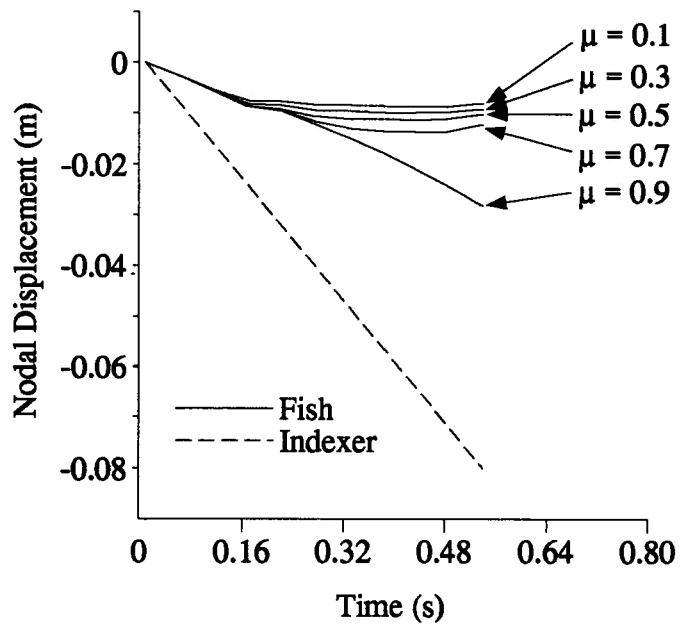

Figure 6.7: Overfeed motion (x-direction) of a large, soft fish as a function of the coefficient of friction between the fish and indexer, when the position of the holder is corrected ($\mu_{fish-table} = 0.1$).

6.2.2 The Role of Structural Deformities

If the structural deformity is best modeled by a change in $\mu_{fish-indexer}$ in a region of the fish skin, then results of section 6.2.1 are applicable. In such a case the action proposed in section 6.2.1 should suffice to eliminate most instances of overfeed error of this type. If on the other hand, the structural deformity is best modeled by a physical structure which protrudes above the surface of the fish, the results of section 6.1 would apply. To reduce the incidence of overfeed of this type, the indexing process should be abandoned in favor of a system which senses the location of the gill cover and positions the cutter for the head cut, or the fish should not be placed on the Iron Butcher for processing, but should be processed manually.

6.3 Summary of Results and Design Recommendations

The results of this chapter are summarized below.

- The minimum initial gap size between the gill cover and the fish for successful indexing to occur is established.
- A modification to the Iron Butcher (i.e. the push–down mechanism) is proposed to increase the size of the gap between the gill cover and the fish so the indexer will more easily engage with the gill cover and collar–bone.
- Operation of the Iron Butcher with the push–down modification is simulated to determine if the push–down mechanism reduces the likelihood of underfeed error occuring.
- Mechanisms responsible for overfeed error are identified.

- Simulations are used to determine the role each mechanism plays in overfeed error. Simulation results are also used to develop guidelines for the design of the indexing system to reduce the occurrence of overfeed error.

The following recommendations are made to improve the indexing system of the Iron Butcher.

Recommendations to Correct Underfeed Error

1. Modify the Iron Butcher to include a push–down mechanism for the indexing process. This mechanism will increase the size of the gap between the gill cover and the fish, and enhance the protrusion of the collar–bone beyond the fish side, so that the indexer can engage the gill cover and collar–bone and index the fish for the head cut.

Recommendations to Correct Overfeed Error

From the above analysis, two modifications to the machine will greatly reduce the incidence of overfeed error from friction between the fish and indexer and from the effects of holding.

1. Spraying water on the fish will act as a lubricant as the indexer slides over the fish. Since the coefficient of friction is reduced, the chance of overfeed occuring from friction alone is reduced. At the same time, grooves should be cut into the table surface to carry the excess water away, as overfeed is sensitive to $\mu_{fish-table}$.

2. Modify the Iron Butcher to permit adjustment of the position of the holder. For optimum results the machine should adjust the position of the holder for each fish. Since this would require sensing, actuation and control, it would be expensive to

implement. However, a manual adjustment which could be made daily or hourly based on the size of the fish running through the machine would reduce overfeed from the holder holding the fish near the tail where the fish is thin. The carousel in which the holders move could be mounted in a track so that the location of the holders could be easily adjusted and locked into place. A conceptual sketch of the movable carousel is shown in Figure 6.8.

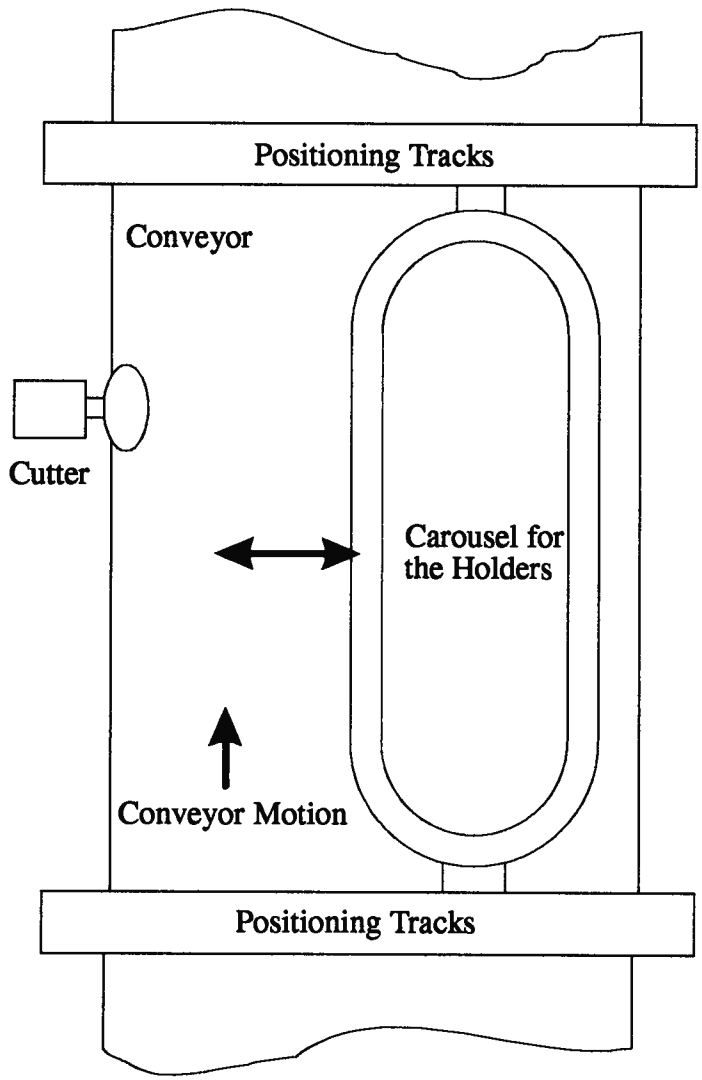

Figure 6.8: A movable carousel system to permit the manual adjustment of the holder position.

Chapter 7

Implementation of Design Improvements

To complement the analytical work in this dissertation and other research carried out in the Industrial Automation Laboratory, Department of Mechanical Engineering at U. B. C., several design improvements are implemented on two seperate butchering machines. The first machine is a laboratory prototype used for research, while the second machine is a prototype built and tested for industrial use. Both of these prototypes have undergone significant change from the current Iron Butcher, and there are some simularities in the design of these prototypes. This chapter describes the configuration and operating mode of these machines. The effects the design changes have on the machine processing of fish are discussed.

7.1 Laboratory Prototype

The components of the laboratory prototype are shown in Figure 7.1. A description of the prototype follows.

Feeding System A fish is placed in a holding pan so that the salmon is oriented with its head pointed towards the cutter and its belly facing away from the conveyor motion. In addition, the collar–bone must lie between two markers.

Conveying System The profile of the holding pan is an arc. The holding pan consists of two components, a small pan to hold and support the head of the fish during conveying, and a large pan to hold and convey the body of the fish. The two

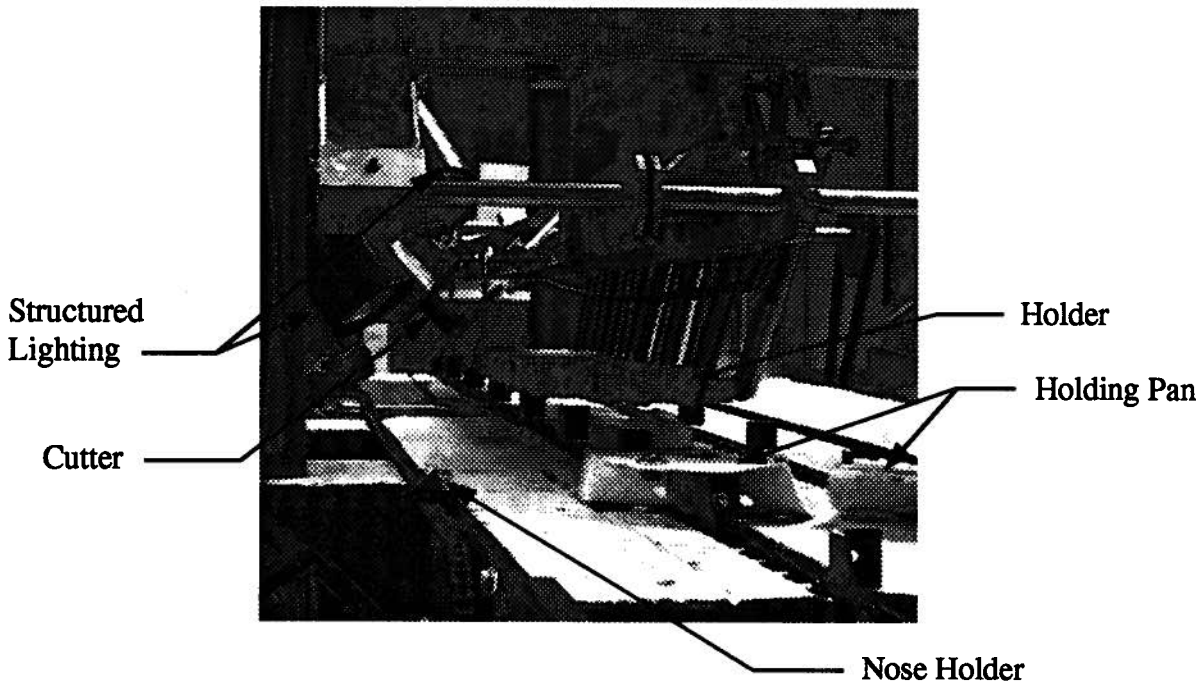

Figure 7.1: The laboratory prototype head–butchering machine.

components of the holding pan are aligned and rotated through 30°. The conveyor moves at a constant speed of 0.5 m/s.

Holding System Holding is accomplished by a group of stationary, active holders. The holders are cylindrical in shape. The cylinders rotate so that the point on the cylinder which is in contact with the fish has the same linear speed as the conveyor. The holders are spring loaded to accomodate different sizes of fish automatically. Holding starts after the feeding stage and continues to the onset of cutting.

Indexing System The mechanical indexing system of the existing Iron Butcher is not used on this protype. Instead of indexing the fish, the cutter is moved to the required location to perform an accurate head cut. Careful placement of the fish in the holding pans during feeding ensures that only a small adjustment in the cutter position is required to obtain an accurate cut. A CCD camera with an

electronic shutter captures an image of the head region of the fish as the fish is conveyed toward the cutter. The location on the fish where the cut is to be made is determined by image processing, and a control signal is sent to a servo–controller to position the cutter. An ultrasound displacement sensor records the thickness of the fish so that the cutter can be adjusted to compensate for the variation in thickness between fish.

Cutting System A double–bladed rotary cutter replaces the old chopping blade of the existing Iron Butcher. The new cutter creates a clean cut that is able to extract meat that was previously lost with the old cutter.

Although not perfect, the laboratory prototype is an improvement over the existing Iron Butcher, due primarily to the improvements to the conveying system and the new approach regarding indexing. The combination of holding pans and active holders provide a firm grip of the fish during the conveying process. This is an important factor in determining the accuracy of the cut, since any lateral movement of the fish with respect to the pan after the CCD camera images the head region of the fish will adversely affect the cut accuracy. The detection of the collar–bone and sensing of the fish thickness using ultrasound are both accurate and reliable. The accuracy of the cut on entry is improved from approximately 6 mm posterior of the collar–bone on the existing Iron Butcher to approximately 1 mm posterior of the collar–bone on this prototype. Although the accuracy of the cut on entry is higher, the accuracy of the rest of the cut diminishes to that of the existing Iron Butcher because of the lack of holding during the cutting process. As the fish is cut, the cutting forces tend to either pull the fish toward and into the cutter or push the fish away and out of the cutter, depending on the direction the cutter blades are rotating, causing the cut to deviate from the calculated optimal cut.

7.2 Industrial Prototype

Figure 7.2 shows the components of the industrial prototype. A description of the prototype follows.

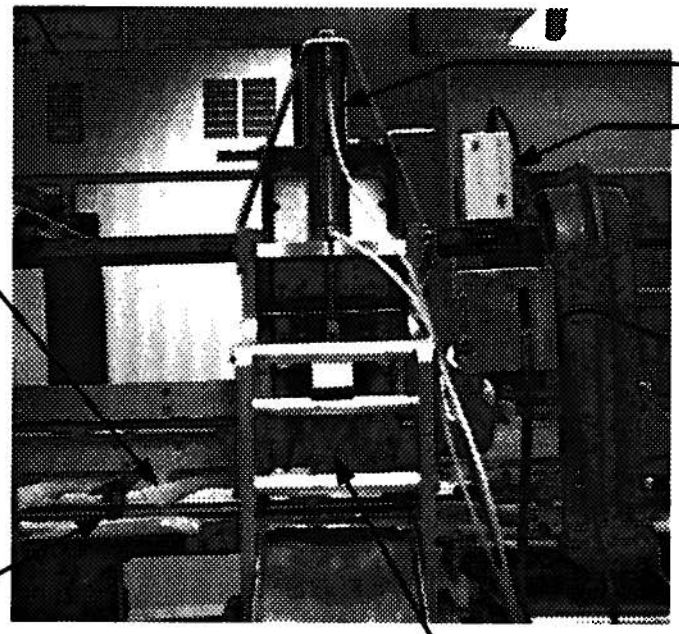

Figure 7.2: The industrial prototype head–butchering machine.

Feeding System The fish is fed onto the table surface with the same orientation used in the laboratory prototype. The fish must also be aligned so that the collar–bone lies within positioning markers.

Conveying System Conveying is accomplished by three lugs, as in the existing Iron Butcher. However, unlike the constant speed conveying of the existing Iron Butcher, the conveying motion of this prototype is intermittent.

Holding System The holders on the prototype maintain a fixed position over the table. Three holders are located at each position corresponding to the location of the fish

when the conveyor pauses. The holders approximate the contour of the fish and are spring loaded to accomodate various sizes of fish. Pneumatics are used to lift the holders while the conveyor is moving.

Indexing System The indexing system employs the same approach as the laboratory prototype. That is, the head region of the fish is imaged using a CCD camera and image processing determines the location on the fish where the cut should be made, and the cutter is moved to this position.

Cutting System A guillotine–style cutter blade is mounted on a single–axis table to position the cutter at the desired cutting location. A pneumatic piston controls the chopping action.

Although the conveying process works well to move the fish along the machine, the head and tail of the fish are not properly constrained, allowing them to oscillate back and forth as the conveyor cycles through its stop–start motion. Because of this extraneous motion of the fish head, the cutter cannot be positioned exactly at the location determined by the imaging system, but must instead be positioned slightly posterior of this position. This results in positional accuracy of cut of between 1 mm and 6 mm, which is an improvement on the existing Iron Butcher, but is not as good as the accuracy of the entry cut on the laboratory prototype. The guillotine–style cutter produces a clean cut, unlike the chopping cutter of the existing Iron Butcher. After the head is removed, only the two tail lugs touch the fish, causing the fish to rotate and jam in the conveyor system. Employing pans would eliminate the extraneous motion of the head and tail of the fish as it is conveyed so that the accuracy of cut could be improved to 1 mm. Furthermore, the pans would prevent the fish from jamming after the head is removed.

Chapter 8

Conclusions and Recommendations

In this final chapter, the main accomplishments of this research are summarized. Recommendations for improving the design of the Iron Butcher are listed. Finally, recommendations for future work on this topic are presented.

8.1 An Overview of the Research

The main accomplishments of this research are summarized below:

1. Finite element models of the fish, the Iron Butcher and the fish–machine interactions have been developed. These models permit the static and dynamic analysis of machine processing of salmon on the Iron Butcher, and serve as a tool for analyzing the operation of the machine in various configurations.

2. An investigation of the conveying process on the Iron Butcher concentrates on design requirements when new configurations and operating requirements are specified.

    - The operation of the Iron Butcher in its present configuration and under the present operating specifications is examined.
    - Pulsed conveying with straight chain lugs, conveying with staggered chain lugs at a constant and pulsed conveyor motion, and the use of holding pans as an alternative to lugs are all investigated.

3. The mechanisms which cause overfeed and underfeed indexing error are investigated. A systematic approach is employed to determine the effect of each mechanism when more than one mechanism is active in producing the indexing error.

4. Design guidelines have been developed from the simulation results and serve to aid the designer in improving the performance of the Iron Butcher.

5. This research demonstrates the usefulness of finite element analysis as a design tool for materials handling problems, particularly when the objects being handled are flexible and the dynamics of the process cannot be ignored.

6. The Iron Butcher has been modified with design changes to the conveying, indexing and cutting systems and has been demonstrated to provide better results.

8.2 Recommendations for Design Improvement

The following recommendations are made to improve the conveying and indexing processes of the Iron Butcher.

1. **Use contoured holders to hold the fish.** The shape of the holder should roughly conform with a range of fish. At least two holders should be used per fish.

2. **Replace the chain lugs with holding pans.** The holding force is greatly reduced when the chain lugs are replaced by holding pans. Furthermore, holding pans greatly reduce the unwanted motion of the head region when the fish is conveyed.

3. **Add a nose push–down mechanism.** The nose push–down mechanism increases the fish–gill cover gap size, thereby decreasing the likelihood of underfeed error.

4. **Spray water on the fish.** Water acts as a lubricant, reducing the fish–indexer coefficient of friction, thereby decreasing the chance of overfeed error.

5. **Permit adjustment of the holder position.** Proper position of the holder is required to reduce overfeed error.

8.3 Recommendations for Further Work

This research has been limited to the investigation of the conveying and indexing processes on the Iron Butcher. Although these two processes are responsible for the extreme cases of waste at the head cut, even if the fish is properly conveyed and indexed, the tearing action of the cutter creates waste with each cut. Therefore, a logical progression of this work would examine the cutting process. Although finite element analysis currently has the capability of modeling processes which have as a feature the removal of material, the criteria used to determine when and how the material should be removed is the critical part of the finite element model. If the generated criteria do not accurately reflect the actual physical process of material removal, then the simulation results will provide information about a quite different process, and the usefulness of these results will be severely limited.

The task of modeling the cutting process becomes a problem of material sciences. The first step is to determine the material properties of the muscle tissue. This description would account for the anisotropic and nonlinear properties of the muscle tissue. Next, an understanding of how muscle fibre fails is required. Controlled experiments may reveal the failure modes of muscle fibre for different loading conditions, but ultimately an understanding of the failure modes during different cutting processes (e.g., chopping or slicing) is required. If an understanding of these processes are attained, would they still be valid for a grouping of muscle fibre? The last step before modeling the process is to translate the understanding of the cutting process into a set of constraint equations which will control the removal of material and the distribution of cutting forces in the finite

element model. The model of the fish and machine must then be modified to incorporate these changes. The process of acquiring an understanding of the cutting process should enable the proper selection of a cutter for a specific cutting task, while simulation results should provide information about how to hold the fish during the cutting process.

Bibliography

[1] Browning, R. J., *FISHERIES OF THE NORTH PACIFIC, History, Species, Gear & Processes (Rev. ed.)*, Alaska Northwest Publishing Co., Anchorage, Alaska, 1974.

[2] de Silva, C. W., "Research Laboratory for Fish Processing Automation", *Proceedings of the 3rd International Symposium on Robotics and Manufacturing*, Vol. 3, A.S.M.E. Press, N.Y., pp. 935–940, 1990.

[3] Mason, M. T., "The Mechanics of Manipulation", *1985 IEEE International Conference on Robotics and Automation*, pp. 544–548.

[4] Mason, M. T., "Mechanics of Pushing", *2nd International Symposium on Robotics Research*, pp. 421–428, August 1984.

[5] Brost, R. C., "Automatic Grasp Planning in the Presence of Uncertainty", *1986 IEEE International Conference on Robotics and Automation*, pp. 1575–1581.

[6] Peshkin, M. A. and Sanderson, A. C., "Manipulation of a Sliding Object", *Proceedings - 1986 IEEE International Conference on Robotics and Automation*, pp. 233–239.

[7] Peshkin, M. A. and Sanderson, A. C., "Planning Robotic Manipulation Strategies for Sliding Objects", *Proceedings - 1987 IEEE International Conference on Robotics and Automation*, pp. 696–701.

[8] Peshkin, M. A. and Sanderson, A. C., "Planning Robotic Manipulation Strategies for Workpieces that Slide", *IEEE Journal of Robotics and Automation*, Vol. 4, No. 5, pp. 524–531, October 1988.

[9] Gilmore, B. J. and Streit, D. A., "A Rule-Based Algorithm to Predict the Dynamic Behaviour of Mechanical Part Orienting Operations", *1988 IEEE International Conference on Robotics and Automation*, pp. 1254–1259.

[10] Wang, Y. and Mason, M. T., "Modeling Impact Dynamics for Robotic Operations", *1987 IEEE International Conference on Robotics and Automation*, pp. 678–685.

[11] Routh, E. J., *Dynamics of a System of Rigid Bodies (Seventh Edition)*, Dover Publications, New York, 1960.

[12] Cai, C. S. and Roth, B., "On the Planar Motion of Rigid Bodies with Point Contact", *Mechanism and Machine Theory*, Vol. 21 No. 6, pp. 453–466, 1986.

[13] de Silva, C. W., *Control Sensors and Actuators*, Prentice-Hall, Inc., Englewood Cliffs, N. J., 1989.

[14] Cai, C. S. and Roth, B., "On the Spatial Motion of a Rigid Body with Point Contact",*IEEE 1987 International Conference on Robotics and Automation*, pp. 686–695.

[15] Montana, D. J., "The Kinematics of Contact and Grasp", *The International Journal of Robotics Research*, Vol. 7 No. 3, pp. 17–32, June 1988.

[16] Montana, D. J., "The Kinematics of Contact with Compliance", *1989 IEEE International Conference on Robotics and Automation*, Vol. 2, pp. 770–774.

[17] Saliba, M. and de Silva, C. W., "An Innovative Robotic Gripper for Grasping and Handling", *Proc. IEEE Conference on Industrial Electronics, Control, and Instrumentation*, Kobe, Japan, pp. 1590–1595, October 1991.

[18] de Silva, C. W. and Saliba, M., "Instrumentation Issues in the Handling of Fish for Automated Processing", *Proc. IEEE Conf. on Industrial Electronics, Control, and Instrumentation*, San Diego, CA, November 1992 (In Press).

[19] Petrell, R. J., Rodriguez, A. C. and Nordin, D. M., "Anisotropic Elastic Properties of Farmed-Salmon Muscle", *Proceedings of the 1990 International Winter Meeting of the American Society of Agricultural Engineers*, Paper No. 906572, December 1990.

[20] Johnson, E. A., Segars, J. G., Kapsalis, M. D. and Peleg, M., "Evaluation of the Compressive Deformability Modulus of Fresh and Cooked Fish Flesh", *Journal of Food Science*, Vol. 45, pp. 1318–1326, 1980.

[21] Borderias, A. J., Lamua, M. and Tejada, M., "Texture analysis of fish fillets and minced fish by both sensory and instrumental methods", *Journal of Food Technology*, Vol. 18, pp. 85–95, 1983.

[22] Chow, W. W. and Odell, E. I., "Deformations and Stresses in Soft Tissues of a Sitting Person", *Journal of Biomechanical Engineering*, Vol. 100, pp. 79–87, 1978.

[23] Yamada, H., *Strength of Biological Materials*, The Williams & Wilkins Company, Baltimore, 1970.

[24] Huebner, K. H. and Thornton, E. A., *THE FINITE ELEMENT METHOD FOR ENGINEERS (Second Edition)*, John Wiley & Sons, Inc., New York, 1982.

[25] Rizzo, A. R., "Estimating Errors in FE Analyses", *MECHANICAL ENGINEERING/CIME*, May 1991, pp. 61–63.

[26] Dunajski, E., "Texture of Fish Muscle", *Journal of Texture Studies*, Vol. 10, pp. 301–318, 1979.

[27] Segars, R. A., Nordstrom, H. A. and Kapsalis, J. G., "Textural Characterstics of Beef Muscles" *Journal of Textural Studies*, Vol. 5, No. 3, pp. 283–297, Oct. 1974.

[28] Bouton, P. E. and Harris, P. V., "The effects of some post-slaughter treatments on the mechanical properties of bovine and ovine muscle", *Journal of Food Science*, Vol. 37, pp. 539–543, 1972.

[29] Fung, Y. C., *Biomechanics, Mechanical Properties of Living Tissues*, Springer-Verlag, New York, N. Y., 1981.

[30] Evans, F. G., *Mechanical Properties of Bone*, Charles C. Thomas, Springfield, Illinois, 1973.

[31] de Silva, C. W. and Riahi, N., "System Integration and Image Processing Techniques in a Fish Processing Workcell", *Advances in Instrumentation*, DSC - Vol. 30, A. S. M. E., N. Y., pp. 73–78, December 1991.

[32] Gamage, L. D. K. B. and de Silva, C. W., " Use of Image Processing for the Measurement of Orientation with Application to Automated Fish Processing", *IECON'90, The 16th Annual Conference of IEEE Industrial Electronics Society*, pp. 482–487, Nov. 1990.